Distributed Space Time Block Coding in Asynchronous Cooperative Relay Networks

by

Abdulghani Mohamed Elazreg

A thesis submitted in partial fulfilment of the requirements for the award of the degree of Doctor of Philosophy, at Loughborough University.

November 2012

Advanced Signal Processing Group
School of Electronic, Electrical and Systems Engineering
Loughborough University, Loughborough
Leicestershire, UK, LE11 3TU.

CERTIFICATE OF ORIGINALITY

This is to certify that I am responsible for the work submitted in this thesis, that the original work is my own except as specified in acknowledgements or in footnotes, and that neither the thesis nor the original work contained therein has been submitted to this or any other institution for a degree.

.... (Signed)

.... (candidate)

I dedicate this thesis to my parents, my wife, my loving children, my brothers and sisters, and my grandmother soul.

ABSTRACT

The design and analysis of various distributed space time block coding schemes for asynchronous cooperative relay networks is considered in this thesis. Rayleigh frequency flat fading channels are assumed to model the links in the networks, and interference suppression techniques together with an orthogonal frequency division multiplexing type transmission approach are employed to mitigate the synchronization errors at the destination node induced by the different delays through the relay nodes.

Closed-loop space time block coding is first considered in the context of decode-and-forward (regenerative) networks. In particular, quasi orthogonal and extended orthogonal coding techniques are employed for transmission from four relay nodes and parallel interference cancellation detection is exploited to mitigate synchronization errors. Availability of a direct link between the source and destination nodes is studied, and a new Alamouti space time block coding technique with parallel interference cancellation detection which does not require such a direct link connection and employs two relay nodes is proposed. Outer coding is then added to gain further improvement in end-to-end performance and amplify-and-forward (non regenerative) type networks together with distributed space time coding are considered to reduce relay node complexity.

Novel detection schemes are then proposed for decode-and-forward networks with closed-loop extended orthogonal coding which reduce the computational complexity of the parallel interference cancellation. Both sub-optimum and near-optimum detectors are presented for relay nodes with single or dual antennas. End-to-end bit error rate simulations confirm the potential of the approaches and their ability to mitigate synchronization errors. A relay selection approach is also formulated which maximizes spatial diversity gain and attains robustness to timing errors.

Finally, a new closed-loop distributed extended orthogonal space time block coding solution for amplify-and-forward type networks which minimizes the number of feedback bits by using a cyclic rotation phase is presented. This approach utilizes an orthogonal frequency division multiplexing type transmission structure with a cyclic prefix to mitigate synchronization errors. End-to-end bit error performance evaluations verify the efficacy of the scheme and its success in overcoming synchronization errors.

ACKNOWLEDGEMENTS

Praise be to Allah (God), the most gracious and the most merciful, without his blessing and guidance my accomplishments would never have been possible.

This dissertation would not have been possible without the help and support of many people during my studies at Loughborough University. A few words mentioned here cannot adequately express my appreciation.

First and foremost, I would like to express my deepest gratitude toward my supervisor, Prof. Jonathon A. Chambers for giving me the opportunity to be a part of his research group and for his patience, constant support from the beginning of my PhD studies, especially the understanding shown during my first year and his guidance throughout my research program at Loughborough University.

I would also wish to thank all the members of the Advanced Signal Processing Group (ASPG), Loughborough University, for creating a friendly environment during my research studies in the Laboratory. Also I would like to express appreciation for all the administrative assistance given to me throughout my study at Loughborough University by June Boot. Moreover, I would also like to thank my friends who worked with me and made my research experience very enjoyable.

Of course, my eternal thanks go to my parents, brothers and sisters for their support, prayers and love. I dedicate this study to them.

I also owe my loving thanks to my beloved wife and my two lovely sons Mohamed and Musaab. Without my wife's endless love, support, prayers, companionship, friendship and caring words, this would not have been possible. I am deeply grateful for her and this dissertation is equally her achievement.

To all these wonderful people, many thanks again.

CONTENTS

Acronyms

3G   Third Generation

4G   Fourth Generation

8PSK   8Phase Shift Keying

A-STBC   Alamouti Space Time Block Coding

AF   Amplify-and-Forward

AMT   Adjacent Mobile Terminal

ASPG   Advanced Signal Processing Group

AWGN   Additive White Gaussian Noise

BER   Bit Error Rate

BPSK   Binary Phase Shift Keying

CDMA   Code Division Multiple Access

CL STBC   Closed-Loop STBC

CL   Closed-Loop

Conv   Conventional

CP   Cyclic Prefix

CRC   Cyclic Redundancy Check

CSI   Channel State Information

dB   Decibel

DFT   Discrete Fourier Transform

DF   Decode-and-Forward

DSP   Digital Signal Processing

DT   Direct Transmission

EO-STBC   Extended Orthogonal-STBC

EP   Error Propagation

EW   Europe Wireless

FFT   Fast Fourier Transform

GAs   Genetic Algorithms

i.i.d   Independently and Identically Distributed

ICACT   International Conference on Advanced Communication Technology

ICASSP   International Conference on Acoustics, Speech and Signal Processing

ICC   International Conference on Communications

IDFT   Inverse Discrete Fourier Transform

IEEE   Institute of Electrical and Electronics Engineers

IET	The Institution of Engineering and Technology
IFFT	Inverse Fast Fourier Transform
ISIT	International Symposium on Information Theory
ISI	Intersymbol Interference
LDPC	Low-Density Parity-Check
LS	Least Squares
LTE	Long Term Evolution
MIC	Multistage Interference Cancellation
MIMO	Multi-Input Multi-Output
ML	Maximum Likelihood
MR	Multi Relay
MS-MR	Multi Source-Multi Relay
MS	Multi Source
O-STBC	Orthogonal Space Time Block Coding
OFDM	Orthogonal Frequency Division Multiplexing
P/S	Parallel to Serial
PAPR	Peak-to-Average Power Ratio
PEP	Pairwise Error Probability
PhD	Doctor of Philosophy
PIC	Parallel Interference Cancellation

PIMRC Personal Indoor and Mobile Radio Communications

PSK Phase Shift Keying

PS Perfect Synchronization

QAM Quadrature Amplitude Modulation

QO-STBC Quasi Orthogonal Space Time Block Coding

QPSK Quadrature Phase Shift Keying

RF Radio Frequency

S/P Serial to Parallel

SIC Successive Interference Cancelation

SNR Signal-to-Noise Ratio

SoftCOM Software, Telecommunications and Computer Networks

SSP Statistical Signal Processing

STBCs Space Time Block Codes

STBC Space Time Block Code

STC Space Time Coding

STTCs Space Time Trellis Codes

TR Time Reversal

VAA Virtual Antenna Array

VTC Vehicular Technology Conference

Wi-Fi Wireless Fidelity

WiMAX Worldwide Interoperability for Microwave Access

WiMob Wireless and Mobile Computing, Networking and Communications

WLAN Wireless Local Area Network

MATHEMATICAL
NOTATIONS

m	Subcarrier index
q	Number of the PIC iteration
M	Size of constellation
N	Duration of one OFDM symbol
P	Total transmitted power
$\mathbf{S}$	Code matrix of STBC
R	Number of relay nodes
$\mathbf{T}$	Number of symbol transmissions
N_T	Number of transmit antennas
N_R	Number of receiver antennas
M_R	Number of antennas on each relay node
E_s	Average power of the source
E_b	Energy per bit

N_o Noise spectral density

D_R Data transmission rate

D_g Diversity gain

C_g Coding gain

C_R Code rate

G_p Guard period

N_S Number of transmission symbols

R_s The set of best relay selection node

N_P Number of transmission periods

I_{Bits} Input bits of convolutional encoder

O_{Bits} Output bits of convolutional encoder

P_1 Transmitted power at the source node

P_2 Transmitted power at the relay nodes

l_{cp} Length of cyclic prefix

τ_{max} Maximum of possible relative timing error

$R_\mathbf{B}$ The rank of matrix $\mathbf{B}$

$N_T \times N_R$ Spatial diversity

Δ Grammian matrix

λ Total channel gain

λ_c Conventional channel gain

λ_f Feedback performance gain

$\angle$ Angle of a complex number

σ_s^2 Variance of transmitted signal

σ_n^2 variance of the AWGN noise

σ_r^2 variance of the received signal

$CN(0,1)$ Circularly symmetric complex Gaussian distribution with zero mean and unit variance

$\otimes$ The Hadamard product

j $\sqrt{-1}$

τ_k Timing misalignments between relay nodes

β_k Reflect the impact of timing misalignments

$h_k(-l)$ Coefficient to reflect ISI from previous symbols

$g_k(-l)$ Coefficient to reflect ISI from previous symbols

log_2 Base-2 logarithm

I_m $m \times m$ Identity matrix

$0_{m \times n}$ $m \times n$ Matrix with all zero entries

$k \in R$ k is an element of R

$\mathbf{E}(.)$ The statistical expectation operator

$\mathbf{det}(.)$ The determinant operator

$\xi(.)$ Time reversal of the signals

$P_e(.)$ Average probability of error

$Q(.)$ Gaussian Q function

$|.|$ Absolute value of a complex number

$||.||$ The Euclidean norm

$||.||_F$ The Frobenius norm

$\min\{.\}$ Select the minimum value

$\max\{.\}$ Select the maximum value

$(.)^T$ Transpose operator

$(.)^*$ Complex conjugate operator

$(.)^H$ Hermitian transpose operator

$\Re\{.\}$ Real part of a complex number

$\arg(a_1, \cdots, a_n)$ Argument of $a_1, \cdots, a_n$

List of Figures

List of Tables

Chapter 1

INTRODUCTION

In recent decades, wireless networks have been motivated by their ability to provide "anywhere, anytime and anymedia" wireless access at a reasonable low price. Nevertheless, in wireless communications, signal transmission can be obstructed by channel impairments such as channel fading, shadowing, path loss and interference [4]. Therefore, recent developments in multi-input multi-output (MIMO) techniques have been proposed to exploit spatial diversity and provide an attractive way to combat the channel impairments in a wireless environment [4], creating different signal paths between the transmitter and the receiver, which can be modelled as a number of separate, independent fading links; although this generally comes with the price of increased transceiver complexity.

The use of the MIMO technique with space-time coding (STC) has been recognized as a promising scheme to exploit spatial diversity gain with a low complexity encoder/decoder through multiple transmit and/or receiver antennas [5]. However, the MIMO technique only promises an increase in spatial diversity if uncorrelated paths are formed between the transmit and receive antennas. In order to overcome this drawback, a new paradigm of gaining spatial diversity gain, called cooperative diversity, which is achieved by utilizing the antennas of other

terminals as relay nodes has been proposed. These relay nodes can generate copies of the same signal, which can provide spatial diversity gain and high signal-to-noise ratio (SNR) benefits by sharing their physical resources through a virtual transmit and receive antenna array.

Recently, space time block coding (STBC) in a distributed fashion for cooperative relay networks has attracted much research interest [6], [7], [8] and [9]. The design of STBC for cooperative relay networks has some new challenges which are different from the design of STBC for point-to-point MIMO systems. The synchronization issue is one of the most important challenges in the design of distributed STBC for cooperative relay networks, since the cooperative systems are asynchronous in nature, e.g., there may exist timing errors and multiple frequency offsets in the relay nodes forming the cooperative system. This will induce intersymbol interference (ISI) between the relay nodes at the destination node, which degrades the system performance and makes it impossible to exploit full cooperative diversity.

The overall context of this thesis is to provide a contributive step towards addressing this challenge, with particular focus on the design of space time block codes (STBCs) for cooperative relay networks with different system models and in asynchronous scenarios over frequency non-selective (flat) Rayleigh fading channels.

Some basic definitions relevant to the work within this thesis are next presented.

1.1   Basic Definitions

1.1.1   Basic Concepts of Cooperative Relay Networks

The concept of cooperative relay networks is to exploit the broadcast nature of wireless networks. Cooperative relay wireless communication networks have gained much interest due to their ability to realize the performance gain of MIMO wireless systems whilst resolving the difficulties of co-located multiple antennas at individual nodes. Figure 1.1 represents the classical example of a two-hop cooperative relay network within which the relay node can cooperate and assist the transmission between the source node and the destination node, in order to increase the link quality, reliability of wireless communication link and possibly the data transmission rate of the system without the requirement of additional antennas and the associated complexity at each node.
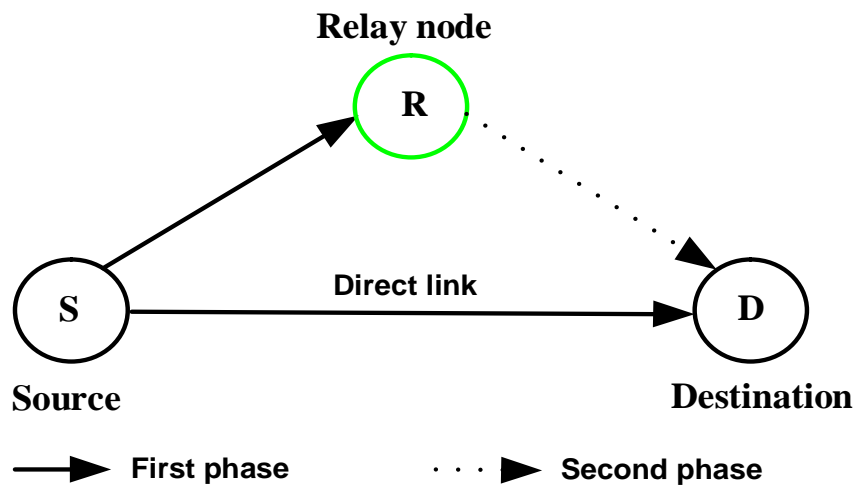
Figure 1.1. Basic structure of a cooperative relay network with two phases for the cooperative transmission process.

Due to the low complexity at each node, it is usually assumed that each node cannot transmit and receive simultaneously in the same frequency band (half-duplex). The overall transmission can be divided

into two phases. The source node first broadcasts its signals to both the relay node and the destination node. Whereas, during the second phase the relay node processes the source signals and then forwards them to the destination node as shown in Figure 1.1. The relay nodes may either just act as a repeater where it amplifies the measured signals from the source node and forwards them or it may decode the measured signals from the source node, re-encode and forward them to the destination node. The former cooperative strategy which can be applied at the relay node to process the received signals from the source node is called non-regenerative or amplify-and-forward (AF) relaying, while the latter technique is called regenerative or the decode-and-forward (DF) strategy [10]. Therefore, the main advantage of cooperative relay wireless communication networks is to increase the communication reliability, decrease power consumption due to transmitting over shorter links and improve the outage probability in a wireless network.

Furthermore, cooperative relay wireless relay networks can take many forms depending on their application [11]. In Figure 1.2 , for example, the source node communicates with the destination node through parallel relay nodes to improve the cooperative diversity gain. The maximum cooperative diversity gain can be achieved by using this model is equal to the number of transmitting relay nodes [6]. When the link between the source node and destination node is too unreliable for example due to high pathloss to guarantee reliable communications [11], the architecture reduces to the case of a cascade multi-stage communication.
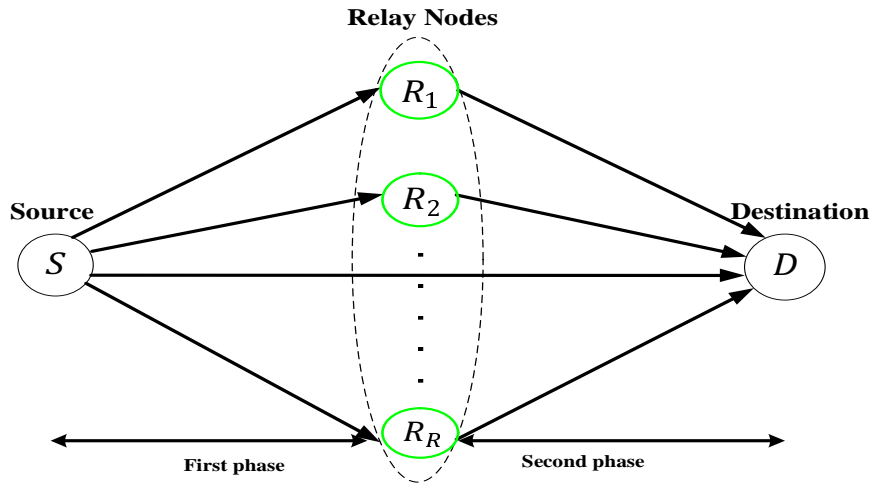
Figure 1.2. Basic structure of a parallel cooperative relay network with two phases for the cooperative transmission process.

However, a solution to overcome this problem as suggested in [12] would be the use of multi-source multi-relay (MS-MR) transmission model as shown in Figure 1.3, which includes an adjacent mobile terminal(AMT).
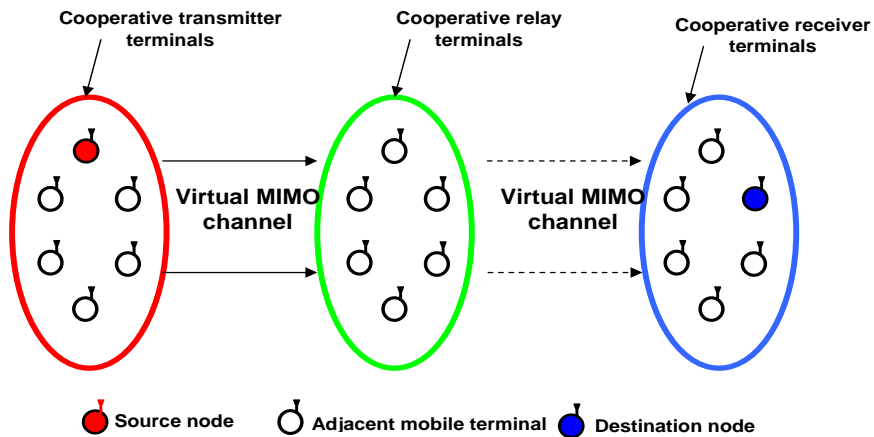
Figure 1.3. Basic structure of MS-MR network with two phases for the cooperative transmission process.

In this model the source node and its adjacent mobile terminal (AMT) share their antennas and send the same information through independent fading paths to the destination node via parallel cooperative relay nodes. then the destination node together with its AMT receives

the information which is jointly decoded and the required information extracted to provide cooperative diversity gain equal to the number of transmitting relay nodes. Recently, the area of cooperative communications has sparked much attention among researchers [10], [11], [13] and [14]. If the transmission from all relay nodes arrives at the destination node at the same time, then the term synchronous cooperative relay networks is used. Otherwise, the expression asynchronous cooperative relay networks is used. Among the several types of cooperative relay networks, this thesis considers asynchronous two-stage relay networks with the assumption that all nodes are equipped with a single or two half-duplex antenna at the relay nodes.

1.1.2 Design of Space-Time Codes and their Enhancement for Cooperative Relay Networks

In recent years it has been found that the framework of distributed[1] STBC also plays an important role in coding for cooperative relay networks. Distributed STBC refers to a cooperative strategy where the conventional STBC for co-located antennas is implemented between the relay nodes in a distributed manner. More specifically, when the relay nodes receive the signals from the source node, they are linearly processed and then broadcast to the destination node in the form of a space time codeword [6] and [7]. Distributed STBC in a cooperative relay network allows the relay nodes to maximize cooperative diversity gain without the availability of channel state information (CSI)[2] at the

---

[1]In this thesis the term "distributed" is used to qualify the use of STBC with relay nodes, either with DF or AF type transmission.

[2]CSI characterizes the channel properties of the communication link and can be estimated at the receiver side during the training period in which the transmitter sends a pilot or training sequences.

relay nodes, similar to the conventional STBC in point-to-point MIMO systems, where transmit diversity is exploited without the need of CSI at the transmit antennas. As a consequence, it is well known that the transmission reliability of the source signals over the cooperative relay networks utilizing distributed STBC can be significantly improved.

Current distributed STBCs include distributed orthogonal STBC (O-STBC) and distributed quasi orthogonal STBC (QO-STBC) [7]. Distributed O-STBC with full transmission rate design and complex elements in its transmission matrix is impossible for more than two relay nodes. The only example of full data transmission rate, full cooperative diversity, complex STBC using orthogonal design is distributed Alamouti STBC (A-STBC) [5]. Consequently, distributed QO-STBC was proposed in which the constraint of orthogonality is relaxed to achieve full data transmission rate. In general distributed QO-STBC does not achieve full cooperative diversity provided in proportion to the number of transmitting relay nodes and it has pair-wise decoding complexity as compared to distributed O-STBC [7]. Therefore, a number of closed-loop (CL STBC) technique were proposed to provide full data transmission rate and full diversity gain with simple-wise decoding complexity in a point-to-point MIMO system [15], [16] and [17]. Basic definitions of closed-loop and open-loop systems are given in the following section.

1.1.3   Closed-Loop Versus Open-Loop System

When the relay nodes do not have any knowledge about the channel coefficients and the destination node is capable of estimating the channel coefficients accurately through some pre-defined training data sequence

and then use the CSI for decoding operations, the system is called an
open-loop system as shown in Figure 1.4 (a). However, if the relay
node can have access to the channel information improvement in the
error rate performance may result and this should be exploited provided
complexity and system overhead is minimized. Therefore, in some com-
munication systems the relay nodes are assumed to obtain knowledge
of the channel condition through a feedback link from the destination
node to the relay node, in this case it is called a closed-loop system as
depicted in Figure 1.4 (b).
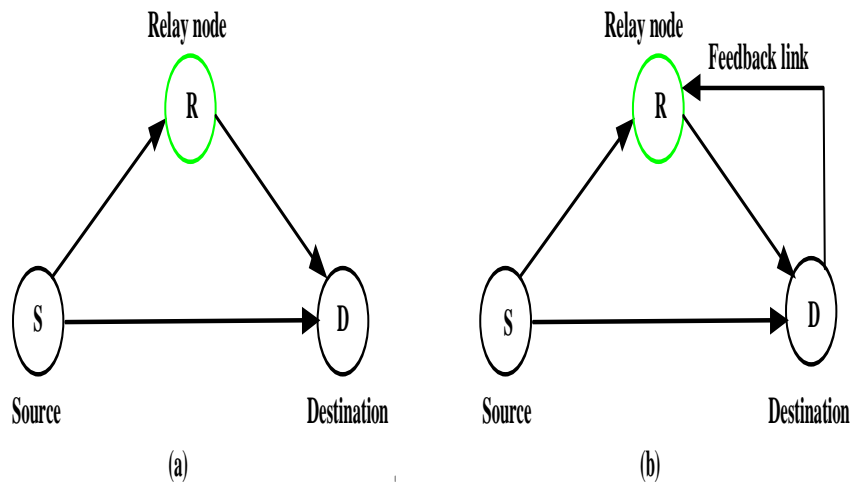
Figure 1.4. Basic structure of (a) open-loop cooperative relay network
and (b) closed-loop cooperative relay network with feedback link from
the destination node to the relay node.

In a closed-loop system, the gain achieved by additional processing
at the relay node and the destination node can be termed as array gain.
Similar to diversity gain, the array gain results in an increase in average
SNR. In most practical applications, the amount of feedback informa-
tion required from the destination node to the relay node should be
kept as small as possible due to limited available feedback bandwidth.
Therefore, the feedback information should be quantized into levels,

and these levels can be fed back to the relay node to improve the system performance [15]. In particular, the feedback can be made available to all relay nodes through a separate feedback channel which is practically achievable in bi-directional control channels present in many communication systems. Thus, in this thesis, distributed CL STBC that achieves full data transmission rate and full cooperative diversity gain with linear decoding for asynchronous two-stage relay networks with and without outer coding is investigated and also a new closed-loop extended orthogonal STBC (EO-STBC) scheme with one-bit feedback information is proposed to enhance the system performance of cooperative relay networks as compared to previous closed-loop methods [15] and [16] in asynchronous distributed manner.

1.2   Impairments on Cooperative Relay Channels

1.2.1   Wireless Fading Channels

One of the most challenging phenomena in wireless communication channels is the signal attenuation caused by the fading nature of the channels. The transmitted signal in a wireless network usually reaches the receiver node via multiple paths and these paths change with time due to the mobility of the user nodes and/or reflectors in the environment [18]. The changing strength of each path and the changing interference between these paths result in fading. Fading can be characterized on large and small time scales. Large fading is a result of movement distance large enough to cause total variation in the overall path between the source node and the receiver nodes. However, the short term fluctuation in the signal amplitude effect by movement

of the user over distances of a small number of wavelengths is called small-scale fading. Small-scale fading itself can be categorized as frequency flat or frequency selective fading [4]. In frequency flat fading, the channel has a constant gain and linear phase response over a bandwidth which is greater than the bandwidth of the transmitted signal. Therefore, all frequencies of the transmitted signal experience the same channel condition. Nevertheless, in frequency selective fading, the channel possesses a constant gain and linear phase over a bandwidth that is smaller than the signal bandwidth, ISI exists and the received signal at the received node is distorted [1].

Throughout this thesis, all communication channels are modelled as frequency flat fading, which is the most common type of fading described in the technical literature due to its simplicity. However, this assumption is always not realistic, since the communication channels often experience time varying frequency selective fading, but orthogonal frequency division multiplexing (OFDM) can convert such channels to frequency flat form.

1.2.2   Interference Between Cooperative Relay Nodes

The use of multiple relaying nodes provides high cooperative diversity gain thereby improving robustness against channel impairments, in order to maximize the cooperative diversity gain of cooperative relay networks in proportion to the number of transmitting relay nodes [19], the relay nodes are scheduled to transmit simultaneously with perfect synchronization among the cooperative relay nodes at the symbol level, which means that the timing, carrier frequency and propagation delay relay nodes are identical as shown in Figure 1.5 (a) [11].

Space

Signal from relay 1

Signal from relay 2

Signal from relay 3

Signal from relay R

Time

(a)

Space

Signal from relay 1

Signal from relay 2

Signal from relay 3

Signal from relay R

Time

τ_{13}

τ_{12}

τ_{1R}

(b)
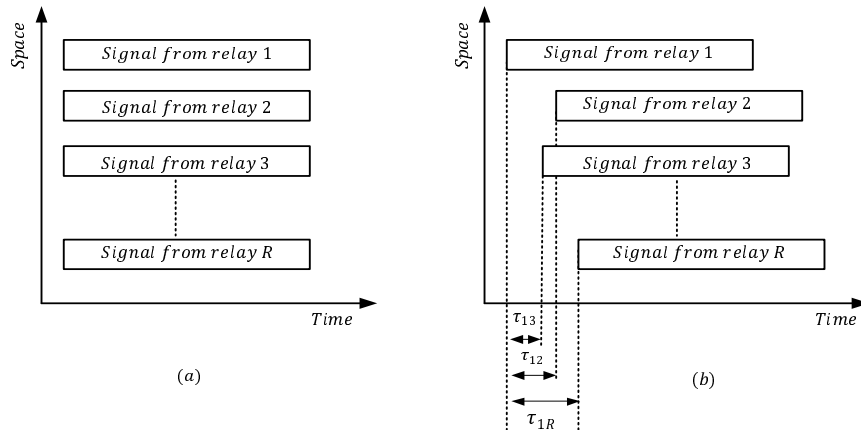
Figure 1.5. Basic structure of the received signals at the destination node from the relay nodes, (a) shows the received signals which arrive at the destination node at the same time instants (perfect synchronization) (b) shows the received signals arrive at the destination node with different time delay τ_{1R} (imperfect synchronization).

However, perfect synchronization in cooperative relay networks does not exist in practice. To achieve exact synchronization among the relay nodes positioned at different locations, which are probably subject to movement, each having its own oscillator, is difficult or impossible to achieve [20]. As shown in Figure 1.5 (b), the major synchronization issue is the time delay τ_{1R} of signals, when they arrive at the destination node in the next hop, where R is the number of relay nodes in the network. Propagation delays may be unknown to them, while transmission time instants may be different at the destination node. This lack of synchronization results in ISI between the received signals from the relay nodes at the destination node. As such the channel becomes dispersive even under a flat fading environment; and will lead to substantial performance degradation. Mitigating this problem is the main research focus of this thesis.

1.3   Challenges and Thesis Contributions

MIMO systems are an emerging technology which involve in using multiple antennas at transmit and/or receive antennas in order to exploit spatial diversity between transmitter and receiver. The success of MIMO technology has led to the concept of cooperative communications where multiple nodes equipped with a single or multiple antenna cooperate together in order to form a virtual MIMO array and offer cooperative diversity. Cooperative system is a promising solution for high data-rate coverage required in future wireless communications systems. Combining a cooperative system with a MIMO transmission is an interesting way to overcome the channel impairments and to improve the system performances [14]. In wireless cooperative communication networks, several previously proposed distributed STBCs have been adapted for use in synchronous cooperative scenarios [6], [8], [20] and [21]. However, the asynchronism between the relay nodes can be a source of system performance degradation as mentioned in the previous section [20], [22], [23], [24] and [25]. Therefore, the scope of this thesis to achieve the objective of eliminating the issue of imperfect synchronization among the relay nodes over frequency flat fading channels. Full cooperative diversity order in proportion to the number of transmitting relay nodes will be exploited together with full data transmission rate over each stage and low decoding and detection complexity either at the relay nodes or the destination node. Furthermore, this thesis focuses on developing a new closed-loop coding scheme with limited feedback information that requires channel knowledge to achieve full data transmission rate, full cooperative diversity and array gain, i.e., exploitation of CSI at the relay nodes for cooperative relay networks.

The work presented in this thesis has been inspired by the contributions of [15], [16] and [17] on STBCs as applied to MIMO systems; [6], [7] and [12] on distributed STBCs for synchronous cooperative relay networks; [2] on distributed STBCs for asynchronous cooperative relay networks over frequency flat fading channels.

Firstly, the core aim of this thesis is to exploit the advantages of the closed-loop EO-STBC (CL EO-STBC) in [15] and [16], and closed-loop QO-STBC (CL QO-STBC) in a point-to-point MIMO system to asynchronous cooperative relay networks in a DF strategy, and thereby provide a framework in which the advantages of theses codes are more likely to be practically realized. Moreover, an important issue in multistage multi-source cooperative relay networks is in the effective use of the available network resources among all participation nodes, this has been studied by many researchers including [12]. The framework provided in [12] has made it possible to extend the resource allocation strategies to asynchronous cooperative communication systems.

Secondly, in [7] the author has used existing distributed STBC designs without outer coding in a synchronous cooperative relay network without any decoding complexity at the relay nodes utilizing AF type transmission. Nevertheless, full cooperative diversity and symbol-wise decoding at the destination node will not be achieved if the number of relay nodes is more than two. In this thesis, the framework in [7] has been extended to distributed A-STBC and distributed CL EO-STBC [15] with outer coding for asynchronous cooperative relay networks and solutions have been proposed to overcome the said issues.

Thirdly, considerable research in [2] has recently considered the case of imperfect synchronization among the relay nodes employing

distributed STBC without outer coding. However, a drawback of the proposed scheme has been highlighted in [26], namely that the near-optimum detector, which is used in this approach can achieve near-Alamouti simplicity, however cannot be extended to the case of more than two relay nodes. A novelty in this thesis is that it lays out a new framework for distributed CL EO-STBC with outer coding for more than two relay nodes under imperfect synchronization with and without a direct transmission (DT) connection between the source node and the destination node, and proposes a solution to overcome the drawback described above.

Finally, several closed-loop methods for STBC in [15] and [16] have been proposed to exploit full data transmission rate and full diversity gain in point-to-point MIMO systems as mentioned earlier. However, these methods require more than a single bit of feedback for each transmission block, which lead to increase feedback overhead. Therefore, in this thesis a new closed-loop method which uses only one-bit feedback in distributed STBC for cooperative relay networks over frequency flat fading channels is proposed and the system performance of it is compared to previous closed-loop methods in [15] and [16] in cooperative relay networks. Furthermore, the work in [27] is extended to achieve full cooperative diversity order of four and full data transmission rate using the combination of the proposed new one-bit feedback scheme with an orthogonal frequency division multiplexing (OFDM) type transmission to overcome the issue of timing error among the relay nodes.

The next section presents the original contribution of this research work that distinctly provides a solution to the above mentioned challenges.

1.3.1   Original Contribution

The contributions of this thesis are concerned with cooperative relay based wireless communications systems with particular emphasis on distributed STBCs under imperfect synchronization. The contributions are supported by six published conference papers, together with one published IET journal in the communications area, and another one submitted to IET journal in the communications area. These contributions can be summarized as follows:

In Chapter 3, a closed-loop method for DF cooperative relay networks with perfect synchronism are proposed using distributed CL EO-STBC and CL QO-STBC to achieve full cooperative diversity gain with full data transmission rate between the relay nodes and the destination node. Parallel interference cancellation (PIC) detection is used at the destination node to overcome the problem of imperfect synchronization among the relay nodes. The performance of the architecture is studied for frequency flat channels. The results have been published in:

- **A.M. Elazreg**, and J.A. Chambers, "Closed-Loop Extended Orthogonal Space-Time Block Coding for Four Relays Node: Under Imperfect Synchronization," IEEE Workshop on Statistical Signal Processing (SSP), pp. 545-548, Aug. 2009.

- **A.M. Elazreg**, F.M. Abdurhaman, and J.A. Chambers, "Distributed Closed-Loop Quasi Orthogonal Space-Time Block Coding for Four Relays Node: Overcoming Imperfect Synchronization," IEEE International Conference on Wireless and Mobile Computing, Networking and Communications (WiMob), pp. 320-325, Oct. 2009.

Moreover, in Chapter 3, a simple Alamouti code for an asynchronous multi-stage multi-source cooperative relay network over frequency flat fading channels is proposed, wherein full data transmission rate and full cooperative diversity STBC scheme is used at each stage. The end-to-end bit error rate (BER) performance is studied when the distributed A-STBC approach is employed at both stages. Furthermore, the problem of synchronization at the relay nodes and destination node and its AMT is solved by using the PIC detection at each stage. The results have been published in:

- **A.M. Elazreg**, S.K. Kassim, and J.A. Chambers, "Cooperative Multi-Hop Wireless Networks with Robustness," IEEE 16th Europe Wireless Conference (EW), pp. 449-453, Apr. 2010.

In Chapter 4, the cooperative strategy of distributed STBC in [6] and [7] with outer convolutive coding in the presence of asynchronism is investigated. The design of end-to-end distributed A-STBC with outer coding for two relay nodes and distributed CL EO-STBC with outer coding for four relay nodes with PIC detection to mitigate the impact of imperfect synchronization among the relay nodes for frequency flat fading channels is addressed and achieves full cooperative diversity and half data transmission rate in each stage. The results have been published respectively in:

- **A.M. Elazreg**, U. Mannai, and J.A. Chambers, "Distributed Cooperative Space-Time Coding with Parallel Interference Cancellation for Asynchronous Wireless Relay Networks," IEEE 18th International Conference on Software, Telecommunications and Computer Networks (SoftCOM), pp. 360-364, Sep. 2010.

- **A.M. Elazreg**, W.M. Qaja, and J.A. Chambers, "PIC Detector with Coded Distributed Closed-loop EO-STBC Under Imperfect Synchronization," IEEE 20th International Conference on Software, Telecommunications and Computer Networks (SoftCOM), pp. 1-5, Sep. 2012.

In Chapter 5, a novel sub-optimum and near-optimum detection scheme in DF asynchronous cooperative relay networks which utilizes distributed CL EO-STBC with convolutive coding is proposed. A sub-optimum detection scheme for four relay nodes, each of which is equipped with a single antenna and with the assumption there is a DT connection between the source node and the destination node is proposed; and a near-optimum detection scheme is designed for two relay nodes, each of which is equipped with two antennas and no DT connection is assumed between the source node and the destination node, owing to path loss between the source node and the destination node. The performance of both proposed schemes is studied for frequency flat fading channels and they are shown to be very effective to mitigate ISI at the destination node with low detection complexity as compared to PIC detection and to achieve full cooperative diversity with unity data transmission rate between the relay nodes and the destination node. Furthermore,a relay selection technique is investigated with near-optimum detection scheme. The results have been published and submitted respectively in:

- **A.M. Elazreg**, and J.A. Chambers, "Sub-Optimum Detection Scheme for Asynchronous Cooperative Relay Networks," IET Communications. vol. 5, no. 15, pp. 2250-2255, Nov 2011.

- W.M. Qaja, **A.M. Elazreg**, and J.A. Chambers, "Near-optimum Detection Scheme with Relay Selection Technique for Asynchronous Cooperative Relay Networks," submitted to IET Communications.

In Chapter 6, a new closed-loop scheme for distributed EO-STBC with one-bit feedback based on selection cyclic phase rotation for two relay nodes, each of which is equipped with two antennas, is proposed. In this scheme, only one-bit feedback is used to determine the transmission phase terms applied to the symbols from the antennas of each relay node. This is considerably lower feedback overhead than previous feedback schemes. This technique can effectively provide full cooperative diversity while satisfying full data transmission rate in each stage. Furthermore, this approach is applied to asynchronous cooperative relay networks using OFDM type transmission over frequency flat fading channels.

- **A.M. Elazreg**, and J.A. Chambers, "Distributed One-Bit Feedback Extended Orthogonal Space Time Coding Based on Selection of Cyclic Rotation for Cooperative Relay Networks," IEEE 36th International Conference Acoustics, Speech and Signal Processing (ICASSP), pp. 3340-3343 , May 2011.

The outlines of this thesis are structured and organized in the following section.

1.4   Outline of Thesis

This thesis is organized as follows: an introduction and discussion of distributed STBCs and wireless communication channel impairments and cooperative diversity are presented in Chapter 1.

In Chapter 2, a detailed literature survey is provided together with the necessary theoretical background for point-to-point MIMO systems, details of transmit and receiver diversity, followed by the introduction of STBCs and a review of uncoded and coding gain. Then the PIC detection scheme and the OFDM type transmission are included. Finally, some background material and a review of previous work in synchronous and asynchronous cooperative relay networks are given.

The core research is presented in Chapters 3, 4, 5 and 6. Chapter 3 focuses on the development of distributd CL EO-STBC and distributed CL QO-STBC with PIC detection for four relay nodes in a DF asynchronous cooperative relay networks with a DT link between the source node and the destination node. Furthermore, without the DT link between the source node and the destination node, the new relaying solution that employs distributed A-STBC with PIC detection at both the relay nodes and the destination node is presented.

Since using the DF strategy at the relay nodes results in increased decoding complexity at the relay node, Chapter 4, investigates distributed A-STBC and distributed CL EO-STBC using two-bit feedback information with outer convolutive coding and a PIC detection scheme for asynchronous two and four relay nodes, respectively; where the relay nodes generate a linear A-STBC and EO-STBC codeword at the destination node, which leads to decrease in the decoding complexity at the relay nodes. Moreover, the pairwise error probability (PEP) is

analyzed to exploit the cooperative diversity of both proposed schemes in this chapter.

Chapter 5, proposes two novel detection schemes for the DF asynchronous cooperative relay networks utilizing distributed CL EO-STBC using two-bit feedback information with outer convolutive coding. Furthermore, the relay selection technique is considered in this chapter.

In Chapter 6, a new closed-loop scheme for distributed EO-STBC using one-bit feedback is proposed based on selection cyclic phase rotation for wireless relay networks over frequency flat fading channels to achieve full data transmission rate with full cooperative diversity and reduce the amount of feedback information required from the destination node. Moreover, to mitigate the timing error between the relay nodes, a one-bit CL EO-STBC is concatenated with the OFDM type transmission. Note that only spatial diversity gain (cooperative diversity gain) is exploited.

Finally, a concluding summary and suggestions for future research are provided in Chapter 7.

Chapter 2

LITERATURE SURVEY AND BACKGROUND ON CONVENTIONAL DISTRIBUTED STBC

2.1 Introduction

In this chapter a necessary theoretical background of communication systems employing multiple transmit and receiver antennas, and a review of previous work in synchronous and asynchronous cooperative relay networks are presented. In Section 2.2 a review of multiple-input multiple-output (MIMO) communication systems is presented both from information theoretic and practical implementation perspectives. In Section 2.3 several types of orthogonal space time block codes (O-STBCs) techniques are investigated leading to the discussion on the concept of maximum likelihood (ML) decoding and pairwise error probability (PEP). The definition of uncoded and coded transmission is introduced in Section 2.4. Then the principle of parallel interference cancellation (PIC) is presented in Section 2.5. Also in Section 2.6 the

principle of the orthogonal frequency division multiplexing (OFDM) type transmission and its advantages and disadvantages are introduced. A review of synchronous cooperative relay networks and cooperative operation is provided in Section 2.7. The ability of a cooperative relay network to mimic the performance advantages of point-to-point MIMO is discussed. Finally, Section 2.8 reviews the literature relevant to asynchronous cooperative relay networks is presented. This background material is essential for the reader to appreciate the research which relates to this thesis.

2.2   Multiple Antenna Communication Systems and Diversity Techniques

2.2.1   Multiple-Input Multiple-Output Communication Systems

MIMO systems can enhance the performance of wireless communication systems to improve the capacity, data transmission rate and reliability of a wireless communication link in a fading environment without the need for additional transmission power or bandwidth [28], [29], [30], [31] and [32]. This is already happening in the IEEE 802.11n system wireless fidelity (WiFi) [33] system, IEEE 802.16e worldwide interoperability for microwave access (WiMax) system [34] and is a major focus for 4G [35] long term evolution (LTE) cellular systems [36].

MIMO channels are constructed through the use of multiple antennas at the transmitter and/or receiver in a communication system which can result in the creation of a number of independent fading channels between the transmitter and the receiver as shown in Figure 2.1. This extra degree of freedom brought about by these independent channels

is termed spatial diversity (antenna diversity). Under this model, consider a transmitter with N_T transmit antennas and a receiver with N_R receiver antennas as shown in Figure 2.1.
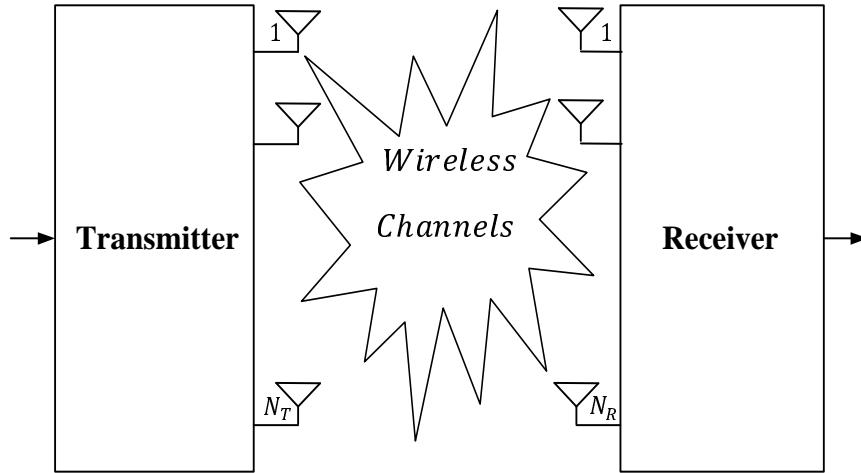
Figure 2.1. Basic structure of wireless MIMO channels with N_T transmitter and N_R receiver antennas which provides spatial diversity.

The channel can be represented by an $N_T \times N_R$ matrix $\mathbf{H}$ of channel gains and the $N_R \times 1$ received signal $\mathbf{y}$ is equal to

$$\mathbf{y} = \mathbf{Hs} + \mathbf{n} \qquad\qquad (2.2.1)$$

where $\mathbf{s}$ is an $N_T \times 1$ transmitted vector and $\mathbf{n}$ is an $N_R \times 1$ additive white circularly symmetric complex Gaussian noise vector (AWGN) [1]. If $\mathbf{H}$ is known to the receiver, it is referred to as the coherent case. The case of unknown $\mathbf{H}$ at both transmitter and receiver sides is called the non-coherent case, but is not considered in this thesis.

To obtain the best use of multiple transmit antennas depends on having channel state information (CSI) available to both the transmitter and receiver sides [32]. Moreover, coding across space and time

---

[1]A complex Gaussian random variable $\mathbf{n}$ is circularly symmetric if for any $\theta = [0, 2\pi]$, the distribution of $\mathbf{n}$ is the same as the distribution of $e^{j\theta}$ times the random variable [32].

is generally necessary to obtain the spatial diversity benefit of MIMO systems [31]. In most practical cases, the system estimates the channel at the receiver side through the exploitation of training sequences [37].

MIMO systems can potentially offer increased diversity gain, array gain and spatial multiplexing gain [38] over conventional single-input single-output (SISO) wireless communication systems. These gains are described in brief below.

- Diversity gain: Spatial diversity gain mitigates fading and is realized by providing the receiver with multiple (ideally independent) copies of the transmitted signal in space, frequency or time. With an increasing number of independent copies[2], the probability that at least one of the copies is not experiencing a deep fade increases, thereby improving the quality and reliability of reception. A MIMO channel with N_T transmit antennas and N_R receive antennas potentially offers $N_T \times N_R$ independently fading links, and hence a spatial diversity order of $N_T \times N_R$ [4] [31].Furthermore, for the MIMO channel shown in Figure 2.1 with N_T transmitter and N_R receiver antennas the diversity gain D_g in terms of error probability is given by [32]

$$D_g = - \lim_{SNR \to \infty} \frac{log(P_e)}{log(SNR)} \qquad (2.2.2)$$

where P_e denotes the probability of error of a communication system at a given signal-to-noise ratio (SNR)[3]. The diversity gain D_g can be defined as the slope of error probability curve in term

---

[2]The number of copies is often referred to as the diversity order.
[3]The SNR at the receiver is equal to the sum of the SNR on the individual transmission paths.

of received SNR on a log-log scale. In other words, the diversity gain D_g describes how fast the probability of the error decreases asymptotically with increasing SNR [39]. Hence diversity gain D_g is an important parameter of interest especially for systems that operate at high SNR.

- Array gain: Refers to the average increase in SNR at the receiver that can be obtained by the coherent combining effect of multiple antennas at the receiver or at the transmitter or at both sides. In MIMO channels, array gain exploitation requires channel knowledge at the transmitter side [31].

- Multiplexing gain: MIMO systems offer a linear increase in data rate through spatial multiplexing [40], i.e., transmitting multiple, independent data streams within the bandwidth of operation. Under suitable channel conditions, such as rich scattering in the environment, the receiver can separate the data streams. Furthermore, each data stream experiences at least the same channel quality that would be experienced by a single-input single-output system, effectively enhancing the capacity by a multiplicative factor equal to the number of streams. In general, the number of data streams that can be reliably supported by a MIMO channel equals the minimum of the number of transmit antennas and the number of receive antennas, i.e., $min\{N_T, N_R\}$. The spatial multiplexing gain increases the capacity of a wireless network. However, only diversity gain and array gain are considered in this thesis.

Coding across space and time is generally necessary to exploit the potential spatial diversity available within MIMO systems to achieve a higher reliability, higher spectral efficiency and higher performance gain. Such coding is well known [5] and [41] to provide diversity as high as the number of transmit antennas times the number of received antennas $N_T \times N_R$. In all chapters of this thesis, these coding techniques are considered for the case that the receiver side (destination node) knows the CSI and are presented in the next section.

2.3   Space Time Block Codes

Space time block codes (STBCs) are already playing an important role in wireless communication systems and are very attractive for next generation wireless communication systems. STBCs refer to coding across space by using multiple transmit antennas and receiver antennas and across time by using multiple symbol transmission periods. Their aim is to exploit the spatial diversity available to the system with linear processing at the receiver, which is preferable in practical wireless communication systems. Furthermore, STBC is easy to concatenate with a convolutional code to enhance the coding gain[4], even though the spatial diversity is achieved from STBC.

There are several types of STBCs, these include Alamouti STBC (A-STBC) [5], orthogonal STBC (O-STBC) [42], quasi orthogonal STBC (QO-STBC) [43] and extended orthogonal STBC (EO-STBC) [16].

---

[4]The effect of coding gain is similar to that of array gain.

2.3.1   Alamouti Space Time Block Coding

The Alamouti code is probably the most well-known STBC and the simplest transmit diversity scheme [5]. It is the first STBC scheme that can provide full diversity order of $2N_R$ and full data transmission D_R rate[5] for complex constellations by transmitting signals across two transmit antennas and N_R receiver antennas with different symbol transmission periods. The block diagram of an A-STBC operation with a single receiver antenna is presented in Figure 2.2.
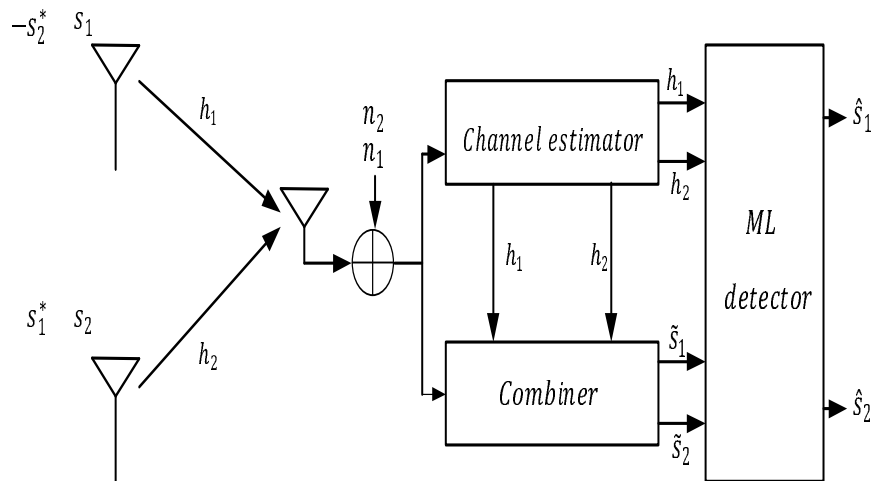
Figure 2.2. Basic structure of Alamouti's STBC for two transmit antennas and one receive antenna, depicting transmission over two symbol periods.

STBCs are represented by a code matrix, which defines what is to be broadcasted from the transmit antennas during the transmission of a block. The code matrix is dimension of $N_T \times T$, where N_T represents the number of transmitter antenna an T the number of symbol transmission periods.

---

[5]Data transmission rate D_R is defined as the ratio between the number of transmitted symbols that can be sent in one codeword and the number of symbol transmission periods used in transmitting the codeword.

As shown in Figure 2.2 for a two transmit antennas and one receive antenna scheme with a frequency flat Rayleigh fading channel, the code matrix for Alamouti's code is given by

$$\mathbf{S} = \begin{bmatrix} s_1 & s_2 \\ -s_2^* & s_1^* \end{bmatrix} \tag{2.3.1}$$

where $(.)^*$ denotes complex conjugate. It is readily apparent that the data transmission rate D_R is unity[6]. The columns of the matrix in (2.3.1) represent the number of transmitter antennas and the rows represent the number of symbol transmission periods. The orthogonality of the columns of the matrix $\mathbf{S}$ can be easily verified by calculating the inner product of the columns $\mathbf{S}_1$ and $\mathbf{S}_2$ of (2.3.1) and the inner product is given by

$$< \mathbf{S}_1, \mathbf{S}_2 >= s_1 s_2^* - s_2^* s_1 = 0 \tag{2.3.2}$$

From (2.3.2) the inner product between columns of matrix is zero, as this is the basis for it to be orthogonal. During the first symbol transmission period, the transmitter sends s_1 from the first antenna and s_2 from the second antenna, during the second symbol transmission period, it transmits $-s_2^*$ and s_1^* from the first and second antenna, respectively. Exploiting the basic feature of code matrix $\mathbf{S}$, the orthogonal columns of code matrix $\mathbf{S}$ as in (2.3.2) provide a linear decoding scheme and give rise to a simplified ML decoding scheme [44]. Therefore, the symbols in the same symbol transmission period must be synchronized and transmitted together so that they can be detected independently at the receiver. As shown in Figure 2.2 in the case of one receive an-

---

[6]Because two symbols are transmitted during two symbol transmission periods.

tenna, the received signals at this antenna, at two symbol transmission periods can be represented with a 2×1 vector $\mathbf{y}$ as follows

$$\mathbf{y} = \begin{bmatrix} y_1 \\ y_2 \end{bmatrix} = \begin{bmatrix} s_1 & s_2 \\ -s_2^* & s_1^* \end{bmatrix} \begin{bmatrix} h_1 \\ h_2 \end{bmatrix} + \begin{bmatrix} n_1 \\ n_2 \end{bmatrix} \qquad (2.3.3)$$

where y_1 and y_2 are the received signals at two symbol transmission periods, h_1 and h_2 are the fading channel coefficients from transmitter antenna one and two which are assumed to remain constant across these two symbol transmission periods, and n_1, n_2 are independent, zero-mean circularly symmetric, additive Gaussian noise terms across the channel at two symbol transmission periods, respectively. Therefore (2.3.3) can be written in matrix form as

$$\mathbf{y} = \mathbf{S}\mathbf{h} + \mathbf{n} \qquad (2.3.4)$$

where $\mathbf{y}$ represents a 2×1 column vector, $\mathbf{h}$ is a 2×1 column vector, $\mathbf{S}$ is a 2×2 vector, and $\mathbf{n}$ represent a 2×1 column vector. Alternately, without loss of generality, by conjugating the second row in (2.3.3), then the received signals can be equivalently written in the following form

$$\begin{bmatrix} y_1 \\ y_2^* \end{bmatrix} = \begin{bmatrix} h_1 & h_2 \\ h_2^* & -h_1^* \end{bmatrix} \begin{bmatrix} s_1 \\ s_2 \end{bmatrix} + \begin{bmatrix} n_1 \\ n_2^* \end{bmatrix} \qquad (2.3.5)$$

also (2.3.5) can be written in matrix form as

$$\tilde{\mathbf{y}} = \mathbf{H}\mathbf{s} + \tilde{\mathbf{n}} \qquad (2.3.6)$$

where $\tilde{\mathbf{y}}$ represents a 2×1 column vector, $\mathbf{H}$ is a 2×2 matrix of the transmission path vector, $\mathbf{s}$ is a 2×1 column vector, and $\tilde{\mathbf{n}}$ represents a 2×1 column vector. Assuming perfect channel knowledge at the

receiver, Alamouti's combiner can be performed by multiplying both sides of (2.3.6) by $\mathbf{H}^H$, where $(.)^H$ denotes Hermitian conjugate, it is a scaled unitary matrix i.e., $\mathbf{H}^H\mathbf{H} = \lambda\mathbf{I}_2$, where $\mathbf{I}_2$ is the 2×2 identity matrix and λ is the gain of the channel with $\lambda = |h_1|^2 + |h_2|^2$, which is due to fact the transmitted symbol block has an orthogonal structure as shown in (2.3.2). Therefore, the combiner combines the received signals as follows

$$\tilde{\mathbf{s}} = \mathbf{H}^H\tilde{\mathbf{y}} \qquad (2.3.7)$$

Thus

$$\tilde{s}_1 = \lambda s_1 + h_1^*\tilde{n}_1 + h_2\tilde{n}_2^*$$
$$\tilde{s}_2 = \lambda s_2 + h_2^*\tilde{n}_1 + h_1\tilde{n}_2^* \qquad (2.3.8)$$

From (2.3.8), it can be noted that the decision for $\tilde{s}_1$ depends on s_1 and the decision for $\tilde{s}_2$ depends on s_2. As shown in Figure 2.2, these combined signals are then sent to the ML decision rule used at the receiver to choose which symbol was actually transmitted by applying least squares (LS) detection as follows

$$\hat{s}_k = arg \min_{s_k \in S} |\tilde{s}_k - \lambda s_k|^2 \qquad \text{for} \qquad k \in 1, 2 \qquad (2.3.9)$$

where S is the alphabet containing M symbols of phase shift keying (PSK) and $|.|$ is a magnitude operator. It can be observed that the ML detection is a very simple decoding scheme which includes decoupling of signals transmitted from different transmitter antennas via linear processing at the receiver side. Alamouti further extended this scheme to the case of two transmit antennas and N_R receive antennas and showed that the new scheme provided a maximal diversity order of $2N_R$ [44].

The Alamouti scheme is a very popular scheme in practical application in several wireless communication systems such as WiFi, WiMax and 3G LTE [45] because it provides two important properties, simple decoding combined with maximal spatial diversity gain advantage.

2.3.2   Orthogonal Space Time Block Coding

Alamouti's code in (2.3.1) is only designed for two transmit antennas to achieve both full diversity order and full data transmission rate (unity) for complex constellations with simple decoding algorithm at the receiver. In [42] a general design of O-STBC for more than two transmit antennas is proposed, which may achieve full diversity order that is identical to the number of transmit antennas however with a data transmission rate less than unity. All O-STBC share the common unitary-type property as follows

$$\mathbf{S}^H\mathbf{S} = (\sum_{k=1}^{n_s} |s_k|^2)\mathbf{I}_{N_T} \qquad (2.3.10)$$

where n_s is the number of symbols to be transmitted within a codeword. Some other examples of O-STBC are given below [9], [42] and [46]

$$\mathbf{S} = \begin{bmatrix} s_1 & s_2 & s_3 \\ 0 & s_1^* & -s_2^* \\ -s_1^* & 0 & -s_2^* \\ s_2^* & -s_3^* & 0 \end{bmatrix} \qquad (2.3.11)$$

and

$$
\mathbf{S} = \begin{bmatrix}
s_1 & s_2 & s_3 & 0 \\
-s_2^* & s_1^* & 0 & -s_3 \\
-s_3^* & 0 & s_1^* & s_2 \\
0 & s_3^* & -s_2^* & s_1
\end{bmatrix}
\qquad (2.3.12)
$$

where the rows of the code matrix $\mathbf{S}$ represent the number of symbol transmission periods and the columns of the code matrix $\mathbf{S}$ denote the number of transmitter antennas. Therefore, the code matrix in (2.3.11) and (2.3.12) correspond to transmission of three symbols s_1, s_2, s_3 over four time symbol transmission periods, achieving full diversity order of four and data transmission rate equal to $D_R = 3/4$ for three and four transmitter antennas, respectively. The zeros in both transmission code matrices $\mathbf{S}$ represent that there is no transmitted signal from that particular antenna during that symbol transmission period. Their performance is presented and simulated in Chapter 3 for asynchronous cooperative relay networks. Furthermore, there are O-STBCs that can achieve a data transmission rate equal to $D_R = 1/2$ for any given number of transmitter antennas. For example the code matrix in (2.3.13) which denotes transmission of four symbols over eight time symbol periods from three transmit antennas, achieving full diversity order of three and 1/2 data transmission rate [42];

$$\mathbf{S} = \begin{bmatrix} s_1 & s_2 & s_3 \\ -s_3 & s_1 & -s_4 \\ -s_3 & s_4 & s_1 \\ -s_4 & -s_3 & s_2 \\ s_1^* & s_2^* & s_3^* \\ -s_2^* & s_1^* & -s_4^* \\ -s_3^* & s_4^* & s_1^* \\ -s_4^* & s_3^* & s_2^* \end{bmatrix} \qquad (2.3.13)$$

In summary, O-STBCs can provide full diversity order and have a simple decoding algorithm. However, they suffer from low data transmission rate when used with more than two transmit antennas and complex constellation, which result in bandwidth expansion. It is desirable to construct STBCs from complex orthogonal design that have higher data transmission rate when there are more than two transmit antennas. This class of codes is called QO-STBCs [43], [46], [47] and [48], which are considered in the following section.

2.3.3   Quasi Orthogonal Space Time Block Coding

QO-STBCs with full data transmission rate for four transmit antennas have been proposed in [43] and [47] to overcome the shortcoming of O-STBCs as mentioned in the previous section. Although the code matrices presented in these publication are different, it has been shown that their properties and performance are identical. Therefore, only the code matrix proposed in [43] is considered in Chapter 3 for cooperative relay networks under imperfect synchronization, which provides more insight into the behavior of QO-STBC. In this scheme, the A-STBC

defined in (2.3.1) is extended to construct the code matrix by using

two Alamouti codes $\mathbf{S}_k$ (hence with four data symbols), where $k \in 1, 3$,

$$\mathbf{S}_k = \begin{bmatrix} s_k & s_{k+1} \\ -s_{k+1}^* & s_k^* \end{bmatrix} \tag{2.3.14}$$

Therefore, the QO-STBC matrix of [43] is represented as

$$\mathbf{S} = \begin{bmatrix} \mathbf{S}_1 & \mathbf{S}_3 \\ -\mathbf{S}_3^* & \mathbf{S}_1^* \end{bmatrix} = \begin{bmatrix} s_1 & s_2 & s_3 & s_4 \\ -s_2^* & s_1^* & -s_4^* & -s_3^* \\ -s_3^* & -s_4^* & s_1^* & s_2^* \\ s_4 & -s_3 & -s_2 & s_1 \end{bmatrix} \tag{2.3.15}$$

It can be clearly observed that from the codeword in (2.3.15), the data

transmission rate D_R is unity[7], nevertheless the diversity order is re-

duced by half $(2N_R)$[8] due to coupling between the symbols in the code-

word (2.3.15) and the relaxation of the orthogonality of QO-STBC

increases the ML decoding complexity and in fact, the ML decoding of

QO-STBC is in general complex symbol pair-wise decoding[9].

To show this, the codeword in (2.3.15) is considered to be transmit-

ted through four transmit and one receive antennas in frequency flat

quasi-static fading environment with Rayleigh distributions. After tak-

ing the complex conjugate of the symbols in the second and third row

of the matrix (2.3.15), the received signal can be expressed as follows

---

[7]Because four data symbols are transmitted over four symbol transmission peri-
ods.

[8]It has proved in [42] that the maximum diversity order of $4N_R$ for unity data
transmission rate is impossible in the case of QO-STBC.

[9]The decoder of QO-STBC works with pair of transmitted symbols instead of
single symbols.

$$
\begin{bmatrix} y_1 \\ y_2^* \\ y_3^* \\ y_4 \end{bmatrix} = \underbrace{\begin{bmatrix} h_1 & h_2 & h_3 & h_4 \\ -h_2^* & h_1^* & -h_4^* & -h_3^* \\ -h_3^* & -h_4^* & h_1^* & h_2^* \\ h_4 & -h_3 & -h_2 & h_1 \end{bmatrix}}_{\mathbf{H}} \begin{bmatrix} s_1 \\ s_2 \\ s_3 \\ s_4 \end{bmatrix} + \begin{bmatrix} n_1 \\ n_2^* \\ n_3^* \\ n_4 \end{bmatrix} \qquad (2.3.16)
$$

Therefore, (2.3.16) can be expressed in vector form as follows

$$
\tilde{\mathbf{y}} = \mathbf{H}\mathbf{s} + \tilde{\mathbf{n}} \qquad\qquad (2.3.17)
$$

where $\tilde{\mathbf{y}}$ represents a 4×1 column vector of the received signal, $\mathbf{H}$ is a 4×4 matrix of the transmission path vector, and $\tilde{\mathbf{n}}$ represents a 4×1 column vector containing the zero-mean circularly symmetric complex valued Gaussian noise components. After applying the matrix $\mathbf{H}^H$ to perform matched filtering, i.e. perfect CSI is assumed to be available at the receiver, then the estimates of the transmitted symbols can be expressed as in (2.3.7). Therefore (2.3.7) can be represented in matrix form as follows

$$
\begin{bmatrix} \tilde{s}_1 \\ \tilde{s}_2 \\ \tilde{s}_3 \\ \tilde{s}_4 \end{bmatrix} = \underbrace{\begin{bmatrix} \gamma & 0 & 0 & \alpha \\ 0 & \gamma & -\alpha & 0 \\ 0 & -\alpha & \gamma & 0 \\ \alpha & 0 & 0 & \gamma \end{bmatrix}}_{\Delta} \begin{bmatrix} s_1 \\ s_2 \\ s_3 \\ s_4 \end{bmatrix} + \mathbf{H}^H \begin{bmatrix} \tilde{n}_1 \\ \tilde{n}_2^* \\ \tilde{n}_3^* \\ \tilde{n}_4 \end{bmatrix} \qquad (2.3.18)
$$

where $\Delta = \mathbf{H}^H \mathbf{H}$ is a 4×4 matrix with entries $\gamma = \sum_{k=1}^{4} |h_k|^2$ and $\alpha = \Re(h_1^* h_4 - h_2^* h_3)$, where $\Re\{.\}$ denotes the real part operator. As mentioned in the previous sections, for O-STBC, all the off-diagonal terms of Δ will be zeros as in Alamouti's scheme [5]. However, for the QO-STBC it can be seen that due to the term α (some non-zeros off

diagonal terms appear), there is a form of coupling between estimated symbols reducing the diversity gain of the code, which increases the complexity of ML decoding to a pair-wise operation.

Several interesting methods have been proposed to increase the performance of the open-loop QO-STBC by minimizing or removing this coupling factor. One methods is proposed in [17] to achieve full diversity order and full data transmission rate for four transmit antennas. A feedback method is used to orthogonalize the QO-STBC and is achieved by rotating the transmitted symbols from the third and fourth antenna with particular angles ϕ and θ while the other two antennas are kept unchanged. Therefore, full diversity order and full data transmission rate are achieved by eliminating the off-diagonal elements $\alpha = 0$, however at the expense of feedback overhead as follows

$$\begin{aligned}
\alpha &= \Re\{h_1^* h_4 e^{j\theta} - h_2^* h_3 e^{j\phi}\} \\
&= |\kappa| \cos(\theta + \angle\kappa) - |\grave{\kappa}| \cos(\phi + \angle\grave{\kappa}) \qquad (2.3.19)
\end{aligned}$$

where $\kappa = h_1^* h_4$ and $\grave{\kappa} = h_2^* h_3$. Here, $|.|$ and $\angle$ denote respectively, the absolute value and the angle operator. In order to orthogonalize the QO-STBC, it is sufficient to set the phase angle value θ to

$$\theta = \cos^{-1}\left(\frac{|\grave{\kappa}|}{|\kappa|} \cos(\phi + \angle\grave{\kappa})\right) - \angle\kappa \qquad (2.3.20)$$

provided that ϕ is in the range $\phi \in [0, 2\pi]$ if $|\grave{\kappa}| < \kappa$, or otherwise, $\phi \in [\pi - \mu - \angle\grave{\kappa}, \mu - \grave{\kappa}] \cup [-\mu - \grave{\kappa}, \pi + \mu - \grave{\kappa}]$, where μ is defined by $\mu = \arccos(\kappa/\grave{\kappa})$ [17]. However, in a practical application this may not be possible due to the very limited feedback bandwidth. It was further shown in the same work that identical performance of the sys-

tem can also be obtained by rotating the third and fourth antennas by a common phaser to keep the feedback from the receiver to transmit antenna as small as possible. It is shown in [49], [50] and [51] that QO-STBC achieves full data transmission rate by using constellation rotation and partial feedback, however all these methods either have increased decoding complexity or reduced diversity order.

In the context of this thesis only the single phase approach in [17] is presented in Chapter 3 for asynchronous cooperative relay networks, as it requires minimum feedback information while minimizing the decoding complexity of ML decoding, thereby making it symbol-wise decoding with full data transmission rate and full cooperative diversity order.

2.3.4   Extended Alamouti Space Time Block Coding

As was discussed in the last section due to data transmission rate limitations in O-STBCs, Alamouti's codeword matrix in (2.3.1) can also be used to build a new class of codes named EO-STBC, which was introduced in [16]. Slightly different from the QO-STBC, this code achieves full data transmission rate of unity[10] with symbol-wise decoding by transmitting two symbols over two symbol transmission periods through four transmitting antennas. Therefore, the codeword matrix of EO-STBC is represented as

$$\mathbf{S} = \begin{bmatrix} s_1 & s_1 & s_2 & s_2 \\ -s_2^* & -s_2^* & s_1^* & s_1^* \end{bmatrix} \tag{2.3.21}$$

---

[10]Because two data symbols are transmitted over two symbol transmission periods.

Assuming that the codeword matrix in (2.3.21) is transmitted over a four transmit and one antenna channel with each path experiencing independent flat fading with a Rayleigh distribution, the received signal at the receiver side over two symbol transmission periods after taking the complex conjugates of the symbols in the second symbol transmission period can be modelled as

$$
\begin{bmatrix} y_1 \\ y_2^* \end{bmatrix} = \begin{bmatrix} h_1 + h_2 & h_3 + h_4 \\ h_3^* + h_4^* & -h_1^* - h_2^* \end{bmatrix} \begin{bmatrix} s_1 \\ s_2 \end{bmatrix} + \begin{bmatrix} n_1 \\ n_2^* \end{bmatrix} \qquad (2.3.22)
$$

Therefore, (2.3.22) can be rewritten in vector form as follows

$$
\tilde{\mathbf{y}} = \mathbf{H}\mathbf{s} + \tilde{\mathbf{n}} \qquad (2.3.23)
$$

where $\tilde{\mathbf{y}}$ denotes a 2×1 column vector of the received signal, $\mathbf{H}$ is a 2×2 matrix of the channel gain vector representing the paths between the transmit antennas and receive antenna, and $\tilde{\mathbf{n}}$ represents a 2×1 column vector containing the additive Gaussian noise term at each receive antenna. Applying the matrix $\mathbf{H}^H$ as in (2.3.7) to perform matched filtering at the receiver, the Grammian matrix can be obtained as follows

$$
\Delta = \mathbf{H}^H\mathbf{H} = \begin{bmatrix} \lambda_c + \lambda_f & 0 \\ 0 & \lambda_c + \lambda_f \end{bmatrix} \qquad (2.3.24)
$$

where $\lambda_c = \sum_{k=1}^{4} |h_k|^2$ is the conventional channel gain for four transmit antennas and $\lambda_f = 2\Re(h_1 h_2^* + h_3 h_4^*)$ can be interpreted as the channel dependent interference parameter. From (2.3.24) it can be noted that the Grammian matrix Δ of the EO-STBC is orthogonal (unlike

that of QO-STBCs), which indicates that the codeword in (2.3.21) can be decoded a simpler receiver decoding with linear detected signal as follows

$$
\begin{bmatrix} \tilde{s_1} \\ \tilde{s_2} \end{bmatrix} = \Delta \begin{bmatrix} s_1 \\ s_2 \end{bmatrix} + \mathbf{H}^H \begin{bmatrix} \tilde{n}_1 \\ \tilde{n}_2^* \end{bmatrix} \tag{2.3.25}
$$

Then, the ML decision is used at the receiver to estimate which symbol was actually transmitted by applying LS detection as in (2.3.9). However, although the decoding complexity is low, λ_f in (2.3.24) may be negative, which leads to some diversity loss [15] and [16]. In order to overcome this issue and maximize the diversity order achieved by the codeword in (2.3.21), several feedback methods are utilized to ensure the channel dependent interference λ_f in (2.3.24) is positive during the whole transmission to achieve full data transmission rate and full diversity order with the array gain.

In [15] and [16] a closed-loop EO-STBC scheme for four transmit and one receive antenna is proposed, where phase rotation is applied to rotate the phases of the symbols for certain transmit antennas based on CSI feedback from the receive antenna. The analysis of these two closed-loop methods are presented in Appendix A, respectively.

Therefore, in the context of this thesis both proposed schemes are adopted for application in an asynchronous cooperative wireless relay network with relay nodes deploying the distributed EO-STBC scheme with and without outer coding and a new one-bit feedback EO-STBC is proposed in Chapter 6.

2.3.5   Maximum Likelihood and Pairwise Error Probability

As mentioned in the previous sections, all STBC are designed for quasi-static channels, where the channels are constant over a block of T symbols periods and the channels are unknown at the transmitter, while the receiver has knowledge of the channel matrix $\mathbf{H}$. Under ML detection it can be shown using similar techniques as in (2.3.9), giving received matrix $\mathbf{Y}$, the ML estimate of the matrix $\hat{\mathbf{S}}$ can be represented as follows [4]

$$\hat{\mathbf{S}} = arg \min_{\mathbf{S} \in \chi^{N_T \times T}} ||\mathbf{Y} - \mathbf{HS}||_F^2 = arg \min_{\mathbf{S} \in \chi^{N_T \times T}} \sum_{k=1}^{T} ||\mathbf{y}_k - \mathbf{Hs}_k||^2 \quad (2.3.26)$$

where $||\mathbf{A}||_F$ is the Frobenius norm[11] of matrix $\mathbf{A}$ and minimization is taken over all possible space time input matrix $\chi^{M_T \times T}$. The pairwise error probability (PEP) for mistaking a transmit matrix $\mathbf{S}$ for another matrix $\hat{\mathbf{S}}$, represented as $P_e(\hat{\mathbf{S}} \rightarrow \mathbf{S})$, depends only on the distance between the two matrices after transmission through channel matrix $\mathbf{H}$ and noise power of $\mathbf{N}$ equal to σ^2 can be represented as follows

$$P_e(\hat{\mathbf{S}} \rightarrow \mathbf{S}) = Q\left(\sqrt{\frac{||\mathbf{HS_s}||_F^2}{2\sigma^2}}\right) \quad (2.3.27)$$

where $Q(.)$ represents the Gaussian Q function and $\mathbf{S_s} = \mathbf{S} - \hat{\mathbf{S}}$ represents the different between these two matrice. By applying the Chernoff bound to (2.3.27), an upper bound of (2.3.27) becomes

$$P_e(\hat{\mathbf{S}} \rightarrow \mathbf{S}) \leq \exp\left[-\frac{||\mathbf{HS_s}||_F^2}{4\sigma^2}\right] \quad (2.3.28)$$

---

[11]The Frobenius norm of a matrix $\mathbf{A}$ is defined to be $||\mathbf{A}|| = \sqrt{\sum_{ij} |\mathbf{a}_{ij}|^2}$.

Let $\mathbf{h}_k$ denote kth row of $\mathbf{H}$, $k \in 1, ..., N_R$. Then

$$||\mathbf{HS_s}||_F^2 = \sum_{k=1}^{N_R} \mathbf{h}_k \mathbf{S_s} \mathbf{S_s}^H \mathbf{h}_k^H \qquad (2.3.29)$$

Substituting (2.3.29) into (2.3.28) and taking statistical expectation relative to all possible channel realizations yields [4]

$$P_e(\mathbf{S} \rightarrow \hat{\mathbf{S}}) \leq \left(det \left[\mathbf{I}_{N_T N_R} + \frac{\mathbf{E}[\mathbf{S_s}^H \mathbf{H}^H \mathbf{H} \mathbf{S_s}]}{4\sigma^2} \right] \right)^{-1} \qquad (2.3.30)$$

Assuming that the channel matrix $\mathbf{H}$ has elements which are uncorrelated Gaussian random variables with zero-mean and unit-variance, then (2.3.30) becomes

$$P_e(\mathbf{S} \rightarrow \hat{\mathbf{S}}) \leq \left(\frac{1}{\det[\mathbf{I}_{N_T} + 0.25\rho\mathbf{B}]} \right)^{N_R} \qquad (2.3.31)$$

where $\mathbf{I}_{N_T}$ is the $N_T \times N_T$ identity matrix and $\mathbf{B} = (1/P)\mathbf{S_s}\mathbf{S_s}^H$, where P denote the signal power. This can be simplified to

$$P_e(\mathbf{S} \rightarrow \hat{\mathbf{S}}) \leq \prod_{k=1}^{R_\mathbf{B}} \left(\frac{1}{1 + 0.25\rho\lambda_k(\mathbf{B})} \right)^{N_R} \qquad (2.3.32)$$

where $\rho = P/\sigma^2$ is the SNR per input symbol, $\lambda_k(\mathbf{B})$ is the kth nonzero eigenvalue of $\mathbf{B}$, $k \in 1, ...R_\mathbf{B}$, where $R_\mathbf{B}$ is the rank of $\mathbf{B}$. In the case of high SNR i.e., for $\rho \gg 1$, this can be simplified to

$$P_e(\mathbf{S} \rightarrow \hat{\mathbf{S}}) \leq \left(\prod_{k=1}^{R_\mathbf{B}} \lambda_k(\mathbf{B}) \right)^{-N_R} \left(\frac{1}{4}\rho \right)^{-R_\mathbf{B} N_R} \qquad (2.3.33)$$

The result of PEP in (2.3.33) indicates that the probability of error decreases as ρ^{-D_g} for $D_g = R_\mathbf{B} N_R$, where $R_\mathbf{B} N_R$ is the diversity gain of the STBC [4]. Therefore, the PEP in (2.3.33) gives rise to the main criteria for design of STBC, described in Section 2.3.

2.4   Uncoded Versus Coded Transmission

2.4.1   Coding Gain

Coding gain is the measure in the difference between the SNR levels between the uncoded system and coded system required to reach the same bit error rate (BER) levels. Therefore, when SNR is in dB the coding gain is defined as [52]

$$C_g = (SNR)_{uncoded} - (SNR)_{coded} \qquad (2.4.1)$$

This also can reduce error rate to improve system performance, but, compared with diversity gain, the nature of coding gain is different.
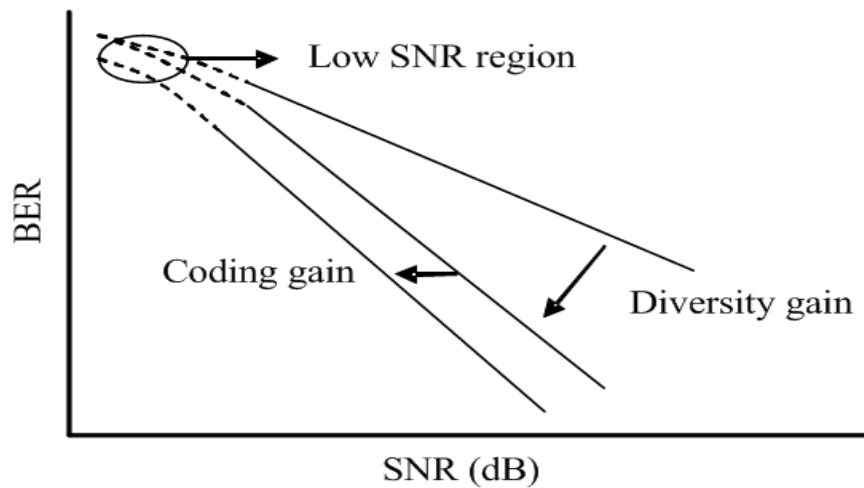
Figure 2.3. The difference in the effects of coding gain and diversity gain on bit error rate [1].

Diversity gain attests itself by rising the magnitude of the slope of the BER curve, whereas coding gain generally just shifts the error rate curve to the left [31] as shown in Figure 2.3 and as mentioned in Section 2.2.

2.4.2   Convolution Coding

Convolutional codes are used extensively in numerous applications in order to achieve reliable data transfer, i.e. third generation (3G) cellular communication system [53] and [54]. A convolution code generates coded symbols by passing the information bits through a linear finite-state shift register as shown in Figure 2.4. The shift register consists of K stages with I_{Bits} bits per stage. There are O_{Bits} binary addition operations with input taken from all K stages: these operators produce a codeword of length O_{Bits} for each I_{Bits} bit input sequence. Moreover, the rate of the code C_R is I_{Bits}/O_{Bits}, because the binary input data is shifted into each stage of the shift register I_{Bits} bits at a time, and each of these shifts produces a coded sequence of length O_{Bits}.
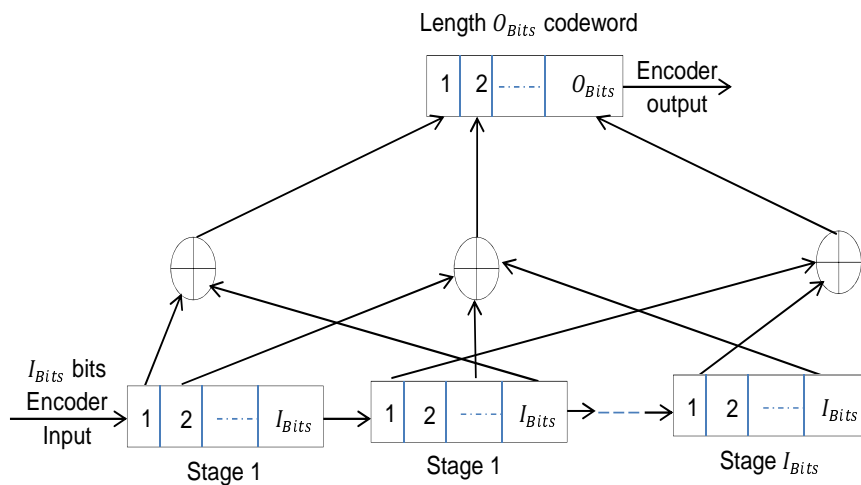
Figure 2.4.   Basic structure of a simple binary linear convolutional encoder.

The number of shift register stages K is called the constraint length. In Chapters 4 and 5, a half rate[12] ($O_{Bits} = 2, I_{Bits} = 1, K = 3$) convolution coding will be used to improve the BER performance. A well

---

[12]For every binary digit that enters the encoder, two code digits are output, hence code rate $C_R = 1/2$.

known scheme can be employed to decode the convolution coding, which is the Viterbi algorithm, full details of which can be found in [1], [53] and [54].

2.5   The Parallel Interference Cancellation Detection

The PIC detector is a popular method for interference cancellation and was presented in [55] and a block diagram of a multistage PIC detector is shown in Figure 2.5. The PIC detector is based on a technique that employs multiple iterations in detecting the desired information bits and cancelling the ISI at the receiver side. As shown in Figure 2.5, the PIC detector at the receiver uses a conventional blank of matched filter at the front end followed by two stages of cancellation.
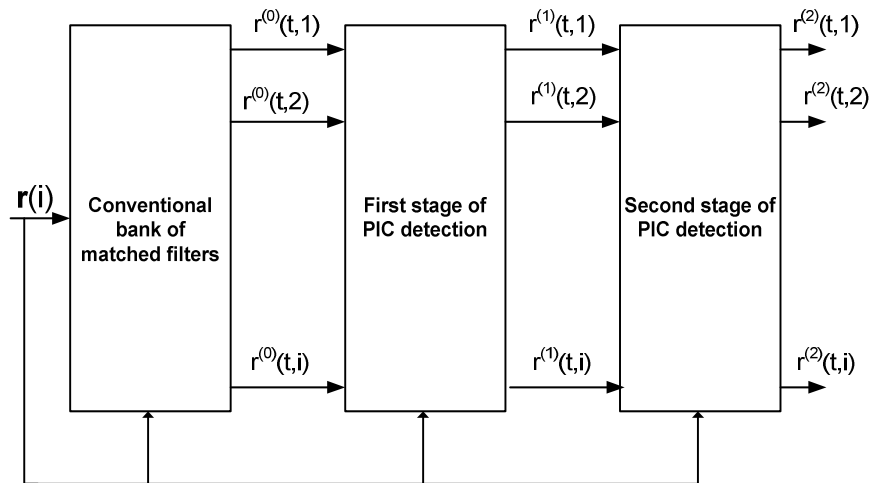
Figure 2.5. Basic structure of parallel interference cancelation (PIC) scheme that uses a two cancellation stage.

In the first and the second stages , the reconstruction, subtraction and re-estimation operations are repeated using the outputs of the previous stage as the information inputs. In this way, a new set of better information bit estimates will be generated at the output of the next stage. multiple cancellation stages maybe used to yield improved

estimates of the received signals at the destination node for further cancellation. In general, the PIC algorithm can be represented as follows

- Initialization

- Set the iteration number $q = 0$

- Remove ISI from the $\mathbf{r}^{(0)}(i)$

- Set the iteration number $q = 1, 2, ..., n$

- Subtract more ISI from the received signals $\mathbf{r}^{(q)}(i)$ using the previous estimated signals

- Repeat the process from point 4 until $q = n$

One problem with the multistage PIC detector is that it cannot guarantee a performance improvement with more stages; when a wrong estimation of the received signal is applied, degradation is introduced. Furthermore, increasing the number of stages of the multistage PIC detector also makes the system computationally more intensive as a greater number of operations have to be preformed. Therefore, in Chapter 3 and 4, the PIC detection scheme is adapted for application in an asynchronous cooperative relay network with the relay nodes utilizing the distributed closed-loop STBC.

2.6   Orthogonal Frequency Division Multiplexing

Recently, wireless communications has evolved towards broadband systems to achieve high data transmission rate and better transmission quality. OFDM is an emerging technology for high data transmission rates, with increased robustness to shadowing and multipath fading,

through insertion of the guard period G_p and using digital signal processing. OFDM modulation for wireless communication networks is designed to more fully utilize existing bandwidth, and can be very effective against the frequency selective fading and narrowband interference [18] [56]. Due to these characteristics of OFDM, it is used widely in many applications such as digital audio broadcasting and the IEEE 802.11a/g WLAN standard, and is the preferred candidate for next generation mobile systems, such as 4G LTE.

A review of OFDM is given in the following sections and it is used in Chapter 6 within a distributed closed-loop EO-STBC-OFDM for asynchronous cooperative relay networks.

2.6.1   OFDM principle

A typical baseband OFDM transmission system is shown in Figure 2.6, which can be divided into three main parts. The first part is the transmitter, the second the channel and finally the receiver. To generate OFDM successfully the relationship between all the subcarriers must be carefully controlled to maintain the orthogonality of the subcarriers [57]. Orthogonality is achieved by making the peak of each subcarrier signal coincide with the nulls of other subcarrier signals. For this reason, OFDM is generated by firstly choosing the frequency spectrum required, based on the input data, and the modulation scheme used can, for example, be binary phase shift keying (BPSK), quadrature phase shift keying (QPSK) and quadrature amplitude modulation (QAM).
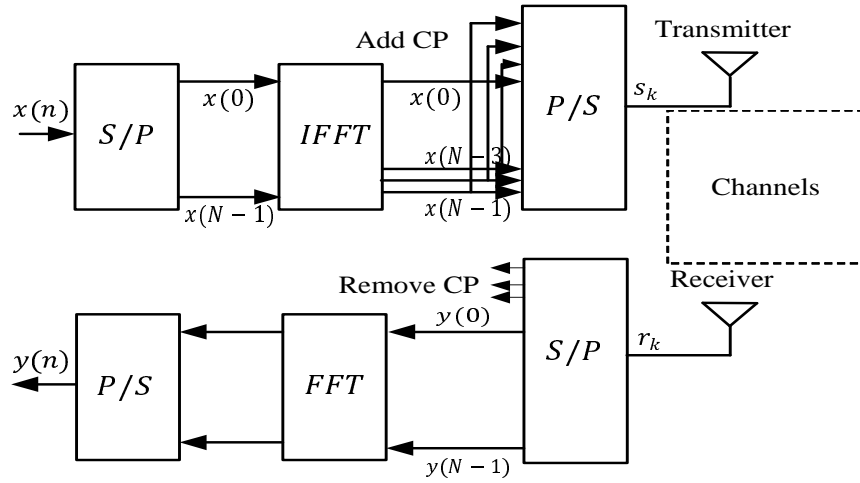
Figure 2.6. Basic diagram of a baseband OFDM transmitter and receiver, exploiting the FFT and serial to parallel and parallel to serial converters.

Then the frequency spectrum is converted into the time domain signal by applying an inverse fast Fourier transform (IFFT). The IFFT is useful for OFDM because it generates samples of a subcarrier with frequency components satisfying the orthogonality condition, assuming perfect synchronization. In addition to that the FFT algorithm provides an efficient way to implement the DFT and the IDFT. "It reduces the number of complex multiplications from of the order of N^2 to $N/2 \log_2 N$ for an N-point DFT or IDFT, hence, with the help of the FFT algorithm, the implementation of OFDM is very simple" [18]. The IFFT calculated from the subcarrier $S(k)$ can be represented as follows

$$s(m) = \frac{1}{\sqrt{N}} \sum_{k=0}^{N-1} S(k)e^{j2\pi km/N} \qquad \text{for} \qquad m \in 0, ..., N-1 \quad (2.6.1)$$

where N denotes the duration of one OFDM symbol, k is the frequency index for the IFFT and m is the index for the samples of $s(m)$. That means, the IFFT converts the discrete frequency domain signal into

a discrete time domain signal which maintains the orthogonality. On the other hand, in the receiver side the FFT converts the time domain signal into the frequency domain to recover the information that was originally sent. However, multipath interference and timing errors are a important phenomena in wireless communication systems. Different versions of the transmitted signals arrive at the receiver side by different paths showing different time delays. Such delayed signals are the result of refections and refractions from objects, which are surrounding the receiver as mentioned in Section 1.2.

This makes the correct synchronization to all signals impossible. To avoid this phenomenon of intersymbol interference (ISI) completely, a cyclic prefix (CP) is introduced, with the constraint that the CP duration at least matches the maximum delay spread of the channel. The time domain duration of the OFDM symbol is extended by the CP, which adds a copy of the last part of the OFDM symbol to the front to create a guard period as shown in Figure 2.7. To avoid destroying the orthogonality the length of the CP should be longer than the delay spread. At the receiver side this extension of the guard period is removed.
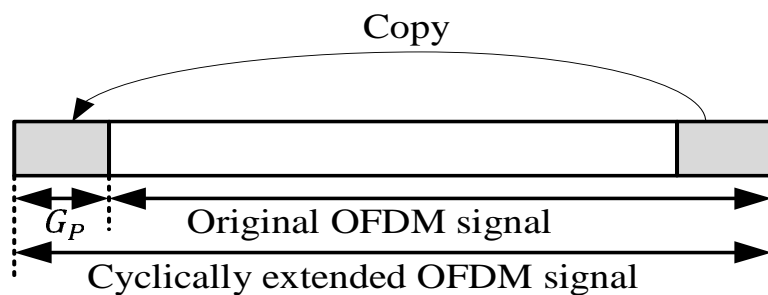
Figure 2.7. Illustration of cyclic prefix (CP) concept to the original OFDM signal.

As long as the length of the guard period is greater than the channel delay spread, then all the time delays of the reflections are removed and the orthogonality still exists. The next step is to convert the received signal from the time domain to the frequency domain by applying the FFT to recover the transmitted signals.

2.6.2   OFDM Advantage and Disadvantage

As discussed earlier, OFDM is commonly implemented in many emerging wireless communication systems, because it provides several advantages over a traditional single carrier modulation approach to wireless communication channels as follows

- OFDM has very high frequency spectrum efficiency.

- By dividing the channel into narrowband flat fading sub channels, OFDM is more resistant to frequency selective fading, which greatly simplifies the structure of the receiver complexity.

- OFDM is computationally efficient by using simple FFT techniques to implement the modulation and demodulation functions.

- The OFDM signal has robustness in the multipath propagation environment and is more tolerant to delay spread[13].

However, OFDM also has some shortcomings as follows

- Relatively higher peak-to-average power (PAPR) compared to a signal carrier system, which tends to reduce the power efficiency of the radio frequency (RF) amplifier.

---

[13]OFDM is robust against multipath effect, first because of using many narrowband subcarriers instead of one wide-band carrier for transmission and secondly because of the inserting of a cyclic prefix.

- OFDM is sensitive to frequency offsets, timing errors and phase noise.

More detailed discussion of these points can be found in [18] and [58].

2.7   Synchronous Cooperative Relay Networks

As mentioned earlier in Section 2.2 , a MIMO system can be used to mitigate the fading phenomena in wireless communication and increase the data transmission rate of the system [4]. It is affordable to have multiple antennas at the base station however impractical to equip the small mobile node with multiple antennas due to space constraints of the mobile node[14], power limitation and hardware complexity of the mobile node [59].

In order to overcome these limitations, a new communication scheme, so-called cooperative communications (also known as cooperative diversity or user cooperation), has been proposed in order to reap the benefits of MIMO communications systems in a wireless scenario with single antenna network nodes cooperatively transmitting and receiveing by forming a virtual antenna array (VAA) [12]. Since cooperative communications is a recent paradigm for wireless relay networks, it has become a very active area of communications and networking research with promising developments, where the signals can be relayed from the source node to the destination node through half-duplex relay nodes.

The basic idea behind cooperative communications was proposed in [60] wherein the relay channel was introduced and then investigated extensively in [61] to provide a number of relaying strategies to find

---

[14]If the antennas are located close to each other, the channel fades may have some correlation which reduces the achievable diversity.

achievable regions and provide upper bounds upon the capacity of a general relay channel in [60], a more detailed description of which can be found in [62].

The recent surge of interest in cooperative communications is represented by [10], [11], [19], [12], [63] and [64]. In [19] and [63], the concept and the potential benefits of cooperative communications have been introduced for a two user code division multiple access (CDMA) cellular network, where both users are active and orthogonal codes are used to avoid multiple access interference. Likewise, cooperative communication strategies have been analyzed in terms of their performance outage behavior in [10]. It has been shown that the outage gains and the cooperative diversity gain are proportion to the number of transmitting relay nodes. These benefits are achieved by deploying the relaying strategies rather than a direct link. The two main relaying strategies studied in [10] are amplify-and-forward (AF) and decode-and-forward (DF), which can be applied at the relay node to process the received signals from the source node and then forward them to the destination node. The key difference between AF and DF strategies is the amount of processing at the relay node. In an AF strategy, the relay node simply receives the signals from the source node, amplifies them and then re-transmit them to the destination node. Therefore, AF does not require sophisticated processing at the relay node, which implies low-complexity relay transceivers and lower power consumption. However, in the DF strategy the relay node decodes its received signals from the source node to eliminate the effects of noise and interference before re-transmitting them to the destination node. Therefore, the AF strategy has the advantage of simple implementation in a practical scenario as

compared to the DF strategy although its noise immunity is lower.

In [12], the ideas in [10] have been extended to a more refined distributed MIMO multi-stage cooperative communications system, where cooperation between spatial distributed nodes not only takes place at the relaying stage, but also at the source node and the destination node. This will achieve the maximum cooperative diversity gain, nevertheless, at the expense of reducing the data rate[15]. Furthermore, in [12] a significant discussion on the fractional power allocation at every stage in the network for different cooperative communications scenarios mentioned. Another technique known as coded cooperation has been introduced in [64] to achieve cooperative diversity and further analysis for coded cooperation can be found in [65].

A different approach, which can obtain the maximum spatial diversity gain, without suffering from the rate loss of repetition coding consists of combining the idea of cooperation with STBC, resulting in what is known as a distributed STBC. The case of distributed STBC has been first applied to wireless relay networks under the framework of cooperative communications in [11] and [8], in order to improve the bandwidth efficiency without losing any spatial diversity order (cooperative diversity) available in cooperative networks. As mentioned earlier in this section, this approach will involve a two phase protocol; in the first phase the relay nodes receive the signals from the source node and then in the second phase the relay nodes linearly process the signals received from the source node and forward them to the destination node such that the signals at the destination node appear as a STBC [5].

One such method can be found in [12], where orthogonal STBCs

---

[15]If the number of relaying stages increases, the total data transmission rate D_R will decrease.

are deployed in distributed fashion for a VAA multi-stage network. Likewise, in [66] and [67] a simple Alamouti design [5] is introduced into cooperative relay networks because of its symbol-wise ML detector which achieves high diversity gain to combat channel impairments in wireless communications environments.

In [6] and [7] a distributed linear dispersion coding scheme for a wireless relay network in which every node is equipped with a single antenna has been proposed, where the signals are sent by the relay nodes in the second phase as a linear function[16] of its received information. It has been shown that by cooperating distributively, the relay nodes generate a linear STBC codeword at the destination node and a full cooperative diversity gain of a multiple antenna system[17] can be obtained, where the relay nodes are assumed to be synchronized at the destination node and also the destination node has full knowledge of the fading channels from the source node to the destination node.

Furthermore, distributed linear dispersion STBC [68] among the relay nodes can be found in [21] and [69]. However, in [70], the idea of distributed STBC has been extended to wireless cooperative relay networks, in which every node has multiple antennas and the achievable cooperative diversity has been analyzed[18]. After these works, [7] has attempted to exploit the distributed coding techniques using orthogonal designs [5] and quasi-orthogonal designs [43] with more cooperating nodes, which leads to reliable communications in wireless relay networks. This approach provides many advantages such as maximum

---

[16]No decoding or demodulation is needed at relay nodes.

[17]Cooperative diversity gain equal to $R \times 1$, where R denotes the number of transmitting relay node antennas.

[18]Cooperative diversity equal to $min\{M, N\}R$ if $M \neq N$ and equal to MR if $M = N$, where M denotes antennas at the source node, N denotes antennas at the destination node and R represent antennas at all the relay nodes.

cooperative diversity, low ML decoding complexity and linear encoding of the information symbols. Regrettably, the maximum data transmission rate of orthogonal design [5] can not be achieved for more than two relay nodes [71] and the linear decoding complexity is no longer available. On the other hand, a quasi-orthogonal design [43] is only applicable to four relay nodes and its decoding complexity is higher than that of an orthogonal design. However, by applying feedback in the form of phase rotations [15], [16] and [17] at the relay nodes, it is possible to extract full data transmission rate at each hop and full cooperative diversity in proportion to the transmitting relay nodes from the orthogonal design [5] for more than two relay nodes and quasi-orthogonal design [43] for four relay nodes with simple linear decoding at the destination node. These approaches are presented in this thesis with the assumption of imperfect synchronization among the relay nodes and other distinctions are outlined in the introductory parts of Chapter 3 and 4.

Most cooperative relay communication scenarios investigated so far are built upon the assumption that all nodes are equipped with a single half-duplex antenna, more recent work has however exploited the benefits of multiple antennas at the relay nodes. It is forward to have a small number of multiple antenna arrays within the infrastructure of fixed relay networks [72]. This model for the cooperative relay node is considered in Chapters 5 and 6.

The next section presents a review of research works that led to the deployments of STBCs in the context of asynchronous cooperative relay networks.

2.8   Asynchronous Cooperative Relay Networks

As mentioned in the previous section to reap the benefits of cooperative communications, it is necessary for the network to operate synchronously . However, perfect synchronization in cooperative relay networks is highly unlikely in practice [20]. This lack of synchronization results in ISI between the received signals from the relay nodes at the destination node, and also when the relay nodes use STBC to forward the received signals from the source node to the destination node, the code structure at the destination node is not orthogonal thereby preventing the transmitted signals from being successfully detected at the destination node with the normal STBC decoder. Therefore, the impact of imperfect synchronization between the relay nodes is one of the most critical and challenging issues when designing a space time cooperative relay network. Recently, there have been studies for asynchronous cooperative systems based on STCs to exploit cooperative diversity.

In [25] and [73], a DF two-phase protocol with a distributed space time trellis codes (STTCs) that achieves full cooperative diversity and coding gain without the synchronization assumption between relay nodes has been proposed. However, the decoding complexity becomes high when the number of relay nodes is not small, this is because the memory size of the corresponding STTCs grows exponentially in term of the number of relay nodes. To overcome this problem, in [23] the systematic construction of such a trellis code with minimum memory size for any number of relay nodes is developed to achieve full cooperative diversity in asynchronous cooperative communications.

Furthermore, there has been limited work reported in the literature addressing distributed STBC regarding the mitigation of interference

at the symbol level in [73] and [22], where an equalization technique is employed at the destination node to reduce the effect of imperfect synchronization among the relay nodes at the destination node, however, this leads to increased receiver complexity at the destination node. While in [74], [75], [76] and [26], the distributed STBC with PIC detection scheme for the case of two and four relay nodes is proposed and shown to be a very effective approach to mitigate the impact of imperfect synchronization at the destination node. Nevertheless, the schemes in [74] and [75] are limited by the number of relay nodes and can only achieve the diversity order between the relay nodes and the destination of two, also the work in [76] and [26] is limited since complex O-STBC with data transmission rate $D_R = 3/4$[19] is used between the relay nodes and the destination node.

To achieve both full cooperative diversity and full data transmission rate for four relay nodes under the assumption of imperfect synchronization, distributed closed-loop EO-STBC [77] and closed-loop QO-STBC [78] with PIC detection scheme as in Section 2.5 are proposed. All these proposed schemes have the potential of delivering cooperative diversity order of cooperating relay nodes using a DF protocol, which leads to complexity increase at the relay nodes.

To avoid this complexity, the proposed scheme in [6] and [7] is extended to the case of imperfect synchronization in [79] and [80], where the signals broadcast by all relay nodes are designed as linear functions of their received information, therefore, no decoding operation at the relay nodes is required as compared to the DF scheme. However, all distributed STBCs based on the PIC detection scheme mentioned above

---

[19]Because three symbols transmit from the relay nodes over four time symbol transmission periods.

have the disadvantage that their computational complexity is dependent upon the number of PIC detection iterations. It has been shown in simulation results that the PIC detection scheme is very effective in mitigating synchronization error and normally two or three iterations will deliver most of the performance gain.

While in [2], an equalizer has been proposed to combat the interference components caused by timing misalignment in a decision feedback manner, and then a symbol-by-symbol ML detection is implemented. Nevertheless, the low computational complexity of the Alamouti code remains but this only applies in the case of two cooperative relay nodes and cannot be extended to more than two cooperative relay nodes. Recently, two novel detection scheme for more than two relay nodes under imperfect synchronization are proposed [3] and [80] to overcome the drawback in [2].

All the above works have been performed under the assumption that the wireless transmission channels are frequency flat fading channels. In [27] and [81] a distributed A-STBC transmission scheme based on OFDM for asynchronous AF protocol is proposed to cancel the timing error among the relay nodes and achieve asynchronous cooperative diversity, where the relay nodes only need to perform a few very simple operations, time reversion and complex conjugation, and the destination node has the Alamouti code structure. However, this proposed scheme is only valid for the case of two relay nodes.

The idea in [27] is extended to the case of any number of relay nodes in [82]. Unfortunately, full cooperative diversity and the data transmission rate[20] decreases as the number of transmitting relay nodes increase,

---

[20]Since a half-duplex protocol is used, the data transmission rate of two-hop relay network is actually unity for each hop.

in other word O-STBC generated from complex constellations for more than two relay nodes do not exist [7]. As mentioned earlier above in this literature survey to achieve both full cooperative diversity and full data transmission rate in each hop for more than two relay nodes using O-STBC, feedback schemes are required. Therefore, in [83] a new one-bit feedback based on selection cyclic phase rotation is proposed along with the OFDM type transmission for asynchronous relay networks over frequency flat channels to exploit full data transmission rate and full cooperative diversity, also outperforms the previous closed-loop methods [15] and [16] in distributed manner .

2.9 Chapter Summary

This chapter has reviewed a research work that has been undertaken prior to the work presented in this thesis. The first section of this chapter focussed on the achievements made in the area of MIMO communications in information theoretic terms to the various developments in STBC and then the application of these background works to cooperative communication under both cases of perfect synchronization and imperfect synchronization. In MIMO, the STBCs used in order to exploit the transmit diversity offered by multiple antennas are introduced, leading to the A-STBC, O-STBCs, QO-STBCs and EO-STBCs. The performance advantages of each were highlighted and also the principle of the OFDM technique with its advantages and disadvantages were highlighted.

The chapter then proceeded to discuss earlier attempts to expand wireless network coverage with the use of cooperative relay networks. Various theoretical and practical issues were also reviewed. Motivated

by the difficulty in deploying multiple antennas in mobile terminals, it was then highlighted that researchers have focused their attention into ways of using multiple single antenna elements to create a MIMO channel through the use of cooperation, this was later extended to cooperative relay networks and the advantages of distributed STBCs was also exploited. Furthermore, the problem of synchronization among the relay nodes was addressed, which is the main research focus in this thesis.

Chapter 3

DISTRIBUTED STBC FOR ASYNCHRONOUS COOPERATIVE RELAY NETWORKS

In this chapter, distributed closed-loop space time block coding (CL STBC) strategies for multiple relay nodes in (decode-and-forward) DF asynchronous cooperative relay networks with and without a direct transmission (DT) connection between the source node and the destination node are considered. These techniques can effectively harness available cooperative diversity gain between the relay nodes and the destination node while addressing the important practical issue of synchronization among the relay nodes.

3.1 Introduction

Synchronization in a wireless relay network is very important, it allows for successful communication between nodes within the wireless cooperative relay network. However, timing errors between the relay

nodes is one of the most critical and challenging issues when designing a space time cooperative relay network. Mitigation of interference at the symbol level has been considered in [20], [75] and [76] to reduce the effect of timing errors among the relay nodes at the destination node and deliver good system performance.

In this chapter, distributed STBCs with closed-loop strategies for multiple relay nodes in a DF cooperative relay network with a DT link between the source node and the destination node. These techniques effectively harness available cooperative diversity gain between the relay nodes and the destination node while addressing the important practical issue of synchronization among the relay nodes. Distributed closed-loop quasi orthogonal STBC (CL QO-STBC) and closed-loop extended orthogonal STBC (CL EO-STBC) with parallel interference cancellation (PIC) detection schemes are proposed under imperfect synchronization in [77] and [78].It is shown that the full data transmission rate and full cooperative diversity gain, which increases in proportion to the number of transmitting relay nodes between the relay nodes and the destination node, are exploited in these two schemes with simple detection, contrary to what was previously achieved in [76].

Moreover, a new relaying solution that employs distributed Alamouti (A-STBC) with PIC detection at both the relay nodes and the destination node without the DT link between the source node and the destination node is proposed in [84], thereby promising to deliver cooperative diversity order close to the number of cooperating relay nodes at the relaying stage and with full data transmission rate in each hop. For comparison purpose, the end-to-end performance of the proposed scheme is shown to outperform previous work in [75] with a DT link.

This chapter is structured as follows: Section 3.2 presents the general structure of the system model of cooperative relay network and defines distributed STBCs with imperfect synchronization for closed-loop QO-STBC and closed-loop EO-STBC are presented in Section 3.3. To mitigate the interference at the symbol level at the destination node, the general full scheme of PIC detection is introduced in Section 3.4. The comparison of the proposed closed-loop QO-STBC and EO-STBC schemes with other schemes [75] and [76] is presented in Section 3.5. In Section 3.6 the multiple level cooperation among all nodes of each hop without DT with the PIC detection scheme under imperfect synchronization is described. Simulation results for the end-to-end performance of the proposed multi-hop cooperative multiple-input multiple-output (MIMO) technique are shown in Section 3.7. Finally, the chapter is concluded with a summary.

3.2   The System Model

A general two-hop cooperative relay network with one source node and destination node communicating via cooperating multiple parallel relay nodes R is depicted in Figure 3.1. It is assumed that there is direct link between the source node and the destination node and every participating node in the network communicates using a single transmit antenna and receive antenna configuration and operates in half-duplex mode, thereby generating virtual multiple antenna. The narrowband flat fading broadcasting channel gain between the source node and each relay node is represented as $h_{sr,k}$, the relaying channel gain from each relay node to the destination node is represented as h_k, where $k \in 1, 2, ..., R$, and the channel between the source node and the destination node is

represented as h_{sd}. It is assumed that all random channel parameters[1] $h_{sr,k}$, h_k and h_{sd} are spatially uncorrelated and they are assumed to be zero mean circularly symmetrical complex Gaussian random variable with unity variance.
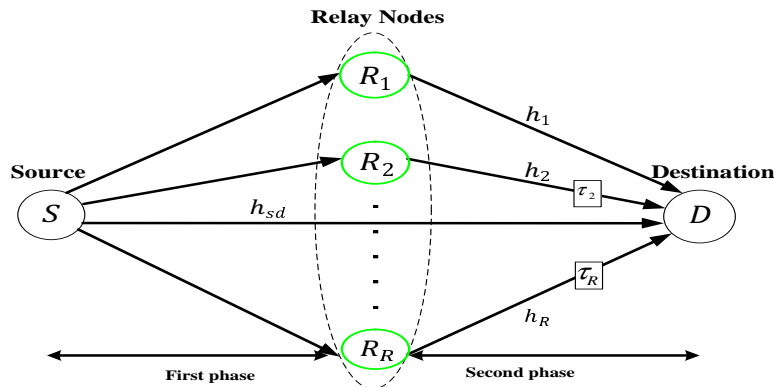
Figure 3.1. Basic structure of general cooperative relay network with one source node, R relay nodes and one destination node, each node is equipped with a single half-duplex antenna.

Moreover, the slowly varying block-fading environment is assumed in this model, where the channels remain constant within at least one transmission cycle duration, and the succeeding realizations of the propagation channels are statistically independent. The flat fading channel is considered in order to isolate the benefits of spatial diversity provided by distributed STBCs. The signals are broadcasted according to a cooperative strategy with a two phase protocol as shown in Figure 3.1. In the first phase, the source node transmits its signals to the destination node through the channel gain h_{sd} and due to the broadcast nature of wireless channels the neighboring relay nodes receive the signals through the channel gains $h_{sr,k}$, . In the second phase, the source node ceases transmission and the multiple relay nodes decode,

---

[1]In practice, the channel parameters can be correlated due to small angular spread and/or not large enough antenna spacing, this will reduce the diversity gain. The uses of estimation channnels in these parameters is not addressed in this Thesis.

re-encode their received signals and forward them to the destination node through the channel gain h_k, $k \in 1, 2, ..., R$. It is assumed that the relay nodes are set to work in the DF strategy. As such, a sufficient level of cyclic redundancy check (CRC) can be included into the signals at the source node, therefore the relaying will happen if the signals are correctly detected at the relay nodes. This arrangement is termed "selective relaying" in [10]. Then, the destination node combines all the received signals and produces an estimate of the original transmitted signals.
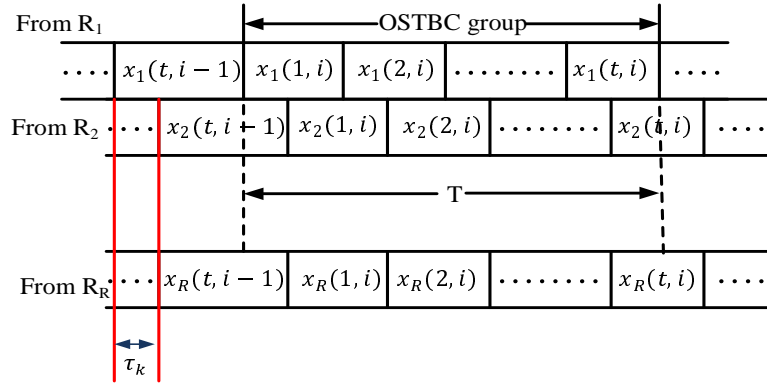
Figure 3.2. Representation of misalignment of the received signals at the destination node which induces intersymbol interference (ISI).

Perfect synchronization becomes unlikely in practice due to the different locations of the relay nodes and their separate timing operations. In this model the timing misalignments τ_k, $k \in 2, 3, ..., R$, among the received versions of the signals at the destination node are considered identical [75] and [76] and as shown in Figure 3.2, however these can be different as shown in Figure 1.3. Without loss of generality, it is also assumed that the destination node is fully synchronized to R_1.

3.3   Distributed Space Time Block Coding for Cooperative Relay Networks

In this section, the principle of distributed QO-STBC [43] and distributed EO-STBC [16] of full data transmission rate with feedback rotation are presented for a cooperative relay network under imperfect synchronization to provide full cooperative diversity gain and as well as to overcome the shortcoming of orthogonal codes in [76], which cannot achieve full data transmission rate[2]. In this model, a four node distributed closed-loop QO-STBC and distributed closed-loop EO-STBC for cooperative relay networks are presented, comprising the source node, the destination node, the four cooperative relay nodes R_k, $k \in 1, 2, 3, 4$, and the closed-loop phase rotation feedback U_1 and U_2 as presented in Section 2.2 for QO-STBC and Appendix A for EO-STBC. Likewise, the DT link between the source node and the destination node is assumed to be available in both schemes.

As mention in Section 3.1, in most cooperative relay networks, the transmission process can be divided in two orthogonal phases. Firstly, the source node broadcasts the sequence of information bits, after modulating and mapping to the destination node and the cooperative relay nodes R_k, $k \in 1, 2, 3, 4$. The transmitted symbols are grouped into number of symbols pairs and denoted by vector $\mathbf{s}(i) = [s(1, i), ..., s(t, i)]^T$, where $[.]^T$ denotes the transpose of the vector $\mathbf{s}(i)$ and i denotes the discrete pair index in two different transmission periods $t \in 1, 2, 3, 4$ in the case of QO-STBC and $t \in 1, 2$ in the case of EO-STBC. Therefore, the received signal vector $\mathbf{r}_{sd}(i) = [r_{sd}(1, i), ..., r_{sd}(t, i)]^T$ at the destina-

---

[2]Data transmission rate $D_R = 3/4$, because three transmission symbols are broadcasted over four symbol transmission periods.

tion node through the DT link during different transmission periods in the first phase can be represented as

$$\mathbf{r}_{sd}(i) = h_{sd}\mathbf{s}(i) + \mathbf{n}_{sd}(i) \qquad (3.3.1)$$

where h_{sd} is the channel gain between the source node and the destination node and it is modelled as a Rayleigh flat fading channel and $\mathbf{n}_{sd}(i) = [n_{sd}(1,i), ..., n_{sd}(t,i)]^T$, $t \in 1, 2, 3, 4$, in the case of QO-STBC and $t \in 1, 2$ in the case of EO-STBC is a noise vector containing independent circularly-symmetric complex additive Gaussian random variables at the destination node, each having distribution $CN(0, \sigma_n^2)$.

To detect which symbol was actually transmitted from the source node through a DT link at the destination node, the least squares (LS) method can be used as follows

$$\hat{s}_{sd}(t,i) = arg \min_{s_t \in S} |h_{sd}^* r_{sd}(t,i) - |h_{sd}|^2 s_t|^2 \quad \text{for} \quad t = \begin{cases} 1, 2, 3, 4 & \text{in} \\ & QO - STBC \\ \\ 1, 2 & \text{in} \\ & EO - STBC \end{cases}$$

$$(3.3.2)$$

where S is the alphabet containing M symbols for PSK. In the second phase, the received signals at the relay nodes R_k, $k \in 1, 2, 3, 4$, in the first phase are re-encoded utilizing QO-STBC [43] or EO-STBC [16] and then transmitted to the destination node in different transmission periods as will be presented in the next sections.

3.3.1   Distributed Closed-Loop Quasi Orthogonal Space Time Block Coding

As mention in Section 3.1, in the second phase the source node terminates transmission and the four relay nodes re-transmit the processed signal to the destination node using the DF strategy. Before transmitting the encoded signal matrix $\mathbf{S}$ in (3.3.3) from the relay nodes R_k, $k \in 1, 2, 3, 4$, in four different transmission periods, the modulated signals from the third and fourth relay nodes are respectively rotated by two phases $U_1 = e^{j\phi}$ and $U_2 = e^{j\theta}$ as shown in Figure 3.3. This is discussed further in Section 2.2 in (2.3.19) and (2.3.20) [17] and shown to provide full cooperative diversity gain between the relay nodes and the destination node in proportion to the number of transmitting relay nodes.
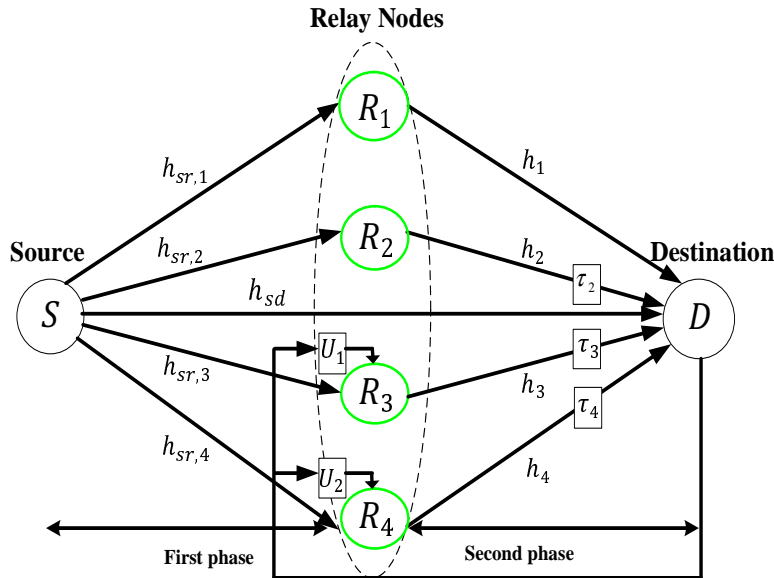
Figure 3.3. Basic structure of distributed closed-loop QO-STBC without outer coding using two-bit feedback for four relay nodes with a two phase cooperative transmission process and time delay offset between R_2, R_3 and R_4 at the destination node.

The information packet at the relay nodes corresponding to $\mathbf{s}(i)$ is $\mathbf{x}_k(i) = [x_k(1,i), ..., x_k(4,i)]^T$, $k \in 1,2,3,4$. Therefore, the transmitted signal matrix $\mathbf{S}$ from the relay nodes can be expressed as

$$\left[\begin{array}{cccc} \mathbf{x}_1(i) & \mathbf{x}_2(i) & \mathbf{x}_3(i) & \mathbf{x}_4(i) \end{array} \right] =$$

$$\mathbf{S} = \left[\begin{array}{cccc} s(1,i) & s(2,i) & s(3,i) & s(4,i) \\ -s^*(2,i) & s^*(1,i) & -s^*(4,i) & s^*(3,i) \\ -s^*(3,i) & -s^*(4,i) & s^*(1,i) & s^*(2,i) \\ s(4,i) & -s(3,i) & -s(2,i) & s(1,i) \end{array} \right] \tag{3.3.3}$$

Therefore, the code matrix $\mathbf{S}$ in (3.3.3) presents a unity data transmission rate between the relay nodes and the destination node as compared to the matrix code in [76]. In the case of distributed open-loop QO-STBC, some of the nonzero off-diagonal terms which appear in the Grammian matrix Δ as shown in [17] will reduce the cooperative diversity gain of the code matrix in (3.3.3) between the relay nodes and the destination node. The bit error rate (BER) performance of this distributed open-loop QO-STBC therefore is degraded.

To overcome this problem, two feedback methods for this distributed QO-STBC are used to achieve full cooperative diversity gain with unity data transmission rate between the relay nodes and the destination node as presented in Section 2.2. The signals transmitted from the third relay node R_3 and the fourth relay node R_4 are instead rotated by $U_1 = e^{j\phi}$ and $U_2 = e^{j\theta}$ respectively as shown in Figure 3.3, while the other two relay nodes R_1 and R_2 are kept unchanged. As shown in Figure 3.2 the accurate synchronization level between the transmitted signals from the relay nodes R_k, $k \in 1,2,3,4$, is difficult or impossi-

ble to achieve, because there is normally timing misalignment of τ_k, $k \in 2, 3, 4$, among the received versions of these signals at the destination node as mentioned in Section 3.1. Moreover in this model it is assumed the received signal at the destination node is perfectly synchronized to the relay node R_1 i.e. $\tau_1 = 0$. Therefore, the received signals $\mathbf{r}_{rd}(i) = [r_{rd}(1, i), ..., r_{rd}(4, i)]^T$ at the destination node in four independent transmission periods are expressed as

$$r_{rd}(1, i) = \sum_{k=1}^{2} h_k x_k(1, i) + \sum_{k=3}^{4} (U_{k-2} h_k x_k(1, i)) + h_2(-1) x_2(4, i - 1) +$$

$$\sum_{k=3}^{4} (U_{k-2} h_k(-1) x_k(4, i - 1)) + n_{rd}(1, i) \tag{3.3.4}$$

$$r_{rd}(t, i) = \sum_{k=1}^{2} h_k x_k(t, i) + \sum_{k=3}^{4} (U_{k-2} h_k x_k(t, i)) + h_2(-1) x_2(t - 1, i) +$$

$$\sum_{k=3}^{4} (U_{k-2} h_k(-1) x_k(t - 1, i)) + n_{rd}(t, i) \quad \text{for} \quad t \in 2, 3, 4 \tag{3.3.5}$$

where $n_{rd}(1, i), ..., n_{rd}(4, i)$ are additive Gaussian noise terms with distribution $CN(0, \sigma_n^2)$ at the destination node, h_k, $k \in 1, 2, 3, 4$, are the channel gains between the relay nodes and the destination node and all channels are assumed frequency flat Rayleigh fading i.e. circularly complex Gaussian random variables and statistically independent from each other, and the channel coefficients $h_k(-1)$, $k \in 2, 3, 4$, reflect the intersymbol interference (ISI) from the previous symbol as shown in Figure 3.2, due to imperfect synchronization between the relay nodes and the destination node. The relative strength of $h_k(-1)$ will be represented as follows

$$\beta_k = \frac{|h_k(-1)|^2}{|h_k|^2} \qquad \text{for} \qquad k \in 2, 3, 4 \tag{3.3.6}$$

All relay nodes are assumed to transmit with $1/4$ of the available power i.e. $\sigma_r^2 = 0.25\sigma_s^2$. By substituting (3.3.3) into (3.3.4) and (3.3.5) gives the received signals at the destination $r_{rd}(t, i)$, $t \in 1, 2, 3, 4$, as in (3.3.5) where the signals $r_{rd}(t, i)$ received in the second and third symbol period are conjugated where, $t \in 2, 3$. Therefore, the received signals at the destination node can be represented in matrix form as follows

$$\mathbf{r}_{rd}(i) = \mathbf{H}\mathbf{s}(i) + \mathbf{I}_{int}(i) + \mathbf{n}_{rd}(i) \tag{3.3.7}$$

where

$$\mathbf{H} = \begin{bmatrix} h_1 & h_2 & U_1 h_3 & U_2 h_4 \\ h_2^* & -h_1^* & U_2^* h_4^* & -U_1^* h_3^* \\ U_1^* h_3^* & U_2^* h_4^* & -h_1^* & -h_2^* \\ U_2 h_4 & -U_1 h_3 & -h_2 & h_1 \end{bmatrix},$$

$\mathbf{n}_{rd}(i) = [n_{rd}(1, i), n_{rd}^*(2, i), n_{rd}^*(3, i), n_{rd}(4, i)]^T$ is an additive Gaussian noise vector with element having distribution $CN(0, \sigma_n^2)$ at the destination during four transmission periods and $\mathbf{I}_{int}(i) = [I_{int}(1, i), I_{int}^*(2, i), I_{int}^*(3, i), I_{int}(4, i)]^T$ contains the interference terms at the destination node from the relay nodes R_k, $k \in 2, 3, 4$, and can be modelled as follow

$$I_{int}(1, i) = h_2(-1)x_2(4, i - 1) + \sum_{k=3}^{4} U_{k-2}h_k(-1)x_k(4, i - 1) \tag{3.3.8}$$

$$I_{int}(t, i) = h_2(-1)x_2(t - 1, i) + \sum_{k=3}^{4} U_{k-2}h_k(-1)x_k(t - 1, i) \tag{3.3.9}$$

where $t \in 2, 3, 4$ denotes the index of the timing misalignment among the received signals from relay nodes at the destination node, $x_k(4, i-1)$ and $x_k(t - 1, i)$ are defined according to (3.3.3).

3.3.2   Distributed Closed-Loop Extended Orthogonal Space Time Block Coding

All the relay nodes can successfully decode $\mathbf{s}(i)$ using a DF strategy as mentioned in Section 3.1. Therefore, in the second phase, all the relay nodes R_k, $k \in 1, 2, 3, 4$, perform distributed EO-STBC encoding on their received vectors and transmit the resulting matrix code $\mathbf{S}$ in (3.3.10) from the relay nodes to the destination node in two different symbol periods to achieve unity data transmission rate between the relay nodes and the destination node.

$$
\left[\begin{array}{cccc} \mathbf{x}_1(i) & \mathbf{x}_2(i) & \mathbf{x}_3(i) & \mathbf{x}_4(i) \end{array} \right] =
$$

$$
\mathbf{S} = \left[\begin{array}{cccc} s(1,i) & s(2,i) & s(2,i) & s(2,i) \\ -s^*(2,i) & -s^*(2,i) & s^*(1,i) & s^*(1,i) \end{array} \right] \tag{3.3.10}
$$

For achieving full cooperative diversity gain between the relay nodes and the destination node, the close-loop method is adapted to improve the system performance as presented in Appendix A [16]. Therefore, the signals from the first relay node R_1 is multiplied by $U_1 = (-1)^a$ and the third relay node R_3 is multiplied by $U_2 = (-1)^b$ as shown Figure 3.4, where $a, b = 0, 1$, prior to transmitting them to the destination node. In this model a and b denote two feedback parameters which are determined by the channel conditions. In particular, when a or $b = 1$ then both U_1 and U_2 equal -1. That means the signals from the first and third relay nodes in (3.3.10) will be rotated by 180° before transmitting to the destination node during two different transmission periods [16]. Otherwise, the signals can be directly transmitted.
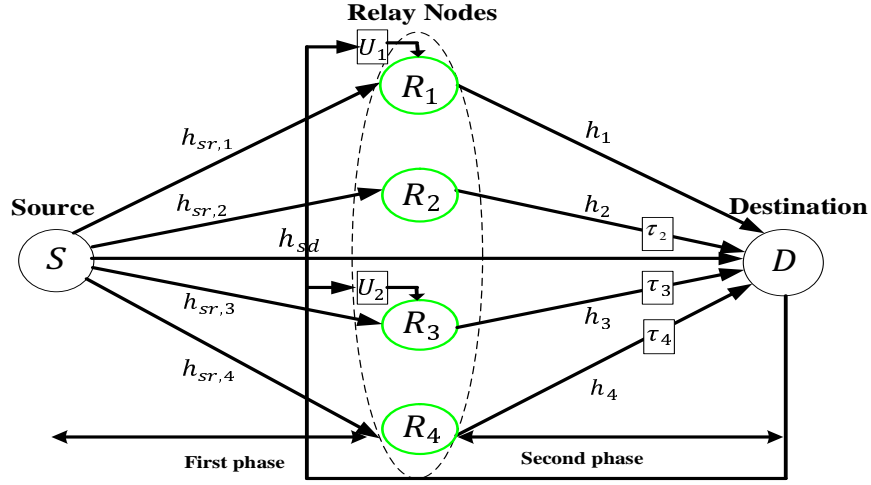
Figure 3.4. Basic structure of distributed closed-loop EO-STBC without outer coding using two-bit feedback for four relay nodes with a two phase cooperative transmission process and time delay offset between R_2, R_3 and R_4 at the destination node.

The perfect synchronization transmission between the first relay R_1 and the destination node is assumed where $\tau_1 = 0$. However, due to imperfect synchronization such as different propagation delay τ_k, the $\mathbf{x}_k(i)$ signals will not arrive at the destination node at the same time from relay nodes R_k and for convenience development (but this can be generalized) the time delay $\tau_k \neq 0$ are assumed to be identical as shown in Figure 3.2, where $k \in 2, 3, 4$ [76]. Therefore, the received signals $r_{rd}(1, i)$ and $r_{rd}(2, i)$ at the destination node in two independent transmission periods are modelled as follows

$$
\begin{aligned}
r_{rd}(1, i) = {} & U_1 h_1 x_1(1, i) + h_2 x_2(1, i) + U_3 h_3 x_3(1, i) + h_4 x_4(1, i) \\
& + h_2(-1) x_2(2, i-1) + U_2 h_3(-1) x_3(2, i-1) + h_4(-1) \\
& x_4(2, i-1) + n_{rd}(1, i)
\end{aligned} \tag{3.3.11}
$$

$$
\begin{aligned}
r_{rd}(2, i) = {} & U_1 h_1 x_1(2, i) + h_2 x_2(2, i) + U_3 h_3 x_3(2, i) + h_4 x_4(2, i) \\
& + h_2(-1) x_2(1, i) + U_2 h_3(-1) x_3(1, i) + h_4(-1) x_4(1, i) \\
& + n_{rd}(1, i)
\end{aligned}
\tag{3.3.12}
$$

where $n_{rd}(1, i)$ and $n_{rd}(2, i)$ are additive Gaussian noise terms at the destination node in the second phase with distribution $CN(0, \sigma_n^2)$ and h_k, $k \in 1, 2, 3, 4$, are the channel gains between relay nodes and the destination node and also are assumed to be Rayleigh fading and constant across two symbols transmission periods. Also the $h_k(-1)$, $k \in 2, 3, 4$, reflect the ISI from the previous symbols due to imperfect synchronization between the relay nodes R_k and the relative strength of $h_k(-1)$ can be represented as the ratio as in (3.3.6), where $k \in 2, 3, 4$.

Substituting (3.3.10) into (3.3.11) and (3.3.12), the received signals $r_{rd}(1, i)$ and $r_{rd}(2, i)$, conjugated for convenience at two independent time intervals are expressed equivalently as

$$
\begin{bmatrix} r_{rd}(1, i) \\ r_{rd}^*(2, i) \end{bmatrix}
=
\begin{bmatrix} U_1 h_1 + h_2 & U_2 h_3 + h_4 \\ U_2^* h_3^* + h_4^* & -U_1^* h_1^* - h_2^* \end{bmatrix}
\begin{bmatrix} s(1, i) \\ s(2, i) \end{bmatrix}
+
\begin{bmatrix} I_{int}(1, i) \\ I_{int}^*(2, i) \end{bmatrix}
$$
$$
+
\begin{bmatrix} n_{rd}(1, i) \\ n_{rd}^*(2, i) \end{bmatrix}
\tag{3.3.13}
$$

where

$$
\begin{aligned}
I_{int}(1, i) = {} & h_2(-1) x_2(2, i-1) + U_2 h_3(-1) x_3(2, i-1) \\
& + h_4(-1) x_4(2, i-1)
\end{aligned}
\tag{3.3.14}
$$
$$
\begin{aligned}
I_{int}^*(2, i) = {} & h_2^*(-1) x_2^*(1, i) + U_2^* h_3^*(-1) x_3^*(1, i) \\
& + h_4^*(-1) x_4^*(1, i)
\end{aligned}
\tag{3.3.15}
$$

Therefore, (3.3.13) can be re-written as follows

$$\mathbf{r}_{rd}(i) = \mathbf{H}\mathbf{s}(i) + \mathbf{I}_{int}(i) + \mathbf{n}_{rd}(i) \qquad (3.3.16)$$

From (3.3.7) and (3.3.16) the conventional distributed closed-loop QO-STBC and distributed closed-loop EO-STBC detection can be carried out via a two step procedure assuming that the channel state information (CSI) is available at the destination node as will be presented in the following section.

3.3.3 Conventional Distributed Closed-Loop Space Time Block Coding

It is well-known from estimation theory that the matched filter is the optimum front-end receiver to obtain sufficient statistics for detection in the sense it preserves information. Assuming the CSI at the destination node, the conventional CL QO-STBC and CL EO-STBC can be carried as follows

1. By multiplying both sides of (3.3.7) in the case of distributed CL QO-STBC and (3.3.16) in the case of distributed CL EO-STBC by the matched filter $\mathbf{H}^H$, where $(.)^H$ denotes the Hermitian conjugate, the estimated signals can be represented as

$$\hat{\mathbf{g}}(i) = [g(t,i), ..., g(t,i)]^T = \mathbf{H}^H\mathbf{r}_{rd}(i)$$
$$= \Delta\mathbf{s}(i) + \mathbf{H}^H\mathbf{I}_{int}(i) + \mathbf{H}^H\mathbf{n}_{rd}(i) \qquad (3.3.17)$$

   - In the case of distributed CL QO-STBC, $t \in 1, 2, 3, 4$ and the Grammian matrix Δ with entries $\gamma = \sum_{k=1}^{2} |h_k|^2 + \sum_{k=3}^{4} |U_{k-2}h_k|^2$ and $\alpha = \Re\{h_1^*h_4U_2 - h_2^*h_3U_1\}$ as follows

$$\Delta = \begin{bmatrix} \gamma & 0 & 0 & \alpha \\ 0 & \gamma & -\alpha & 0 \\ 0 & -\alpha & \gamma & 0 \\ \alpha & 0 & 0 & \gamma \end{bmatrix},$$

where $\Re\{.\}$ denotes the real part of a complex number, by minimizing the off-diagonal term α maximizes the signal-to-noise ratio (SNR). The value of α can be reduced to zero by rotating the transmitted signal to improve cooperative diversity gain between the relay nodes and the destination node. The phase rotated method can be designed as presented in Section 2.2 [17].

- In the case of distributed CL EO-STBC, $t \in 1, 2$ and the Grammian matrix Δ can be represented as follows

$$\Delta = \begin{bmatrix} \lambda_c + \lambda_f & 0 \\ 0 & \lambda_c + \lambda_f \end{bmatrix},$$

where $\lambda_c = \sum_{k=1}^{4}(|h_k|^2)$ is the conventional diversity gain for four relay nodes and $\lambda_f = 2\Re(U_1 h_1 h_2^* + U_2 h_3 h_4^*)$ changes with the defined values of U_1 and U_2 which are determined by two information bits as presented in Appendix A. The two-bit feedback has been chosen to maximize the value of λ_f which leads to a larger received SNR at the destination node which shows that the distributed CL EO-STBC scheme achieves full cooperative diversity gain with array gain and unity data transmission rate between the relay nodes and

the destination node as compared to distributed O-STBC[3] codeword in (2.3.13) [76].

- The SNR can be calculated at the destination node as

$$
SNR = \begin{cases} \frac{\gamma^2 + \alpha^2}{\gamma} \frac{\sigma_s^2}{\sigma_n^2} & \text{if} \quad \text{CL QO-STBC} \\ \\ \frac{\lambda_c + \lambda_f}{4} \frac{\sigma_s^2}{\sigma_n^2} & \text{if} \quad \text{CL EO-STBC} \end{cases}
$$

where σ_s^2 is the total power of the transmitted signal from the relay nodes at the destination node and σ_n^2 is the noise power at the destination node.

2. Applying least squares (LS) detection

$$
\hat{s}(t, i) = arg \ \min_{s_t \in S} |\hat{g}(t, i) - \Delta s_t|^2 \tag{3.3.18}
$$

where $t \in 1, 2, 3, 4$ in the case of CL QO-STBC and $t \in 1, 2$ in the case of CL EO-STBC.

The above conventional procedure will suffer from significant detection error, because the interference component $\mathbf{H}^H \mathbf{I}_{int}(i)$ in (3.3.17) will damage the orthogonality of both closed-loop schemes. The PIC detection scheme can solve this issue of imperfect synchronization among the relay nodes at the destination node as presented in Section 2.5 and in the following section.

---

[3]O-STBC codeword in (2.3.13) achieves only 3/4 data transmission rate, because three symbols transmit from the relay nodes over four time symbol transmission periods.

3.4   The Parallel Interference Cancellation Detection

The PIC detection is applied to remove the impact of imperfect synchronization of the interference term $\mathbf{I}_{int}(i)$ in (3.3.17), assuming the CSI at the destination node. Since $x_k(t, i-1)$, $k \in 2, 3, 4$, and $t \in 1, 2, 3, 4$, is already known if the detection process has been initialized properly, for example through the use of pilot symbols in the signal packet, therefore, $I_{int}(1, i)$ can be removed during the initialization stage. The general PIC iteration process can be used to mitigate the impact of $\mathbf{I}_{int}(i)$ in (3.3.17) as follows

1. Initialization

2. Set iteration $q = 0$

3. Remove the ISI from $r_{rd}(1, i)$

$$r^{'(0)}(1, i) = r_{rd}(1, i) - I_{int}(1, i)$$

4. Due to poor performance of the conventional distributed STBC detector[4]. Therefore, the DT link detection result in (3.3.2), where $t \in 1, 2, 3, 4$, in the case of distributed CL QO-STBC and $t \in 1, 2$, in the case of distributed CL EO-STBC

$$\mathbf{s}^{(0)}(i) = [s^{(0)}(1, i), ..., s^{(0)}(t, i)]^T = [\hat{s}_{sd}(1, i), ..., \hat{s}_{sd}(t, i)]^T$$

5. Set iteration $q = 1, 2, ..., n$

---

[4]It has shown that the conventional distributed STBC detector for more than two relay nodes will fail due to increase timing error among the relay nodes [26] and [76].

6. Remove more ISI from the received signal $r_{rd}(t, i)$, $t \in 2, 3, 4$.

   In the case of distributed CL QO-STBC

   $$\mathbf{r}'^{(q)}(i) = \begin{bmatrix} r'^{(0)}(1, i) \\ r_{rd}^*(2, i) - I_{int}^{*(q-1)}(2, i) \\ r_{rd}^*(3, i) - I_{int}^{*(q-1)}(3, i) \\ r_{rd}(4, i) - I_{int}^{(q-1)}(4, i) \end{bmatrix}$$

   In the case of distributed CL EO-STBC

   $$\mathbf{r}'^{(q)}(i) = \begin{bmatrix} r'^{(0)}(1, i) \\ r_{rd}^*(2, i) - I_{int}^{*(q-1)}(2, i) \end{bmatrix}$$

   where $I_{int}^{*(q-1)}(t, i)$, $t \in 2, 3, 4$, is determined using $\mathbf{s}^{(q-1)}(i)$ with $x_k^{(q-1)}(t, i)$, in (3.3.9) and in (3.3.15), where $t \in 2$, and where $k \in 2, 3, 4$.

7. In both cases of CL QO-STBC or CL EO-STBC, substitute $\mathbf{r}_{rd}(i)$ in (3.3.17) with $\mathbf{r}'^{(q)}(i)$ to obtain $\hat{\mathbf{g}}^{(q)}(i)$ and then apply LS detection to detect the $\hat{\mathbf{s}}^{(q)}(i)$ by replacing $\hat{\mathbf{g}}(i)$ in (3.3.18) with $\hat{\mathbf{g}}^{(q)}(i)$, where $t \in 1, 2, 3, 4$ in the case of CL QO-STBC and $t \in 1, 2$ in the case of CL EO-STBC, then go to the next step.

8. Repeat the process from point 5 until $q = n$

The above approach will achieve maximum likelihood (ML) detection due to the structure of the STBC, if the interference component of $\mathbf{I}_{int}(i)$ in (3.3.7) in the case of CL QO-STBC and in (3.3.16) in the case of CL EO-STBC is removed. Most of the performance of cooperative diversity gain between the relay nodes and the destination node will be achieved in 2-3 iterations of the PIC detection process [75] and [76],

which means the PIC detection is very effective in mitigating the impact of imperfect synchronization between the relay nodes at the destination node as will be shown in the next section.

3.5   Simulation Results

The error performance of the proposed schemes in quasi-static flat fading channels is demonstrated in this section. The fading is constant with each frame but independent from one frame to another. For all schemes, the BER against SNR[5] in dB utilizing 8-phase shift keying (8PSK) gray mapping scheme is simulated and all simulations which have been presented in this section are without outer coding. The SNR is defined as SNR σ_s^2/σ_n^2 and all nodes transmit at 1/4 power. Table 3.1 shows comparisons of data transmission rate D_R which can be achieved by using the existing distributed A-STBC [75] and distributed O-STBC [76] with the proposed distributed CL QO-STBC and distributed CL EO-STBC.

It can be observed that to achieve unity data transmission rate the A-STBC, QO-STBC or EO-STBC should be employed in the network, while by using distributed O-STBC in [76], the data transmission rate is limited to 3/4. However, distributed A-STBC is available for two relay nodes and can only achieve diversity order of two, whilst the proposed distributed CL QO-STBC and distributed CL EO-STBC can achieve unity data transmission rate with fourth order diversity as shown in Table 3.1. From Table 3.1 can be observed that all schemes achieve full cooperative diversity equal to the number of transmitting relay nodes.

---

[5]In this thesis all the BER simulations are presented as a function of SNR rather than E_b/N_o to be consistent with other researchers [2], [75] and [76].

Table 3.1. Data transmission rate D_R for different STBCs with the available diversity order in the network for each code.

Space-Time Coding Scheme	A-STBC	O-STBC	CL QO-STBC	CL EO-STBC
Number of transmission symbols N_S	2	3	4	2
Number of transmission periods N_P	2	4	4	2
Data Transmission Rate $D_R = \frac{N_S}{N_P}$	1	3/4	1	1
Cooperative diversity order= R	2	4	4	4

Figure 3.5 shows comparisons of BER performance with the proposed distributed CL QO-STBC and distributed CL EO-STBC, and existing distributed A-STBC [75] and distributed O-STBC [76] with the assumption that the DT link received signals does not combine with the received signals of the relay nodes at the destination node.

It can be observed that, at a bit error probability of 10^{-3}, the proposed distributed CL EO-STBC scheme provides approximately 2 dB improvement over the proposed distributed CL QO-STBC scheme and distributed O-STBC in [76], and approximately 6 dB improvement over distributed A-STBC in [75]. Furthermore, it is clear that the proposed distributed CL EO-STBC outperforms proposed distributed CL QO-STBC, this is because in distributed CL QO-STBC there is only diversity gain and no array gain, however in the distributed CL EO-STBC there is both diversity gain of order four and array gain.
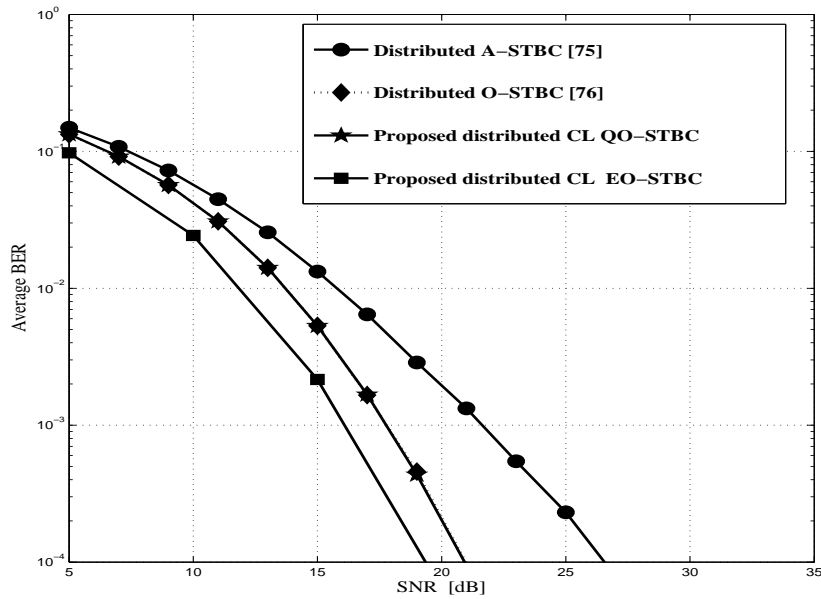
Figure 3.5. The BER performance of different distributed STBC schemes (A-STBC, O-STBC, CL QO-STBC and CL EO-STBC) using conventional detection under perfect synchronization without DT combining.

While both diversity gain and array gain improves system performance (decreases error rate), the nature of these gains are very different as mentioned in Section 2.2. Diversity gain manifests itself in increasing the magnitude of the asymptotic slope of the BER curve, while array gain shifts the error rate curve to the left.

On the other hand, Figure 3.6 shows the BER performance of all distributed STBC schemes mentioned earlier combined with the DT link under perfect synchronization, which greatly improves the system performance due to the higher diversity order as compared to the performance systems in Figure 3.5. For example, it is seen that the distributed CL EO-STBC combined with DT link between the source node and the destination node outperforms the distributed CL EO-STBC without combing the DT link with approximately 3 dB improvement.
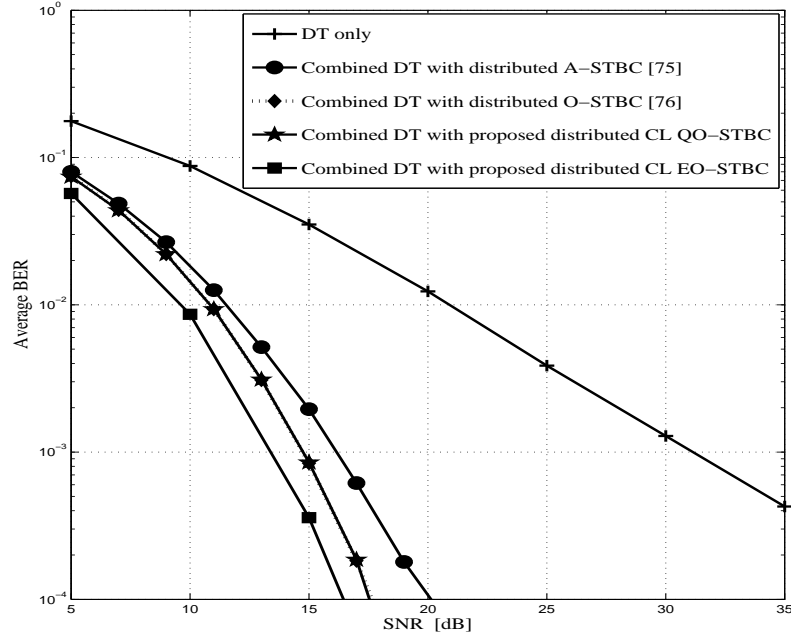
Figure 3.6. The BER performance of different distributed STBC schemes (A-STBC, O-STBC, CL QO-STBC and CL EO-STBC) using conventional detection under perfect synchronization with DT link combining.

However, in Figures 3.7 and 3.8, the impact of synchronization errors is shown by changing the value of β_k, that means β_k reflects the impact of time delay τ_k between transmission from relay nodes R_k at the destination node where $k \in 2, 3, 4$, and can be calculated as shown in Table 3.2.

Table 3.2. Shows the calculation of the impact of time delay between relay node R_1 and the other relay nodes.

β_k	$dB = 10\log_{10}(\beta_k)$	τ_k
1	0	0.5T
0.5	-3	0.25T
0.3	-5	0.15T
0.25	-6	0.125T
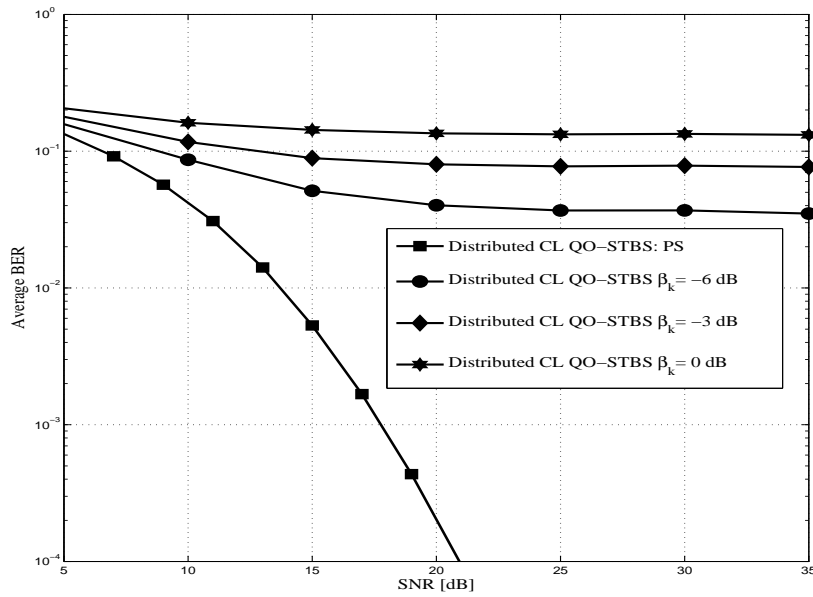
Figure 3.7. The BER performance of distributed CL QO-STBC using conventional detection under imperfect synchronization $\beta_k = 0, -3, -6$ dB without DT link combining.
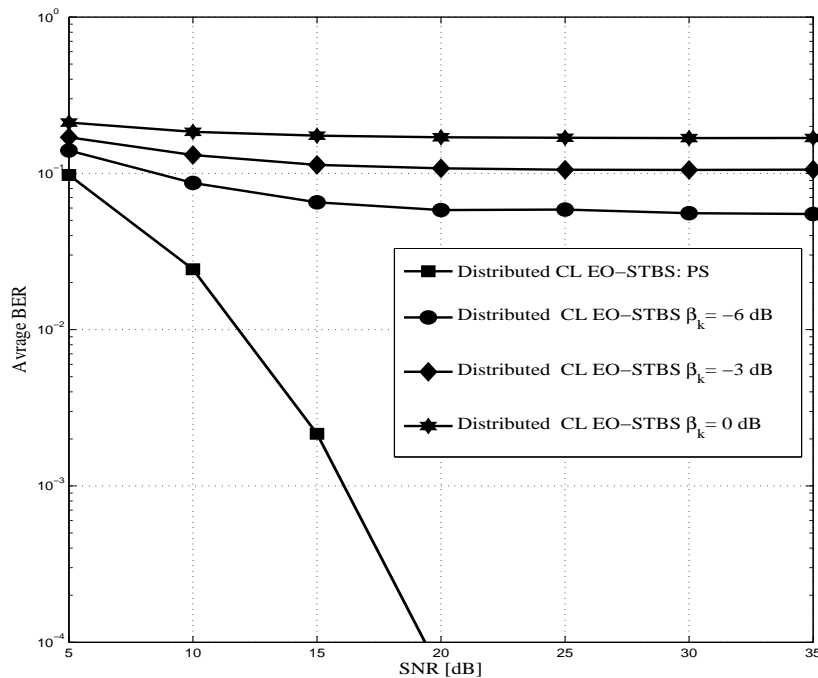
Figure 3.8. The BER performance of distributed CL EO-STBC using conventional detection under imperfect synchronization $\beta_k = 0, -3, -6$ dB without DT link combining.

Figures 3.7 and 3.8 show the result of the conventional detector under imperfect synchronization for both distributed CL STBC schemes presented in this section, likewise including the conventional detector under perfect synchronization (PS) as reference. The figures show that both distributed CL STBC schemes using the conventional detector are not effective with synchronization error even under small time misalignments $\beta_k = -6$ dB, $k \in 2, 3, 4$.

On the other hand, Figures 3.9 and 3.10 show the BER performance of distributed CL QO-STBC and CL EO-STBC schemes, respectively; with three iterations of the PIC detector q = 0,1,3 [75] and [76], under $\beta_k = 0, -3, -6$ dB, also the BER performance of the DT link between the source node and the destination node and perfect synchronization of both proposed distributed CL STBC schemes considered in this chapter are included to compare the results.
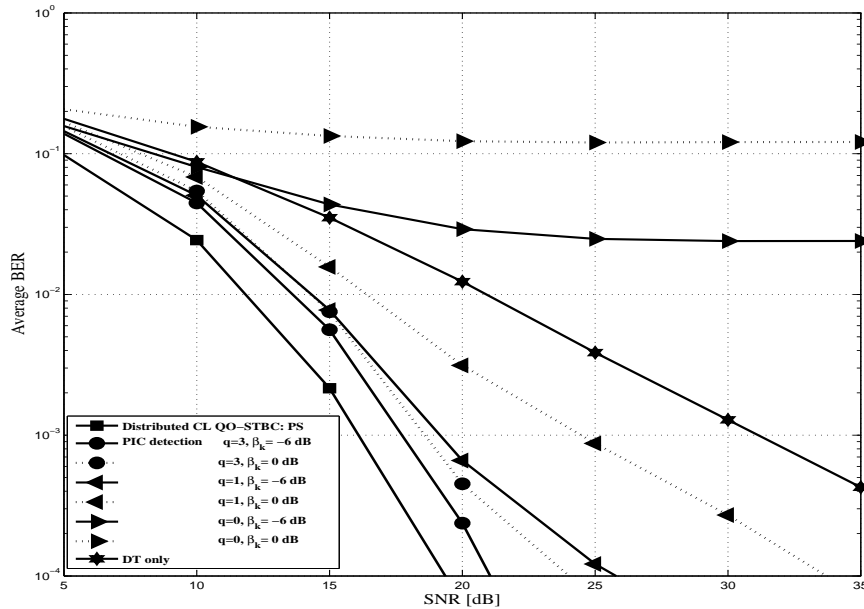
Figure 3.9. The BER performance of distributed closed-loop QO-STBC with PIC detection for different numbers of iterations q = 0,1,3 and under different $\beta_k = 0, -3, -6$ dB without DT link combining.
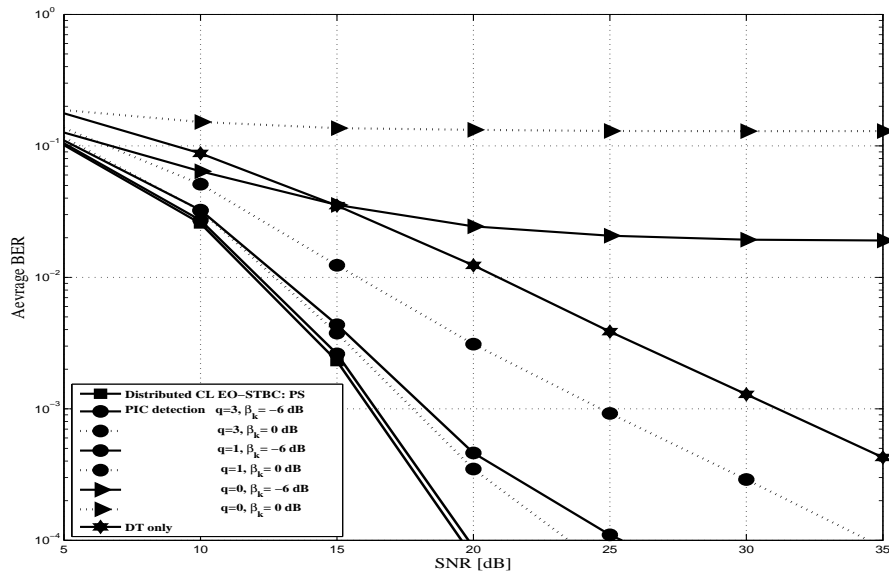
Figure 3.10. The BER performance of distributed closed-loop EO-STBC with PIC detection for different numbers of iterations q = 0,1,3 and under different $\beta_k = 0, -3, -6$ dB without DT link combining.

Both figures show that the performance of the PIC detector with q = 3 when $\beta_k = -6$ dB approach to that of the perfect synchronized case. It can be observed that there is a large improvement on the performance over the conventional detector. For example, in both distributed CL STBC, the value of BER $= 10^{-2}$ can not be achieved by the conventional detector as shown in Figures 3.8 and 3.9 whereas by the PIC detector, it is achieved at approximately 14 dB of SNR in the case of distributed CL QO-STBC and 12 dB of SNR in the case of distributed CL EO-STBC when the number of PIC iterations q = 3 and $\beta_k = -6$ dB, $k \in 2, 3, 4$. Furthermore, both approaches are simulated when $\beta_k = 0$, which considers relatively large amount of imperfect synchronization. It can be observed that the PIC detector is still effective when q = 1, however, its affectiveness is far less than the case of $\beta = -6$ dB when

q = 1. For example at 10^{-2} approximately 16 dB of SNR is necessary in the case of distributed CL QO-STBC and approximately 15.5 dB of SNR in the case of distributed CL EO-STBC.

3.6   Multi-Hop Cooperative MIMO Technique

In this section the example of wireless dual hop networks is described with cooperative relaying nodes where the relay nodes can communicate with both end points. The DT link between the source node and the destination node is assumed to be blocked by some obstacles and also the distributed A-STBC [5] is applied in both hops. This model has an information source node cooperating with one of its adjacent mobile terminal (AMT) node, two relay nodes cooperate with each other and a destination node also cooperates with one of its AMT nodes as shown in Figure 3.12 and as presented in Section 1.1. All nodes are equipped with a single antenna which can be used for both transmission and reception. All transmissions are assumed to be half-duplex and therefore a relay nodes can not transmit and receive at the same time.

As in most cooperative communication systems there are two phases involved. During the first phase the source node cooperates with one of its AMTs to encode its signals $\mathbf{s}(i)$, which are grouped into pairs $s(1, i)$ and $s(2, i)$ and then it transmits codeword $\mathbf{S}^1$ as in (3.6.1) while the relay nodes R_k, $k \in 1, 2$, receive the signals and prepare for the distributed A-STBC operation in the second phase.

$$\mathbf{S}^1 = \begin{bmatrix} x_1(1, i) & x_2(1, i) \\ x_1(2, i) & x_2(2, i) \end{bmatrix} = \begin{bmatrix} s(1, i) & s(2, i) \\ -s^*(2, i) & s^*(1, i) \end{bmatrix} \qquad (3.6.1)$$

In the first transmission period the signal transmitted from the source node is denoted by $s(1,i)$ and from its AMT by $s(2,i)$. During the next transmission period signal $-s^*(2,i)$ is transmitted from the source node and signal $s^*(1,i)$ is transmitted from the AMT.
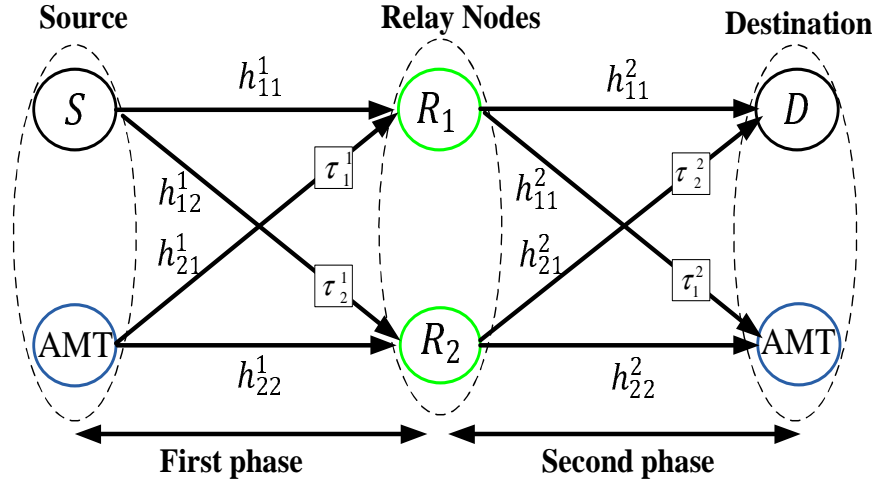
Figure 3.11. Basic structure of distributed A-STBC for two hop cooperative MIMO technique with a two phase cooperative transmission process and time delay offset between the received signals at either relay nodes or the destination node.

Due to imperfect synchronization resulting from different propagation delays in both hops, the transmitted signal in the first hop will not arrive at the relay nodes R_k, $k \in 1,2$, at the same time due to time delay between the source node and its AMT node, similarly in the second hop the received signal will not reach the destination node and its AMT node at the same time due to time delay between the relay node R_1 and the relay node R_2 as shown in Figure 3.12. There is normally a timing misalignment of τ_k^l, among the received versions of the signals where $l \in 1,2$ is the number of hop. At this point, it is assumed that τ_k^l is smaller than the sample period T in both hops, such relative time delay will cause ISI from neighboring symbols at relay nodes or the destination node and its AMT node, owing to sampling

or matched filtering whatever pulse shaping is used. In the first hop it is assumed that the relay nodes R_k, $k \in 1, 2$, are synchronized to the source node, while in the second hop the destination node and its AMT node are synchronized to R_1. The interference is added to the received signals in both hops due to the asynchronism with the source AMT in the first hop and with the relay node R_2 in the second hop, where integer sampling is assumed as all interference is modelled by a single additive term, the received signal in both hops can be expressed as

$$r_k^l(t, i) = h_{1k}^l S_{t1}^l + h_{2k}^l S_{t2}^l + I_{int_k}^l(t, i)$$
$$+ n_k^l(t, i) \qquad \text{for} \qquad l, k, t \in 1, 2 \qquad (3.6.2)$$

where

$$I_{int_k}^l(1, i) = h_{2k}^l(-1)s^*(1, i-1) \qquad (3.6.3)$$
$$I_{int_k}^l(2, i) = h_{2k}^l(-1)s(2, i) \qquad (3.6.4)$$

These quantities are vectorised for convenience in the following as

$$\mathbf{r}_{Hop_l}(i) = [r_1^l(1, i), r_1^{*l}(2, i), r_2^l(3, i), r_2^{*l}(4, i)]^T, \qquad (3.6.5)$$
$$\mathbf{n}_{Hop_l}(i) = [n_1^l(1, i), r_1^{*l}(2, i), n_2^l(3, i), n_2^{*l}(4, i)]^T$$

and

$$\mathbf{I}_{Hop_l}(i) = [I_{int_1}^l(1, i), I_{int_1}^{*l}(2, i), I_{int_2}^l(3, i), I_{int_2}^{*l}(4, i)]^T$$

where $n_k^l(t, i)$, $l, k, t \in 1, 2$, are additive Gaussian noise terms at the received node in both hops with distribution $CN(0, \sigma_n^2)$, h_{1k}^l and h_{2k}^l are the channel gains between the nodes which are assumed to be constant

during both hops with Rayleigh fading and $h_{2k}^l(-1)$, $l, k \in 1, 2$, reflect the ISI from the previous symbols due to imperfect synchronization at the relay nodes in the first hop and at the destination node and its AMT node in the second hop; $h_{2k}^l(-1)$ depends upon timing delay τ_k^l and the particular pulse shaping waveforms used and its relative strength will be expressed as a ratio as follows

$$\beta_k^l = \frac{|h_{2k}^l(-1)|^2}{|h_{2k}^l|^2} \qquad \text{for} \qquad l, k \in 1, 2 \qquad (3.6.6)$$

where β_k^l is defined to reflect the impact of time delay τ_k^l and pulse shaping waveforms [75]. For a fair comparison with a non-relay scheme, all terminal nodes use $1/2$ power i.e. $\sigma_{r_k^l(t,i)}^2 = 0.5\sigma_s^2$, $l, k, t \in 1, 2$ [85].

During the second phase, the received signals at the relay nodes R_k, $k \in 1, 2$ are re-encoded and utilize the A-STBC technique [5] and are then transmitted to the destination node and the AMT at the destination side which is cooperating with the destination node to deliver good end-to-end performance. The relay DF strategy is used in this model as has been explained in Section 3.2. The encoding signals are denoted at the relay nodes corresponding to $\mathbf{s}(i)$ as $\mathbf{r}_k^1(i) = [r_k^1(1,i), r_k^2(2,i)]^T$, $k \in 1, 2$, as in (3.6.2). The codeword $\mathbf{S}^2$, which is transmitted by the relay nodes during two transmission periods can be expressed as follows

$$\mathbf{S}^2 = \begin{bmatrix} r_1^1(1,i) & r_2^1(1,i) \\ r_1^1(2,i) & r_2^1(2,i) \end{bmatrix} = \begin{bmatrix} s(1,i) & s(2,i) \\ -s^*(2,i) & s^*(1,i) \end{bmatrix} \qquad (3.6.7)$$

The transmitted signals $r_k^1(t,i)$, $k, t \in 1, 2$, from the relay nodes in the second hop, are different by different propagation delays. The received signals at the destination node and its AMT at the destination side can then also be represented as in (3.6.2). From (3.6.2) the conventional distributed A-STBC in both hops can be carried out via the

following standard two step procedure assuming CSI at the received side in both hops.

- Applying the linear transform as in (3.3.16) into (3.6.2) to detect the detection signal $\hat{\mathbf{g}}_{Hop_l}(i)$

$$
\begin{aligned}
\hat{\mathbf{g}}_{Hop_l}(i) &= [g_{Hop_l}(1,i), g_{Hop_l}(2,i)]^T = \mathbf{H}_{Hop_l}^H \mathbf{r}_{Hop_l}(i) \\
&= \Delta_{Hop_l} \mathbf{s}(i) + \mathbf{H}_{Hop_l}^H \mathbf{I}_{Hop_l}(i) \\
&+ \mathbf{H}_{Hop_l}^H \mathbf{n}_{Hop_l}(i) \qquad \text{for} \qquad l \in 1,2 \qquad (3.6.8)
\end{aligned}
$$

Due to the Alamouti structure [5]

$$
\Delta_{Hop_l} = \mathbf{H}_{Hop_l}^H \mathbf{H}_{Hop_l} = \begin{bmatrix} \lambda_{Hop_l} & 0 \\ 0 & \lambda_{Hop_l} \end{bmatrix} \qquad (3.6.9)
$$

where

$$
\mathbf{H}_{Hop_l} = \begin{bmatrix} h_{11}^l & h_{21}^l \\ h_{21}^{*l} & -h_{11}^{*l} \\ h_{12}^l & h_{22}^l \\ h_{22}^{*l} & -h_{12}^{*l} \end{bmatrix} \qquad (3.6.10)
$$

and

$$
\lambda_{Hop_l} = |h_{11}^l|^2 + |h_{21}^l|^2 + |h_{12}^l|^2 + |h_{22}^l|^2 \qquad \text{for} \qquad l \in 1,2
$$

- Apply the LS method to detect which symbols were actually transmitted.

$$
\hat{s}_{Hop_l}(t,i) = arg \min_{s_t \in S} |\hat{g}_{Hop_l}(t,i) - \lambda_{Hop_l} s_t|^2 \qquad \text{for} \qquad l,t \in 1,2
$$
$$
(3.6.11)
$$

where S is the alphabet containing M symbols for PSK. Due to imperfect synchronization in both hops, the above procedure will suffer from significant detection error, because the $\mathbf{H}_{Hop_l} \mathbf{I}_{Hop_l}(i)$ component

in (3.6.8) will damage the orthogonality of the distributed A-STBC in both hops. To overcome the issue of imperfect synchronization in both hops PIC detection is again used as in the following section.

3.6.1   The Parallel Interference Cancelation Detection

As mentioned in Section 3.4, the PIC detection scheme is used to mitigate the ISI at the receiver side in both hops and multiple iterations are utilized in detecting the desired signal. To overcome the impact of imperfect synchronization in both hops the interference component of $I^l_{int_k}(t,i)$ should be removed from (3.6.2) in both hops, assuming CSI at both received nodes. Therefore, the principle of PIC detection is applied to combat the interference component $I^l_{int_k}(t,i)$, $l,k,t \in 1,2$. Since $s^*(1, i-1)$ in (3.6.3) is already known in both hops if the detection process has been initialization properly, $I^l_{int_k}(1,i)$, $l,k \in 1,2$, can be mitigated during the initialization stage from both hops at the received node. The PIC iteration process can be represented as follows

- Set iteration number $q = 0$

- From the received signal $\mathbf{r}_{Hop_l}$ in (3.6.5) is calculated as

$$\mathbf{r}^{'(0)}_{Hop_l} = \begin{bmatrix} r^l_1(1,i) - I^l_{int_1}(1,i) \\ r^{*l}_1(2,i) \\ r^l_2(1,i) - I^l_{int_2}(1,i) \\ r^{*l}_2(2,i) \end{bmatrix}$$

- Substitute $\mathbf{r}_{Hop_l}(i)$ with $\mathbf{r}^{'(0)}_{Hop_l}(i)$ to obtain $\hat{\mathbf{g}}^{(0)}_{Hop_l}(i)$ as in (3.6.8) and then apply LS detection in (3.6.11) to detect $\hat{\mathbf{s}}^{(0)}_{Hop_l}(i)$ by replacing $\hat{\mathbf{g}}_{Hop_l}(i))$ with $\hat{\mathbf{g}}^{(0)}_{Hop_l}(i)$

- Set iteration number $q = 1, 2, ..., n$

- Remove additional ISI by calculating

$$
\mathbf{r}_{Hop_l}^{'(q)} = \begin{bmatrix} r_1^l(1, i) - I_{int_1}^l(1, i) \\ r_1^{*l}(2, i) - I_{int_1}^{l(q-1)}(2, i) \\ r_2^l(1, i) - I_{int_2}^l(1, i) \\ r_2^{*l}(2, i) - I_{int_2}^{l(q-1)}(2, i) \end{bmatrix}
$$

where $I_{int_k}^{l(q-1)}(2, i) = h_{2j}^{*l}(-1)[s_{Hop_l}^{(q-1)}(2, i)]^*$, where $l, k \in 1, 2$

- Substitute $\mathbf{r}_{Hop_l}(i)$ with $\mathbf{r}_{Hop_l}^{'(q)}(i)$ to obtain $\hat{\mathbf{g}}_{Hop_l}^{(q)}(i)$ as in (3.6.8) and then apply LS detection in (3.6.11) to detect $\hat{\mathbf{s}}_{Hop_l}^{(q)}(i)$ by replacing $\hat{\mathbf{g}}_{Hop_l}(i))$ with $\hat{\mathbf{g}}_{Hop_l}^{(q)}(i)$

- Repeat the process from point 4 until $q = n$

The above algorithm will mitigate the interference component $I_{int_k}^l(t, i)$, $l, k, t \in 1, 2$, and most of the end-to-end performance cooperative diversity gain will be achieved in 2-3 iteration of the PIC process [75] and [76]. .Therefore, the PIC detection is an effective in mitigating the error of synchronization in both hops as will be shown in the next section. Furthermore, the end-to-end bit error rate performance is studied when the distributed A-STBC approach is employed at both stages (see Appendix B).

3.7   Simulation Results

In this section, the simulation of the algorithms developed in this section is carried out. The channel coefficients are modelled as circularly symmetric complex valued i.i.d. Gaussian random values with zero

mean and unit variance. All simulations performed in this section are without outer coding and the end-to-end BER performance against SNR in dB is simulated by using an 8PSK Gray mapping scheme. The SNR is defined as SNR σ_s^2/σ_n^2 and all nodes transmit at 1/2 power.

Figure 3.12 compares the performance of two stage perfect synchronization (PS) with DT link assisted cooperation in [75] under imperfect synchronization i.e. no time delay and the proposed solution of two stage multi-source multi-relay (MS-MR) scheme without DT link between the source nodes and the destination nodes as shown in Figure 3.11.
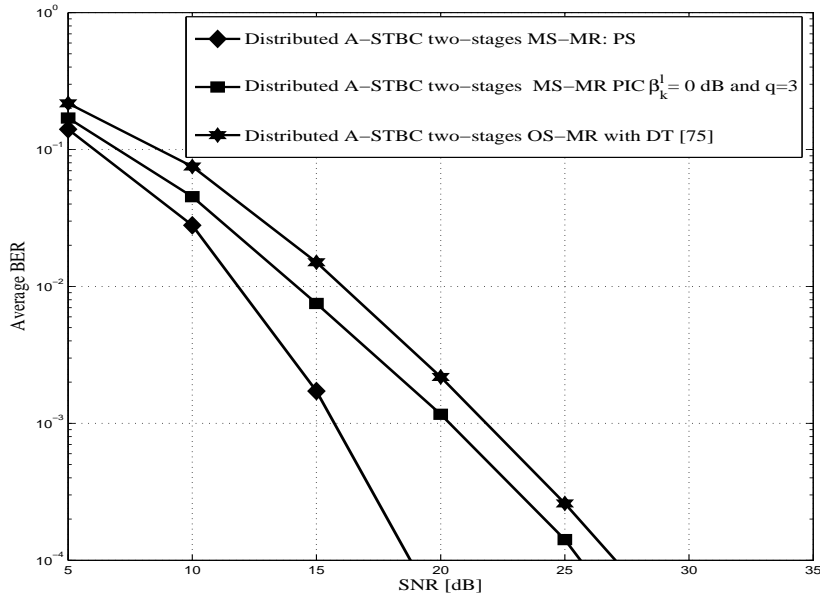
Figure 3.12. End-to-end performance of two-stages perfect synchronization (PS) with DT in [73] compared with the proposed solution and when $\beta_k^l = 0$ dB and $q = 3$.

It is clear that from Figure 3.12 the proposed relaying solution still provides an improved performance, for instance at BER of 10^{-3}, the proposed two stages MS-MR scheme in perfect synchronization pro-

vides a power saving of approximately 8 dB and 2 dB under large time misalignments $\beta_k^l = 0$ dB and when PIC iteration is $q = 3$, as compared with the DT link assisted cooperation scheme in [75]. Hence, the rest of the simulations do not consider the DT link between the source nodes and the destination nodes.

However, Figure 3.13 shows the end-to-end BER performance of a conventional detector when there is perfect synchronization in a distributed A-STBC in an MS-MR scheme, and also when there is imperfect synchronization under different $\beta_k^l = 0, -3, -5$ dB. From the figure, it can be observed that the conventional approach is not effective with synchronization error even under small time misalignment $\beta_k^l = -5$ dB.
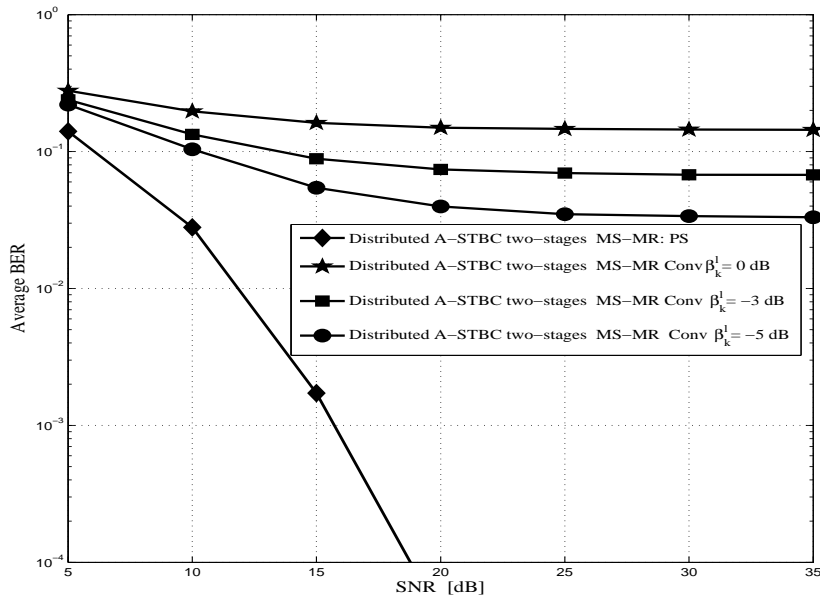
Figure 3.13. End-to-end performance for two-stage multi-source (MS) multi-relay (MR) conventional detector under different β_k^l values compared with conventional detector perfect synchronization (PS).

However, Figure 3.13 shows the end-to-end BER performance of a conventional detector when there is perfect synchronization in a dis-

tributed A-STBC in an MS-MR scheme, and also when there is imperfect synchronization under different $\beta_k^l = 0, -3, -5$ dB. From the figure, it can be observed that the conventional approach is not effective with synchronization error even under small time misalignment $\beta_k^l = -5$ dB.

On the other hand, the PIC detection scheme is an effective in mitigating synchronization error at both the relay nodes and the destination node and its AMT node, even under large time misalignments $\beta_k^l = 0$ dB as shown in Figure 3.14 when the number of PIC detector iteration $q = 3$.
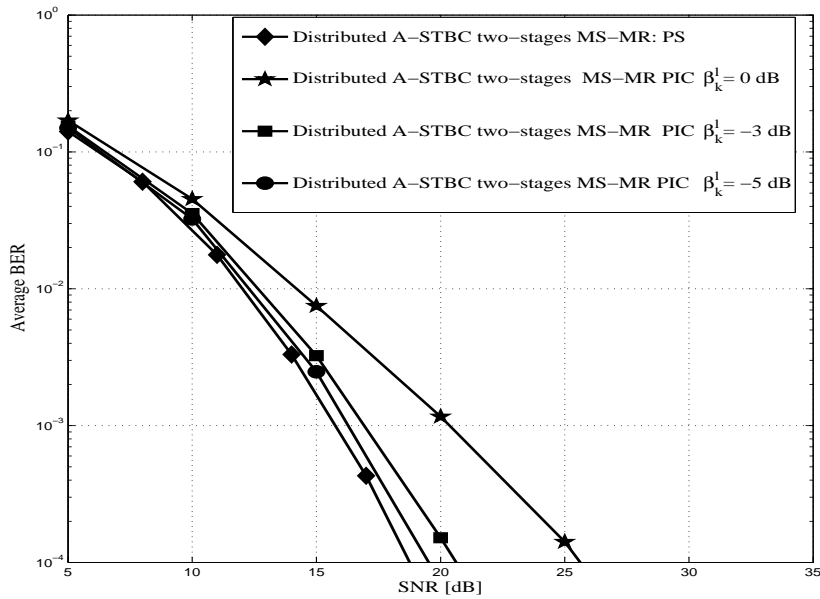
Figure 3.14. End-to-end performance with the PIC detector under different β_k^l values, when the number of PIC iterations $q = 3$.

Figure 3.14 illustrates the end-to-end BER performance with the PIC detector iteration $q = 3$ with different $\beta_k^l = 0, -3, -5$ dB. To achieve a bit error probability of 10^{-3} approximately 17 dB SNR is necessary in the two stage MS-MR scheme in the perfect synchronization case. However, in the case of using the PIC detection scheme

when $q = 3$ and $\beta_K^l = 0, -3, -5$ approximately 23, 19, 18 dB SNR, respectively, are required in the two stage MS-MR scheme under perfect synchronization case. Therefore, the PIC detection scheme is a very effective method to overcome error synchronization even under large time misalignments and the third iteration will deliver the performance gain in both hops, while the conventional detector does not deliver the performance gain under imperfect synchronization between any two nodes in both hops.

3.8   Chapter Summary

In this chapter the potential advantage of using distributed STBCs in DF relaying systems with and without the DT link between the source node and the destination node under imperfect synchronization at the receiver node have been presented. In particular, it was shown that with an appropriate coding scheme across the relay nodes coupled with increase in number of cooperating relay nodes, results in a significant performance improvement in the entire network.

Having established the importance of using four relay nodes in the network, the chapter compared the distributed closed-loop QO-STBC and closed-loop EO-STBC with distributed A-STBC [75] and distributed O-STBC [76]. In both closed-loop schemes, a good performance with full data transmission rate between the relay nodes and the destination node has been achieved with simple linear detection, contrary to distributed O-STBC [76]. Furthermore, the results showed the performance gain by deploying distributed closed-loop EO-STBC scheme as against the distributed A-STBC, distributed O-STBC and distributed closed QO-STBC over the relay nodes. This suggests that

in a cooperative relay network, an increase in the number of cooperating relay nodes must be accompanied with appropriate coding techniques to maximize the network performance.

However, the DT link between the source node and the destination node is considered in all cases, which leads to a reduction in the effect of path loss on the data transmitted from the source node to destination node [86] and also a reduction in the end-to-end BER at the destination node. Next, the use of multiple level cooperation among all nodes of each hop without DT link between the source node and the destination node under imperfect synchronization at both the relay nodes and the destination node was demonstrated in this chapter. Therefore, the use of a multilevel cooperative multi-hop solution provides a significant improvement in networks as compared to the DT link assisted cooperation using distributed A-STBC [75] and provides more robustness to the small scale fading.

In all cases considered, the effect of imperfect synchronization at the receiver nodes is shown to induce ISI. To mitigate the effect of interference on the system performance at the symbol level and due to the interference component in the received signals, the conventional detector is subject to performance degradation. Therefore, to improve the performance of the interference cancellation in the system, the PIC detection scheme was employed in all cases and provided an effective method to mitigate the impact of imperfect synchronization.

Although multi-hop cooperative relay networks have gained much attention and meet the high coverage requirements in beyond 3G mobile radio systems [87], with the higher data transmission rate applications demanded of future wireless systems, there is need to consider

cooperative relay networks which will guarantee higher end-to-end performance and achieve more cooperative diversity in wireless networks. To this end the next chapter will focus on analyzing a cooperative relay network with practical distributed STBC and convolutive coding within asynchronous cooperative wireless relay networks without channel information at the relay nodes.

Chapter 4

DISTRIBUTED STBC WITH OUTER CODING FOR ASYNCHRONOUS COOPERATIVE RELAY NETWORKS

This chapter investigates the cooperative strategy for distributed space time block coding (STBC) design which is based on a linear dispersion code and exploits outer convolutive coding for asynchronous cooperative relay networks. Furthermore, to overcome this lack of synchronization and achieve high performance, a parallel interference cancellation (PIC) detection scheme with distributed Alamouti STBC (A-STBC) design with outer coding for two relay nodes and distributed closed-loop extended orthogonal STBC (CL EO-STBC) design with outer coding for four relay nodes are considered. Finally, the pairwise error probability (PEP) is analyzed to reveal the available cooperative diversity which can be utilized with distributed A-STBC and distributed CL EO-STBC within cooperative relay networks.

4.1 Introduction

A new cooperative strategy of distributed STBC in the case of perfect synchronization among the relay nodes was presented in [6] and [7] using real orthogonal, complex orthogonal and quasi-orthogonal designs. As mentioned in Chapter 2, in most cooperative relay networks, the transmission process can be divided in two orthogonal phases. In the first phase, the source node broadcasts signals to the relay nodes, while in the second phase, the relay nodes forward the received signals from the source node to the destination node without any decoding operations at the relay nodes. The signals transmitted by every relay node in the second phase are a linear function of their respective received signals and their conjugates. Therefore, the relay nodes generate a linear STBC codeword at the destination node.

This strategy is similar to the amplify-and-forward (AF) type transmission, which does not need channel information at the relay nodes, however, full channel information for the channels from the source node to the relay nodes and for the channels from the relay nodes to the destination node is required at the destination node. Furthermore, compared to the decode-and-forward (DF) strategy, it does not need any decoding operation at the relay nodes.

In [75] and [77] asynchronous cooperative relay networks were demonstrated using distributed A-STBC without outer coding for two relay nodes and distributed CL EO-STBC without outer coding for four relay nodes with the PIC detection technique at the destination node, respectively. These proposed schemes have the potential of delivering cooperative diversity order equal to the number of cooperating single antenna relay nodes between the relay nodes and the destination node

using a DF strategy, which leads to increased relay node complexity due to decoding and encoding operations at the relay nodes.

To overcome this complexity, in this chapter, the new distributed STBC strategy in [6] and [7] based on a linear dispersion code is designed for asynchronous cooperative relay networks utilizing distributed A-STBC and distributed CL EO-STBC designs with outer convolutive coding for two and four relay nodes, respectively. Applying PIC detection with these two designs at the destination node can mitigate the impact of imperfect synchronization caused by timing misalignment between the relay nodes and deliver full data transmission rate in each stage as well as achieving full cooperative diversity gain with a coding gain. Furthermore, the PEP analysis for both proposed schemes is presented to confirm the available cooperative diversity for synchronous cooperative relay networks.

This chapter is organized as follows, in Section 4.2 the distributed coherent STBC with outer coding is presented and asynchronous wireless relays networks with outer convolutive coding model using distributed A-STBC design and distributed CL EO-STBC design are demonstrated. In Section 4.3 described the problem of imperfect synchronization and its solution using the PIC detection scheme. The PEP analysis for distributed A-STBC and CL EO-STBC is analyzed in Section 4.4. Simulated end-to-end performance of both distributed STBC designs with outer coding is given in Section 4.5. Section 4.6 contains the summary of the chapter.

4.2 Distributed Coherent Space Time Block Coding with Outer Coding

4.2.1 Using A-STBC Design for two Relay Nodes

In this section the use of Alamouti's orthogonal design in networks with two relay nodes, where each relay node has a single antenna and can be used for both transmission and reception (half-duplex), under imperfect synchronization is considered, the basic structure is depicted in Figure 4.1. During the first phase, the source node transmits the signal vector $\mathbf{s}(i) = \sqrt{P_1}[s(1,i), -s^*(2,i)]^T$, where $[.]^T$ denotes the transpose of the vector $\mathbf{s}(i)$ and i denotes the discrete pair index in two different transmission periods, after being encoded by a convolutional encoder and passed through the interleaver as shown in Figure 4.1, where the average power per transmission used at the source node is denoted by P_1.
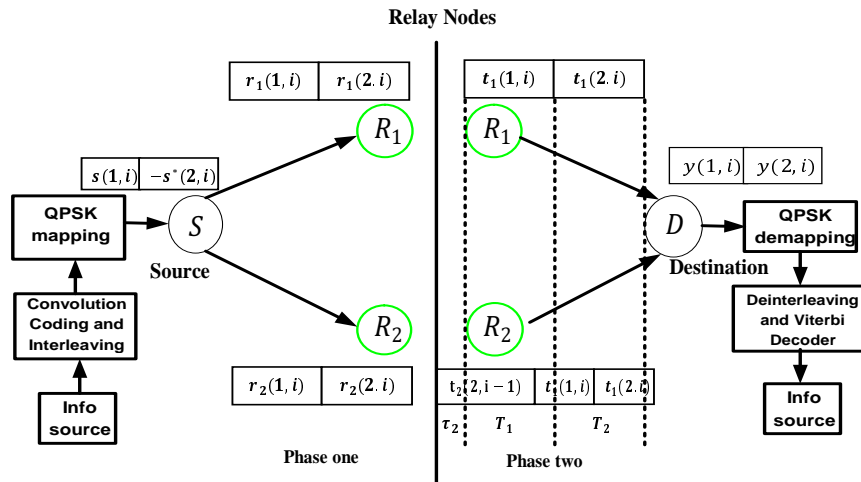
Figure 4.1. Basic structure of distributed A-STBC with outer coding for two relay nodes with two phases for the cooperative transmission process and time delay offset between the relay nodes at the destination node.

Therefore, the received signal vectors at the relay nodes are denoted by $\mathbf{r}_k(i)$, $k \in 1, 2$, and can be represented as follows

$$\mathbf{r}_k(i) = f_k \mathbf{s}(i) + \mathbf{v}_k(i) \tag{4.2.1}$$

where f_k, $k \in 1, 2$, is the channel coefficient between the source node and the relay nodes also f_k is assumed unchanged during a signal code block of two transmission periods (quasi-static frequency flat fading) and $\mathbf{v}_k(i) = [v_k(1, i), v_k(2, i)]^T$ is an additive Gaussian noise vector with elements having zero-mean and unit-variance at the relay nodes.

During the second phase, which also has two channel uses, the relay nodes transmit the received signal from the source node to the destination node. Distributed STBC in [6] and [7], which uses the idea of linear dispersion in [68][1] is used to design A-STBC at the relay nodes. Each relay node is equipped with a pair of fixed 2×2 unitary matrices, therefore the matrices used at the relay node are designed as in [7]

$$A_1 = \begin{bmatrix} 1 & 0 \\ 0 & 1 \end{bmatrix}, B_1 = 0_{2\times 2}, A_2 = 0_{2\times 2}, B_2 = \begin{bmatrix} 0 & -1 \\ 1 & 0 \end{bmatrix} \tag{4.2.2}$$

Therefore, each relay node will transmit a linear combination of symbols in $s(t, i)$ or $s^*(t, i)$, $t \in 1, 2$, (two transmission periods), however not both. Therefore, the transmitted signal vectors at both relay nodes are modelled as follows

$$\mathbf{t}_k(i) = \sqrt{\frac{P_1 P_2}{P_1 + 1}} (f_k A_k \mathbf{s}(i) + f_k^* B_k \mathbf{s}^*(i))$$
$$+ \sqrt{\frac{P_2}{P_1 + 1}} (A_k \mathbf{v}_k(i) + B_k \mathbf{v}_k^*(i)) \tag{4.2.3}$$

---

[1]This means no decoding complexity at the relay nodes as compared to the DF strategy.

By substituting (4.2.1) and (4.2.2) into (4.2.3) the transmitted signal from R_1 to the destination node during two transmission periods can be expressed as

$$
\begin{bmatrix} t_1(1,i) \\ t_1(2,i) \end{bmatrix} = \sqrt{\frac{P_1 P_2}{P_1 + 1}} \begin{bmatrix} f_1 s(1,i) \\ -f_1 s^*(2,i) \end{bmatrix}
$$
$$
+ \sqrt{\frac{P_2}{P_1 + 1}} \begin{bmatrix} v_1(1,i) \\ v_1(2,i) \end{bmatrix} \tag{4.2.4}
$$

and the transmitted signal from R_2 to the destination node during two transmission periods can be expressed as

$$
\begin{bmatrix} t_2(1,i) \\ t_2(2,i) \end{bmatrix} = \sqrt{\frac{P_1 P_2}{P_1 + 1}} \begin{bmatrix} f_2^* s(2,i) \\ f_2^* s^*(1,i) \end{bmatrix}
$$
$$
+ \sqrt{\frac{P_2}{P_1 + 1}} \begin{bmatrix} -v_2^*(1,i) \\ v_2^*(1,i) \end{bmatrix} \tag{4.2.5}
$$

However, the performance of the distributed A-STBC systems is limited by the symbol-level synchronization problem among the relay nodes at the destination node. The transmitted signal $\mathbf{t}_2(i) = [t_2(1,i), t_2(2,i)]^T$ from the second relay node R_2 will arrive at the destination node at different transmission periods as shown in Figure 4.1. This will induce ISI at the destination node, which will destroy the structure of the distributed A-STBC at the destination node and the performance of the network is degraded severely as the interference level grows. There is normally a timing misalignment of τ_2 from the second relay node R_2 at the destination node and it is assumed that τ_2 is smaller than the sample period T and without loss of generality, the first relay node R_1 is assumed to be fully synchronized with the destination node as shown

in Figure 4.1. Therefore, the received signals over two independent transmission periods at the destination node with the interference term due to inter-relay node synchronization with the second relay node R_2 can be represented as follows

$$
\begin{bmatrix} y(1,i) \\ y(2,i) \end{bmatrix} = g_1 \begin{bmatrix} t_1(1,i) \\ t_1(2,i) \end{bmatrix} + g_2 \begin{bmatrix} t_2(1,i) \\ t_2(2,i) \end{bmatrix}
$$

$$
+ \underbrace{g_2(-1) \begin{bmatrix} t_2(2,i-1) \\ t_2(1,i) \end{bmatrix}}_{\mathbf{I}_{int}(i)} + \begin{bmatrix} w(1,i) \\ w(2,i) \end{bmatrix} \qquad (4.2.6)
$$

where $\mathbf{I}_{int}(i)$ represents the ISI from the second relay node R_2 and $w(1,i)$ and $w(2,i)$ are the total additive Gaussian noise terms with zero-mean and unit-variance at the destination node in two different transmission periods. Due to imperfect synchronization $g_2(-1)$ reflects the ISI from the previous symbols under imperfect inter node synchronization. Substituting (4.2.4) and (4.2.5) into (4.2.6) the received signals at the destination node, conjugated for convenience at two independent transmission periods can be represented as follows

$$
\begin{bmatrix} y(1,i) \\ y^*(2,i) \end{bmatrix} = \sqrt{\frac{P_1 P_2}{P_1 + 1}} \underbrace{\begin{bmatrix} g_1 f_1 & g_2 f_2^* \\ g_2^* f_2 & -g_2^* f_2^* \end{bmatrix}}_{\mathbf{H}} \begin{bmatrix} s(1,i) \\ s(2,i) \end{bmatrix}
$$

$$
+ \sqrt{\frac{P_1 P_2}{P_1 + 1}} \underbrace{\begin{bmatrix} g_2(-1) f_2^* s^*(1,i-1) \\ g_2^*(-1) f_2 s^*(2,i) \end{bmatrix}}_{\mathbf{I}_{int}(i)}
$$

$$
+ \underbrace{\begin{bmatrix} w(1,i) \\ w^*(2,i) \end{bmatrix}}_{\mathbf{w}(i)} \qquad (4.2.7)
$$

where

$$
\mathbf{w}(i) = \begin{bmatrix} w(1,i) \\ w^*(2,i) \end{bmatrix} = \sqrt{\frac{P_2}{P_1+1}} \left(\begin{bmatrix} g_1 v_1(1,i) \\ g_1^* v_1^*(2,i) \end{bmatrix} + \begin{bmatrix} -g_2^* v_2^*(2,i) \\ g_2^* v_2(1,i) \end{bmatrix} \right)
$$
$$
+ \begin{bmatrix} n_{rd}(1,i) \\ n_{rd}^*(2,i) \end{bmatrix}
$$

$$(4.2.8)$$

where g_k, $k \in 1,2$, is the channel used between the relay nodes and the destination node, and it is modeled as circularly symmetric complex Gaussian random with zero-mean and unit-variance and $n_{rd}(1,i)$ and $n_{rd}(2,i)$ are the additive Gaussian noise terms at the destination node with zero-mean and unit-variance distribution in two different transmission periods. Due to unity variance assumption of additive noise $\mathbf{v}_k(i)$ from the source node to the relay nodes in (4.2.3) the average power of the signal at the relay nodes is $P_1 + 1$. Considering P_2 is the average transmission power at each relay node, therefore the power allocation scheme can be written as [6]

$$
P_1 = \frac{P}{2} \quad \text{and} \quad P_2 = \frac{P}{2R} \tag{4.2.9}
$$

where $R = 2$ is the number of relay nodes in the network. Therefore, from (4.2.9), it is observed that the optimum power allocation is such that the source node uses half the total power and the relay nodes share the other half. Therefore, the received signal in (4.2.7) at the destination node can be re-written in matrix form as

$$
\mathbf{y}(i) = \sqrt{\frac{P_1 P_2}{P_1+1}} (\mathbf{H}\mathbf{s}(i) + \mathbf{I}_{int}(i)) + \mathbf{w}(i) \tag{4.2.10}
$$

where $\mathbf{I}_{int}(i)$ is the ISI from neighboring symbols at the destination node and it is modelled as in (4.2.7). Since the equivalent channel $\mathbf{H}$ matrix is known at the destination node and the equivalent noise vector $\mathbf{w}(i)$ is a circularly symmetric complex Gaussian random vector whose mean is zero and covariance matrix is $\left[1 + \frac{P_2}{P_1+1}(|g_1|^2 + |g_2|^2)\right]\mathbf{I}_2$, where $\mathbf{I}_2$ is the 2×2 identity matrix. Therefore, the ML decoding at the destination node is thus

$$\hat{\mathbf{s}}(i) = \arg \min_{\mathbf{s}_k(i) \in \mathbf{S}} \left\| \mathbf{y}(i) - \sqrt{\frac{P_1 P_2}{P_1 + 1}} \mathbf{H}\mathbf{s}_k(i) \right\|_F^2 \qquad (4.2.11)$$

where $||.||_F$ is the Frobenius norm and $\mathbf{S}$ is the set of all possible vector symbols. Due to the interference term $\mathbf{I}_{int}(i)$ in (4.2.10), the ML decoding will not exploit the full cooperative diversity order as will be seen in the simulation results.

4.2.2 Using Closed-loop Extended Orthogonal Space Time Block Coding Design for Four Relay Nodes

As shown in Figure 4.2, the outer coding wireless relay network with one source node, one destination node and four relay nodes, where each node only utilizes one antenna element is considered. The direct transmission (DT) link is assumed to be available between the source node and the destination node and all channels between any two nodes are quasi-static flat Rayleigh fading. The distributed open-loop EO-STBC code word $\mathbf{S}$ that is needed to be generated at the destination node has the following form

$$\mathbf{S} = \begin{bmatrix} s(1,i) & s(1,i) & s(2,i) & s(2,i) \\ -s^*(2,i) & -s^*(2,i) & s^*(1,i) & s^*(1,i) \end{bmatrix} \qquad (4.2.12)$$
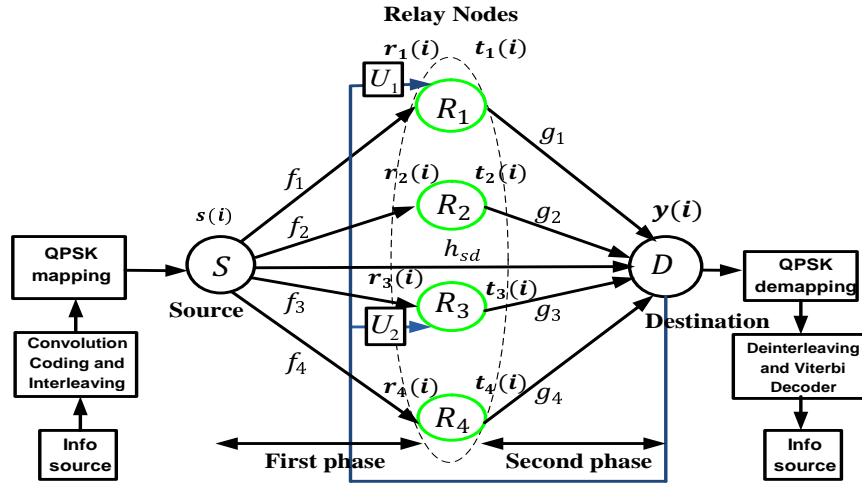
Figure 4.2. Basic structure of distributed CL EO-STBC with outer coding using two-bit feedback based on phase rotation for four relay nodes with single antenna in each relay node and one antenna in the source and the destination node with two phases for the cooperative transmission process.

Therefore, the information sequence after being encoded by the convolutional encoder is passed through the interleaver at the source node as shown in Figure 4.2. It is then mapped into quadrature phase shift keying (QPSK) symbols $\mathbf{s}(i) = \sqrt{P_1}[s(1,i), -s^*(2,i)]^T$. During the first phase the received signal through the DT link between the source node and the destination node can be represented as follows

$$\mathbf{r}_{sd}(i) = h_{sd}\mathbf{s}(i) + \mathbf{n}_{sd}(i) \qquad (4.2.13)$$

where h_{sd} is the channel gain between the source node and the destination node and it is modelled as a Rayleigh flat fading channel and $\mathbf{n}_{sd}(i) = [n_{sd}(1,i), n_{sd}(2,i)]^T$ is a noise vector containing independent circularly-symmetric complex additive Gaussian random variables at the destination node, each having zero-mean and unit-variance. Furthermore, the received signals at the relay nodes can be represented

as in (4.2.1), $k \in 1, 2, 3, 4$. During the second phase, the relay nodes will process and transmit the received noisy signals to the destination node using linear dispersion coding as in [68]. The transmit signals at the relay node R_k are designed to be linear functions of their received signals and their conjugates as in (4.2.3), where A_k and B_k are the matrices at the relay nodes R_k, $k \in 1, 2, 3, 4$, and the relay nodes have been designed to use the following matrices

$$A_1, A_2 = \begin{bmatrix} 1 & 0 \\ 0 & 1 \end{bmatrix}, B_1, B_2 = 0_{2 \times 2}, A_3, A_4 = 0_{2 \times 2}, B_3, B_4 = \begin{bmatrix} 0 & -1 \\ 1 & 0 \end{bmatrix}$$

As mentioned in Section 4.2, in order to achieve the maximum cooperative diversity gain between the source node and the destination node, the relay nodes are scheduled to broadcast their signals simultaneously. However, synchronous reception at the destination node is often unrealistic due to propagation delay among the relay nodes as shown in Figure 4.3. There is normally a timing misalignment of $\tau_2 = \tau_3 = \tau_4 \neq 0$ from relay nodes R_k, $k \in 2, 3, 4$.
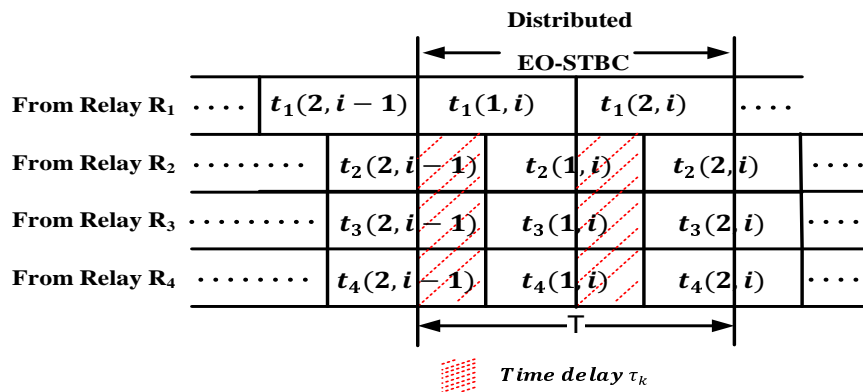
Figure 4.3. Representation of time delay of imperfect synchronization between relay nodes at the destination node, which induces ISI from R_2, R_3 and R_4 [57] and [76].

The time delay τ_k is assumed to be smaller than sample period T and all time delays τ_k are also assumed for convenience to be identical as shown in Figure 4.3 [75] and [76]. Such a relative time delay from R_k, $k \in 2, 3, 4$, will induce ISI from neighboring symbols at the destination node owing to sampling or matched filtering (whatever pulse shaping is used). Nevertheless, the destination node is assumed to be fully synchronized to R_1 i.e. $\tau_1 = 0$. Therefore, the received signals at the destination node at two different transmission periods can be represented as follows

$$\mathbf{y}(i) = \sum_{k=1}^{4} g_k \begin{bmatrix} t_k(1,i) \\ t_k(2,i) \end{bmatrix} + \underbrace{\sum_{k=2}^{4} g_k(-1) \begin{bmatrix} t_k(2,i-1) \\ t_k(1,i) \end{bmatrix}}_{\mathbf{I}_{int}(i)} + \begin{bmatrix} w(1,i) \\ w(2,i) \end{bmatrix}$$

$$(4.2.14)$$

where g_k, $k \in 1, 2, 3, 4$, denote the channel coefficients between the relay nodes and the destination node and they are assumed to be zero-mean and unit-variance complex Gaussian random variables, $\mathbf{y}(i) = [y(1,i), y(2,i)]^T$ is the received signal vector at the destination node over two different transmission periods under imperfect synchronization level, $\mathbf{I}_{int}(i) = [I_{int}(1,i), I_{int}(2,i)]^T$ denotes the total interference vector at the destination node, $g_k(-1)$, $k \in 2, 3, 4$, reflect the ISI from the previous symbols under synchronization error and $w(1,i)$ and $w(2,i)$ are the additive Gaussian noise terms with zero-mean and unit-variance at the destination node in two different transmission periods. By taking the conjugate of $y(2,i)$ in (4.2.14), the equivalent channel $\mathbf{H}$ matrix corresponding to the codeword in (4.2.12) used over four relay nodes is given by

$$\mathbf{H} = \begin{bmatrix} f_1 g_1 + f_2 g_2 & f_3^* g_3 + f_4^* g_4 \\ f_3 g_3^* + f_4 g_4^* & -f_1^* g_1^* - f_2^* g_2^* \end{bmatrix} \tag{4.2.15}$$

Applying the matched filtering at the destination node and thereby forming the $\mathbf{H}^H \mathbf{H}$ matrix, where $(.)^H$ denotes Hermitian (complex conjugate transpose), the Grammian matrix Δ can be represented by

$$\Delta = \begin{bmatrix} \lambda_c + \lambda_f & 0 \\ 0 & \lambda_c + \lambda_f \end{bmatrix} \tag{4.2.16}$$

where λ_c denotes the total channel gain for four relay nodes and λ_f is denoted as the channel dependent interference parameter. Although the decoding complexity is low, the λ_f term may be negative which leads to some diversity loss. In order to achieve a full cooperative diversity gain between the relay nodes and the destination node, two-bit feedback $U_1 = (-1)^a$ and $U_2 = (-1)^b$ is used to rotate the phases of the signals before they are transmitted from the first and third relay nodes respectively, to ensure that the λ_f term is positive during the whole transmission; while the other two relay nodes are kept unchanged as shown in Figure 4.2 and presented in Appendix A, where $a, b \in 0, 1$, here a, b, are two feedback parameters determined by the channel condition[2] [16]. Therefore, the received signal in (4.2.14) at two independent transmission periods after taking the conjugate of $y(2, i)$ can be re-written as follows

$$y(t, i) = t_1(t, i) U_1 g_1 + t_2(t, i) g_2 + t_3(t, i) U_2 g_3 + t_4(t, i) g_4$$
$$+ I(t, i) + w(t, i) \quad \text{for} \quad t \in 1, 2 \tag{4.2.17}$$

---

[2]In particular, when a or $b = 1$, U_1 or $U_2 = -1$, which means the signals from the first and third relay nodes will be phase rotated by $180°$ before transmission. Otherwise, they can be directly transmitted.

where

$$
\begin{aligned}
I_{int}(1,i) &= \sqrt{\frac{P_1 P_2}{P_1 + 1}}(g_2(-1)f_2 s(2, i-1) + (g_3(-1)U_2 f_3^* \\
&\quad + g_4(-1)f_4^*)s^*(1, i-1)) \\
I_{int}(2,i) &= \sqrt{\frac{P_1 P_2}{P_1 + 1}}(g_2(-1)f_2 s(1, i) + (g_3(-1)U_2 f_3^* + g_4(-1)f_4^*)s(2, i))
\end{aligned}
$$

$$(4.2.18)$$

and

$$
\begin{aligned}
w(t,i) &= \sqrt{\frac{P_2}{P_1 + 1}}(U_1 g_1 v_1(t, i) + g_2 v_2(t, i) + U_2 g_3 v^*(t, i) \\
&\quad + g_4 v_4^*(t, i)) + n_{rd}(t, i) \quad \text{for} \quad t \in 1, 2
\end{aligned}
$$

$$(4.2.19)$$

where $n_{rd}(t, i)$, $t \in 1, 2$, is the noise term at the destination node whose entries represent independent complex Gaussian random variables with zero-mean and unit-variance and the equivalent channel matrix $\mathbf{H}$ in (4.2.15) becomes

$$
\mathbf{H} = \begin{bmatrix} U_1 f_1 g_1 + f_2 g_2 & U_2 f_3^* g_3 + f_4^* g_4 \\ U_2^* f_3 g_3^* + f_4 g_4^* & -U_1^* f_1^* g_1^* - f_2^* g_2^* \end{bmatrix}
$$

$$(4.2.20)$$

Therefore, the received signal in (4.2.17) at the destination node can be re-written in matrix form as in (4.2.10) and the power allocation scheme can be represented as in (4.2.9), where $R = 4$, which represents the number of the relay nodes in the network. With the estimated results of $\mathbf{H}$, the signal-to-noise ratio (SNR) at the destination node can be calculated as follows

$$SNR = \left(\underbrace{\sum_{j=1}^{4}(|f_j g_j|^2)}_{\lambda_c} + \underbrace{2\Re(U_1 f_1 g_1 f_2^* g_2^* + U_2 f_3^* g_3 f_4 g^*)}_{\lambda_f} \right) \frac{\sigma_s^2}{\sigma_n^2} \quad (4.2.21)$$

where $\Re\{.\}$ denotes the real part of a complex number and σ_s^2 is the to-tal transmit power of the desired signal and σ_n^2 is the noise power at the destination node. It is clear from the above analysis in (4.2.21) that if $\lambda_f > 0$, the designed CL EO-STBC can obtain additional performance gain, which leads to an improved whole channel gain and correspond-ingly the SNR at the destination node. According to the analysis in Appendix A, the value of U_1 and U_2 can be formed from the following design criteria

$$a = \begin{cases} 0, & \text{if} \quad f_1 g_1 f_2^* g_2^* \geq 0 \\ 1, & \text{otherwise} \end{cases} \quad (4.2.22)$$

$$b = \begin{cases} 0, & \text{if} \quad f_3^* g_3 f_4 g_4^* \geq 0 \\ 1, & \text{otherwise} \end{cases} \quad (4.2.23)$$

Since the equivalent channel $\mathbf{H}$ matrix is known at the destination node and the equivalent noise vector $\mathbf{w}(i)$ is a circularly symmetric complex Gaussian random vector whose means is zero and covariance matrix is $\left[1 + \frac{P_2}{P_1+1}((\sum_{k=2,4} |g_k|^2) + |U_1 g_1|^2 + |U_2 g_3|)\right] \mathbf{I}_2$[3]. Therefore, the ML decoding at the destination node can be represented as in (4.2.11). As mentioned in Section (4.2.2), the ML detection in (4.2.11) for dis-tributed CL EO-STBC can suffer from synchronization error at the destination node, because the $I(t,i)$ component in (4.2.17) will destroy the orthogonality of distributed CL EO-STBC at the destination node, where $t \in 1, 2$.

---

[3]Since $|U_1|^2 = |U_2|^2 = 1$, the covariance matrix becomes $\left[1 + \frac{P_2}{P_1+1} \sum_{k=1}^{4} |g_k|^2\right]$.

4.3 The Synchronization Problem and Parallel Interference Cancellation Detection

As mentioned above, signals transmitted from the relay nodes are received asynchronously at the destination node. Such assumptions will damage the orthogonality for any kind of distributed STBC, also this will lead to substantial system performance degradation. Therefore, the coefficients of $g_k(-1)$, $k \in 2$, in the case of two relay nodes and $k \in 2, 3, 4$, in the case of four relay nodes, depends upon timing delay τ_k and the particular pulse shaping waveform used and its relative strength can be represented by ratio as follows

$$\beta_k = \frac{|g_k(-1)|^2}{|g_k|^2} \begin{cases} k \in 2 & \text{if } R = 2 \\ k \in 2, 3, 4 & \text{if } R = 4 \end{cases} \tag{4.3.1}$$

As discussed in Section 3.4 the PIC is a promising detection technique for interference cancellation. Furthermore, this technique relies on simple processing elements constructed around the matched filter concept. Therefore, the PIC detection scheme presented in Section 2.5 is used with the proposed schemes in Sections 4.2 to remove the interference term $\mathbf{I}_{int}(i)$ in (4.2.10) for both designs. Since $s^*(1, i-1)$ in (4.2.7), and $s^*(1, i-1)$ and $s(2, i-1)$ in (4.2.18) are in fact known if the detection process has been initialized properly, $I_{int}(1, i)$ in (4.2.7) and (4.2.18) can be removed during the initialization stage as mentioned in Section 3.4. Therefore, the general PIC iteration process can be applied to eliminate the interference term of $\mathbf{I}_{int}(i)$ in (4.2.10) for both proposed schemes as follows

1. Initialization

2. Set iteration $q = 0$

3. From the received signal $\mathbf{y}(i)$ in (4.2.7) for the case of distributed A-STBC and in (4.2.17) for the case of distributed CL EO-STBC, calculate

$$\mathbf{y}'^{(0)}(i) = \begin{bmatrix} y(1,i) - I_{int}(1,i) \\ y^*(2,i) \end{bmatrix}$$

   substitute $\mathbf{y}(i)$ in (4.2.11) with $\mathbf{y}'^{(0)}(i)$ to detect the $\hat{\mathbf{s}}^{(0)}(i)$

4. If the number of relay nodes $R = 2$ then go to point 6

5. If the number of relays nodes $R = 4$

   The received signal of the DT link between the source node and the destination node in (4.2.13) can be detected and used as follows

$$\hat{s}_{sd}(t,i) = arg\{\min_{s_m \in S} |\Lambda - \sqrt{P_1}|h_{sd}|^2 s_m|^2\} \qquad \text{for} \quad t \in 1,2$$

   where

$$\Lambda = \begin{cases} h_{sd}^* r_{sd}(1,i) & \text{if} \quad t = 1 \\ -h_{sd} r_{sd}^*(2,i) & \text{if} \quad t = 2 \end{cases}$$

   Due to the poor performance of the ML detector within distributed CL EO-STBC in (4.2.11) [75] and [76]. Therefore, the detection result of the DT link is next used to initialize

$$\mathbf{s}^{(0)}(i) = [s^{(0)}(1,i), s^{(0)}(2,i)]^T = [\hat{s}_{sd}(1,i), \hat{s}_{sd}(2,i)]^T$$

6. Set iteration $q = 1, 2, ..., n$

7. Remove additional ISI from the received signal $y(2, i)$

$$\mathbf{y}^{'(q)}(i) = \begin{bmatrix} y^{'(0)}(1, i) \\ y^*(2, i) - I_{int}^{*(q-1)}(2, i) \end{bmatrix}$$

where $I^{(q-1)}(2, i)$ in the case of distributed A-STBC is

$$I_{int}^{(q-1)}(2, i) = \sqrt{\frac{P_1 P_2}{P_1 + 1}} (g_2(-1) f_2^* s^{(q-1)}(2, i))$$

and in the case of distributed CL EO-STBC is

$$\begin{aligned} I^{(q-1)}(2, i) = {} & \sqrt{\frac{P_1 P_2}{P_1 + 1}} ((g_2(-1) f_2 s^{(q-1)}(1, i) \\ & + (g_3(-1) U_2 f_3^* + g_4(-1) f_4^*) s^{(q-1)}(2, i)) \end{aligned}$$

8. Substitute $\mathbf{y}(i)$ in (4.2.11) with $\mathbf{y}^{'(q)}(i)$ to detect the $\hat{\mathbf{s}}^{(q)}(i)$

9. Repeat the process from point 6 until $q = n$

As will be seen in the simulation results, the above approach shows that, the PIC detection can mitigate the impact of imperfect synchronization among the relay nodes at the destination node. In distributed A-STBC and distributed CL EO-STBC, the performance of cooperative diversity gain can be achieved in 2-3 iterations of the PIC detection process as demonstrated in the simulation results.

4.4   Pairwise Error Probability Analysis

Pairwise error probability (PEP) is one of the common performance measure metrics used in evaluating wireless communication systems as presented in Section 2.3. It is simply referred to the probability of de-

tecting one symbol when another symbol is transmitted. Therefore, the system with the minimum PEP can be considered as the best system performance. In this section, the PEP of distributed STBC is analyzed by employing the distributed A-STBC and distributed CL EO-STBC assuming perfect synchronization among the relay nodes. Following the approach in [6] and assuming the destination node knows the channel coefficients f_k and g_k, $k \in 1, 2$, in the case of using A-STBC and $k \in 1, 2, 3, 4$, in the case of using CL EO-STBC the following Chernoff bound is

$$P_e\big(\mathbf{s}_k(i) \rightarrow \hat{\mathbf{s}}_k(i)\big) \leq \mathbf{E}_{f_k, g_k} \, \exp^{-\big(\hat{P}(\mathbf{h}_c^H \mathbf{S}_e^H \mathbf{S}_e \mathbf{h}_c + \zeta)\big)} \qquad (4.4.1)$$

where $\mathbf{E}(.)$ represents the statistical expectation operation with respect to the channel coefficients f_k and g_k, and ζ^4 can be represented as follows

$$\zeta = \begin{cases} 0 & \text{if} \quad \text{Using A-STBC} \\ \\ \lambda_f \mathbf{s}_e^H \mathbf{s}_e & \text{if} \quad \text{Using CL EO-STBC,} \end{cases}$$

$\mathbf{s}_e = \mathbf{s}_k(i) - \hat{\mathbf{s}}_k(i)$, $\mathbf{S}_e = \mathbf{S}_k(i) - \hat{\mathbf{S}}_k(i)$, $\mathbf{h}_c = [f_1 g_1, f_2^* g_2]^T$ in the case of using A-STBC and $\mathbf{h}_c = [U_1 f_1 g_1, f_2 g_2, U_2 f_3^* g_3, f_4^* g_4]^{T5}$ in the case of using CL EO-STBC, and $\hat{P} = \frac{P_1 P_2}{4(1 + P_1 + P_2 g)}$ with $g = (\sum_{k \in 2, 4} |g_k|^2 + |U_1 g_1|^2 + |U_2 g_3|^2)$. Since $|U_1|^2 = |U_2|^2 = 1$, then the channel gain for four relay nodes becomes $g = \sum_{k=1}^4 |g_k|^2$ in the case of distributed CL EO-STBC and the channel gain for two relay nodes becomes $g = \sum_{k=1}^2 |g_k|^2$ in the case of distributed A-STBC. It is important to note that $\mathbf{S}_k(i)$

---

[4]ζ denotes the array gain which can be achieved by using CL EO-STBC.

[5]Where in general $\mathbf{h}_c = [\hat{f}_1 g_1, ..., \hat{f}_R g_R]^T$ and the coefficient $\hat{f}_k$ can be calculated as $\hat{f}_k = f_k$ if $B_k = 0$ and $\hat{f}_k = f_k^*$ if $A_k = 0$, $k \in 1, 2$ in the case of using A-STBC and $k \in 1, 2, 3, 4$ in the case of using CL EO-STBC.

and $\hat{\mathbf{S}}_k(i)$ $(\mathbf{S}_k(i)\neq \hat{\mathbf{S}}_k(i))$ are two possible codewords of A-STBC or EO-STBC. Next, integrating over f_k as in [6] yields

$$P_e(\mathbf{s}_k(i) \to \hat{\mathbf{s}}_k(i)) \leq \mathbf{E}_{g_k} \exp^{-(\hat{P}\zeta)} \det^{-1}\left[\mathbf{I}_4 + \hat{P}\mathbf{S}_e^H\mathbf{S}_e D\right] \qquad (4.4.2)$$

With the optimum power allocation in (4.2.9), when $P \gg 1$ and the number of relay nodes R is large $g = \sum_{k=1}^{R}|g_k|^2 \approx R$, where $R = 2$ in the case of distributed A-STBC and $R = 4$ in the case of distributed CL EO-STBC, then (4.4.2) becomes

$$P_e(\mathbf{s}_k(i) \to \hat{\mathbf{s}}_k(i)) \leq \mathbf{E}_{g_k} \exp^{-\left(\frac{P}{16R}\zeta\right)} \det^{-1}\left[\mathbf{I}_R + \frac{P}{16R}\mathbf{S}_e^H\mathbf{S}_e D\right] \qquad (4.4.3)$$

where $D = diag\{|g_1|^2, ..., |g_R|^2\}$ and define $\mathbf{B} = \mathbf{S}_e^H\mathbf{S}_e$. The upper bound for the PEP using the minimum nonzero singular value of $\mathbf{B}$, which is denoted as σ_{min}^2, from (4.4.3) becomes

$$P_e(\mathbf{s}_k(i) \to \hat{\mathbf{s}}_k(i)) = \mathbf{E}_{g_k} \exp^{-\left(\frac{P}{16R}\zeta\right)} \prod_{j=1}^{R_\mathbf{B}}\left(1 + \frac{P\sigma_{min}^2}{16R}|g_k|^2\right)$$

$$= \exp^{-\left(\frac{P}{16R}\zeta\right)}\left(\frac{P\sigma_{min}^2}{16R}\right)^{-R_\mathbf{B}}$$

$$\left[-\exp^{\left(\frac{16R}{P\sigma_{min}^2}\right)}\mathbf{Ei}\left(-\frac{16R}{P\sigma_{min}^2}\right)\right]^{R_\mathbf{B}} \qquad (4.4.4)$$

where

$$\mathbf{Ei} = \int_{-\infty}^{\chi}\frac{e^t}{t}dt, \qquad \chi < 0$$

is the exponential integral function and $R_\mathbf{B}$ is the rank of $\mathbf{B}$

$$P_e(\mathbf{s}_k(i) \to \hat{\mathbf{s}}_k(i)) \lesssim \exp^{-\left(\frac{P}{16R}\zeta\right)}\left(\frac{16R}{P\sigma_{min}^2}\right)^{R_\mathbf{B}}\left(\frac{\log P}{P}\right)^{R_\mathbf{B}}$$

$$= \exp^{-\left(\frac{P}{16R}\zeta\right)}\left(\frac{16R}{P\sigma_{min}^2}\right)P^{-R_\mathbf{B}\left(1-\frac{\log\log P}{\log P}\right)}$$

$$(4.4.5)$$

which yields the same diversity as in [6], therefore when $\mathbf{B}$ is full rank, the diversity gain is $2\left(1 - \frac{\log\log\ P}{\log\ P}\right)$ in the case of distributed A-STBC and $4\left(1 - \frac{\log\log\ P}{\log\ P}\right)^6$ in the case of distributed CL EO-STBC with a smaller PEP due to the array gain λ_f.

4.5   Simulation Results

In this section, the simulation results shows how the synchronization error can cause a degradation in the system end-to-end BER performance and how it can be mitigated. The simulated performance of distributed STBC with outer coding and the comparison between distributed A-STBC and distributed CL EO-STBC is demonstrated. In all figures, the horizontal axis indicates the total power used in the network, while the vertical axis indicates end-to-end BER. Furthermore, all simulations which are presented in this section are simulated by using the QPSK mapping scheme. In order to show the BER performance, it is assumed that the channels from the source node to the relay nodes and from the relay nodes to the destination node are both quasi-static flat fading channels.

From Figure 4.4, it can be observed that the end-to-end BER performance of the relaying system based on distributed STBC without outer convolutive performs worse when compared to end-to-end BER performance of distributed STBC with outer convolutive coding. The performance of the proposed distributed CL EO-STBC with outer convolutive coding provides approximately 9 dB of gain at BER 10^{-3} as compared with distributed A-STBC with outer convolutive cod-

---

[6]When P is very large ($\log\ P \gg \log\log\ P$), the diversity gain is approximately equal to the number of cooperating relay nodes R.

ing. When the total power P is in dB, the coding gain is defined as $C_g = (P)_{Uncoded} - (P)_{Coded}$. Approximately C_g=18.5-16=2.5 at BER 10^{-3} in the case of distributed CL EO-STBC and approximately C_g=27.5-25=2.5 at BER 10^{-3} in the case of distributed A-STBC.
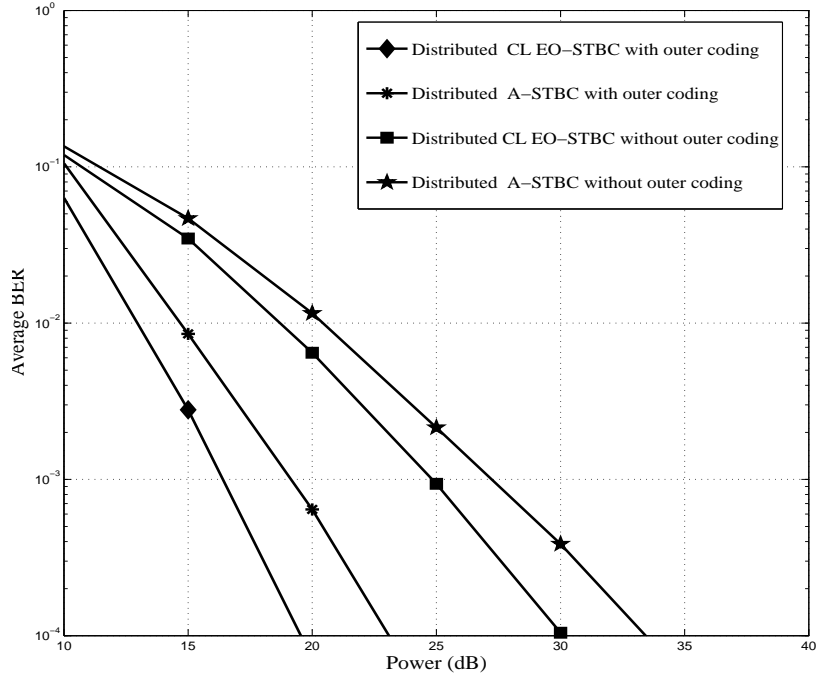
Figure 4.4. The end-to-end BER performance comparisons of proposed distributed STBC with and without outer coding schemes.

Figures 4.5 and 4.6 show the results of ML detection with different time misalignment among the relay nodes at the destination node for both proposed schemes, including the performance of both schemes under perfect synchronization (PS) as reference. It can be observed that from both figures and Table 4.1 the ML detection does not achieve the available cooperative diversity gain and cannot deliver a good end-to-end performance under imperfect synchronization errors even under small time misalignment $\beta_k = -6$ dB, $k \in 2$, in the case of distributed A-STBC and $k \in 2, 3, 4$, in the case of distributed CL EO-STBC.
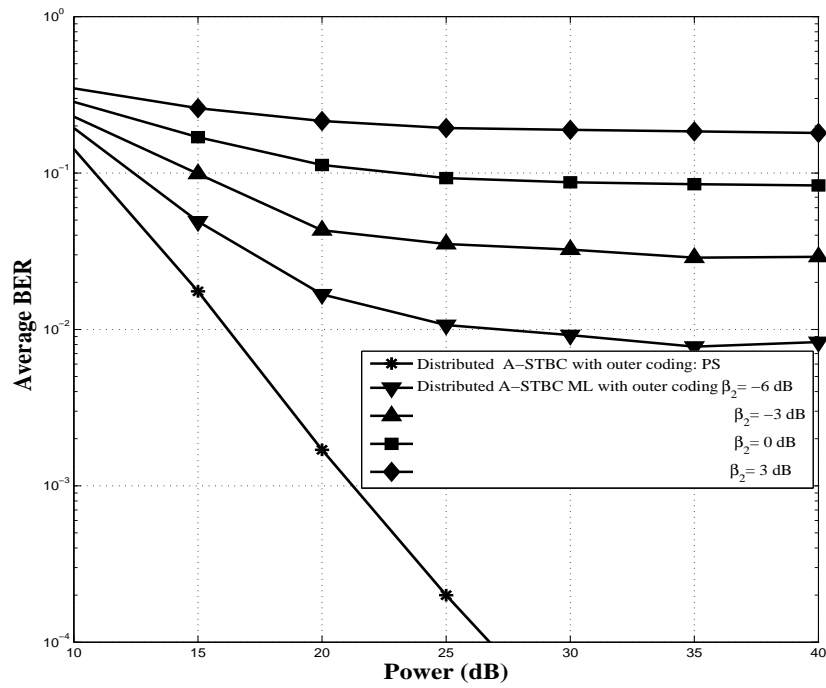
Figure 4.5. The end-to-end BER performance of distributed A-STBC with outer convolutive utilize ML detection under imperfect synchronization $\beta_k = 3, \ 0, \ -3, \ -6$ dB.
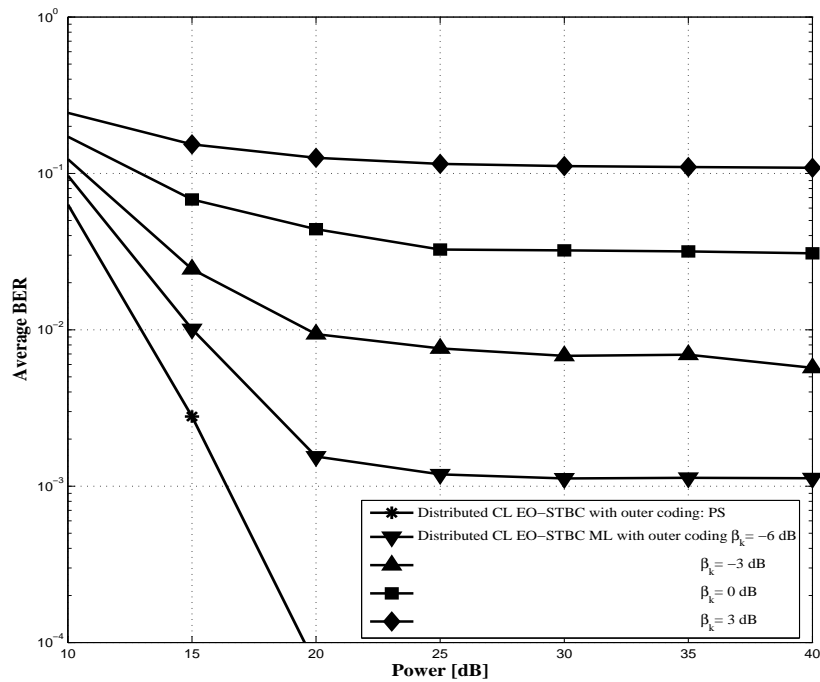
Figure 4.6. The end-to-end BER performance of distributed CL EO-STBC with outer convolutive coding utilizing ML detection under imperfect synchronization $\beta_k = 3, \ 0, \ -3. \ -6$ dB.

Table 4.1. End-to-end BER comparison between ML detection and PIC detection for distributed A-STBC and distributed CL EO-STBC under imperfect synchronization.

Distributed STBC schemes	β_k (dB)	BER	ML Power (dB)	number of iterations	PIC Power (dB)
A-STBC	0	10^{-2}	None	3	~ 20
	-6	10^{-2}	None	3	~ 18
CL EO-STBC	0	10^{-2}	None	3	~ 16
	-6	10^{-2}	None	3	~ 14

Figures 4.7 and 4.8 show the BER of PIC detection with distributed A-STBC and distributed CL EO-STBC under imperfect synchronization when $\beta_k = 3, 0, -3, -6$ dB and when the PIC iteration $q = 3$, respectively. It can be observed that in both proposed schemes the PIC detection is an effective approach to improve the performance of distributed STBC which mitigate the ISI and also has improved its efficiency over large amount of time misalignments.

For example as shown in Table 4.1, the value of 10^{-2} BER cannot be achieved by ML detection in both proposed schemes even under small time misalignment $\beta_k = -6$ dB whereas with the PIC detector it just required approximately 14 dB of gain in the case of distributed CL EO-STBC when $\beta_k = -6$ dB and $q = 3$ and approximately 20 dB of gain in the case of distributed A-STBC when $\beta_k = 0$ dB and $q = 3$. Furthermore, as can be observed in Figure 4.9, even under large time misalignment $\beta_k = 3$ dB and q=3, it required approximately 18 dB of gain to achieve 10^{-2} as compared to DT link performance, which required approximately 22 dB to achieve 10^{-2} BER.
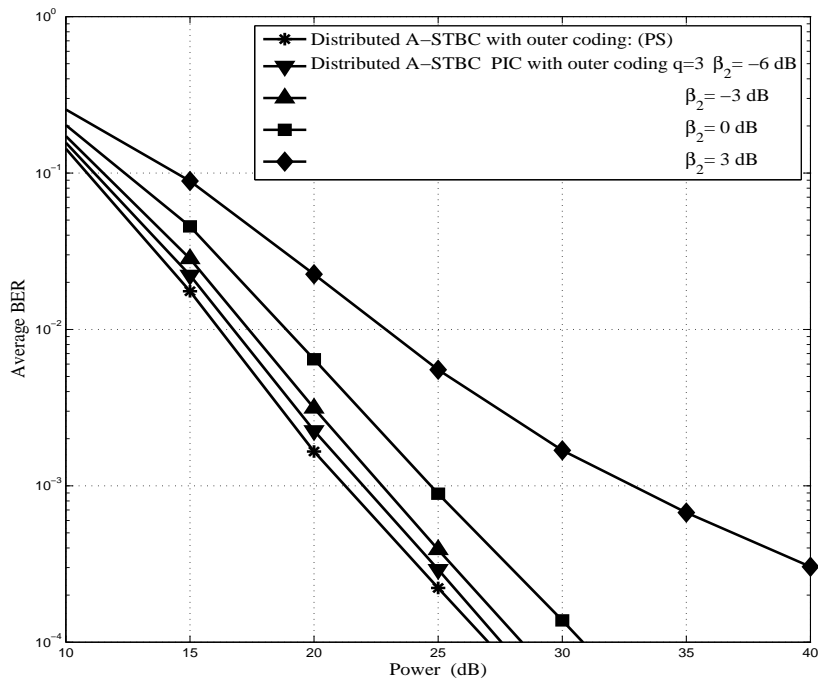
Figure 4.7. The end-to-end BER performance of distributed A-STBC with outer convolutive coding utilizing PIC detection under different time error $\beta_k = 3, 0, -3, -6$ dB and when the iteration $q = 3$.
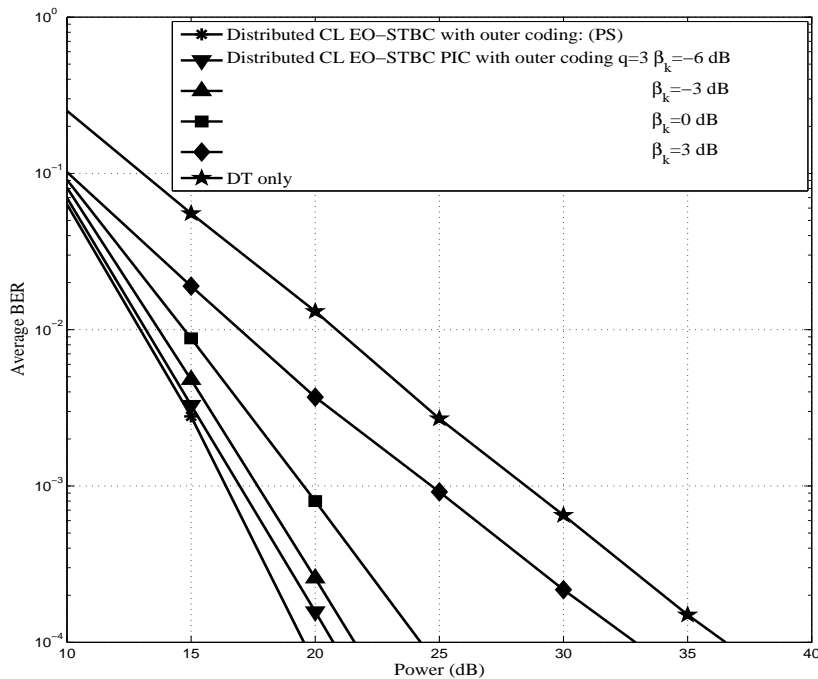
Figure 4.8. The end-to-end BER performance of distributed CL EO-STBC with outer convolutive coding utilizing PIC detection under different time error $\beta_k = 3, 0, -3, -6$ dB and when the iteration $q = 3$.

4.6 Chapter Summary

This chapter investigated applying distributed STBC in [6], and outer convolutive coding for a relay network with two and four relay nodes by utilizing A-STBC and CL EO-STBC respectively. With one antenna at all nodes, the impact of imperfect synchronization among the relay nodes at the destination node was considered. To overcome this issue a signal detector was proposed based on the principle of PIC detection, to cancel the ISI caused by imperfect synchronization and achieve full diversity order of R with coding gain and full data transmission rate in each hop for both proposed schemes, even without channel knowledge at the relay nodes.

Distributed A-STBC only applies for two relay nodes to achieve full data transmission rate with diversity gain of order two between the relay nodes and the destination nodes and cannot be extended for more than two relay nodes. Therefore, using a feedback scheme with distributed EO-STBC both diversity gain of order four and array gain with full data transmission rate between the relay nodes and the destination node were exploited for more than two relay nodes. Furthermore, the PEP utilizing distributed A-STBC and CL EO-STBC for a synchronous cooperative relay network was analyzed to confirm that the cooperative diversity gain is equal to the number of transmitting relay nodes in the case of distributed A-STBC and with a smaller PEP due to array gain in the case of distributed CL EO-STBC. This result was based on the destination node having full knowledge of all fading channels.

Finally, the simulation results of the PIC approach with both proposed schemes showed that there was significant performance improvement over ML detection under synchronization error and the perfor-

mance close to the perfect synchronized case was achieved in just three iterations, whereas ML detection fails to mitigate the impact of imperfect synchronization even under small time misalignment.

With the complexity of the number of PIC iterations, the next chapter will focus on analyzing asynchronous cooperative relay networks and proposing two novel detection schemes with low detection complexity only dependent on the constellation size.

Chapter 5

NOVEL DETECTION SCHEMES FOR ASYNCHRONOUS COOPERATIVE RELAY NETWORKS

In this chapter, two novel detection schemes for a decode-and-forward (DF) asynchronous cooperative relay network are proposed which utilize distributed closed-loop extended orthogonal space time block coding (CL EO-STBC). These techniques are both designed to remove effectively the interference induced by different time delays from the antennas of each relay node at the destination node and achieve full cooperative diversity gain with unity data transmission rate between the relay nodes and the destination node. Moreover, a simple max-min relay selection is proposed for cooperative relay networks to enhance the system performance.

5.1   Introduction

In wireless relay networks, different relay nodes are exploited to communicate cooperatively with the destination node to achieve spatial diversity, that is, cooperative diversity [19] [63]. To enhance the spatial diversity in cooperative relay networks, in [6], the idea of distributed space time block coding (STBC) was proposed for wireless relay networks with a single half-duplex antenna in each node. For a wireless relay network with a single antenna at the source and the destination node and multiple, M_R, antennas on each relay node, and using distributed STBC among the relay nodes, the cooperative diversity gain of $M_R R \left(1 - \frac{log log P}{log P}\right)$ can be achieved as shown in Section 4.4, where R is the number of relay nodes in the whole network and P is the total transmit power in the whole network [88]. Therefore, when the total transmit power P is very large, the wireless relay networks with distributed STBC can theoretically achieve cooperative diversity of $M_R R$ [88].

To achieve full cooperative diversity, the synchronization between the relay nodes is required [8], [10] and [89]. However, unlike in point-to-point multiple-input multiple-output (MIMO) systems, the relay nodes are distributed at different places and each relay node is equipped with its own local oscillator. Therefore, wireless relay communication is generally asynchronous in nature as mentioned in previous chapters [24], [75], [76] and [90].

To address the issue of imperfect synchronization among the relay nodes, in [16] a CL EO-STBC scheme requiring only two-bit feedback was considered. This approach is extended in [77] to the distributed case of four relay nodes with a parallel interference cancellation (PIC) detection to overcome the imperfect synchronization issue in cooper-

ative relay networks. This distributed CL EO-STBC can achieve full data transmission rate and full cooperative diversity gain between the relay nodes and the destination node, however it also has the disadvantage that its detection complexity is dependent upon the number of a PIC iterations and the feedback angles have not been chosen to maximize the array gain as presented in Section 3.3.

However, in [2] a near-optimum detection scheme for the case of two relay nodes was proposed and shown to be a very effective approach to mitigate the impact of imperfect synchronization between relay nodes and its detection complexity dependent upon the constellation size. Nevertheless, this detection scheme is limited by the number of relay nodes and cannot be extended to more than two relay nodes [26].

The work presented in this chapter is concerned with two novel detection schemes for asynchronous wireless relay networks to cancel the interference component at the destination node caused by timing misalignment from the relay nodes. Namely, a sub-optimum detection scheme for four relay nodes, each of which is equipped with a single antenna and with the assumption there is a direct transmission (DT) connection between the source node and the destination node; and a near-optimum detection scheme for two relay nodes each of which is equipped with two antennas and no DT connection is assumed between the source node and the destination node.

It is shown that both approaches do not require multiple iterations and the detection complexity is only dependent upon the constellation size. Since the essence of relaying is to reduce the effect of pathloss on the data transmitted from the source node to the destination node [14] and [91], the near-optimum detection scheme has lower detection

complexity at the destination node as compared to the sub-optimum detection scheme in [3], because the sub-optimum detection scheme relies on the information from the DT link between the source node and the destination node, otherwise this detection will fail. Moreover, the complexity of the near-optimum detection scheme is the same as compared with the scheme in [2] with the advantage of cooperative diversity of order four is achieved between the relay nodes and the destination by utilizing two antennas on each relay node.

Furthermore, the relay selection technique [92] and [93] is considered in this chapter for two dual antenna relay nodes which offer the possibility to improve the system performance as compared to the cooperative relay system without relay selection scheme and also to select the smallest time delay error among the relay nodes.

To this end, the remainder of this chapter is structured as follows: in Section 5.2, the distributed CL EO-STBC for a single antenna relay node with phase rotation and quantization under imperfect synchronization is presented. Section 5.3 introduces a novel sub-optimum detection scheme, which is used to mitigate the intersymbol interference (ISI) induced by the asynchronous between the transmission from the relay nodes. Simulation results are presented in Section 5.4 to illustrate the superiority of the sub-optimum detection scheme for asynchronous wireless relay networks. In Section 5.5, distributed CL EO-STBC for two relay nodes with dual antennas at each relay node with phase rotation for asynchronous wireless relay networks is described. To combat the interference term induced by the different transmissions of the relay nodes at the destination node, a novel near-optimum detection scheme and relay selection scheme are discussed in Section 5.6 and 5.7 respec-

tively. Simulation results which show the performance of the proposed near-optimum detection scheme and relay selection scheme are given in Section 5.8. Finally, the chapter summary is presented in Section 5.9.

5.2   Distributed CL EO-STBC for Relay Nodes with Single Antennas

Distributed CL EO-STBC for the asynchronous cooperative scenario with four relay nodes and outer convolutive coding is considered in this section as represented in Figure 5.1. This model has a source node, four cooperative relay nodes R_k, $k \in 1, 2, 3, 4$, and the destination node which provides feedback to the antennas of relays R_1 and R_3 as shown in Figure 5.1, where all relay nodes are equipped with a single antenna and are assumed to operate in half-duplex mode.

Figure 5.1. Basic structure of coded distributed CL EO-STBC using two-bit feedback based on phase rotation for an asynchronous wireless relay with a single antenna in each node with two phases for the cooperative transmission process and time delay offset between the antenna of R_2, R_3 and R_4 and the destination node.

The feedback scheme in [15] is used in this model to attain full cooperative diversity between the relay nodes and the destination node as presented in Appendix A. In addition, performance improvement

with outer coding is also investigated by combining an outer convolutive code at the source node with a Viterbi decoder at the destination node as depicted in Figure 5.1 to further exploit coding gain as presented in Section 4.2. Furthermore, the source node is assumed to encode the block of its information bits using a cyclic redundancy check (CRC), so that the relay nodes can detect whether the received symbol is correct or not. As mentioned in all models in Chapters 3 and 4, the information bits are transmitted according to a two phase protocol. During the first phase, at the source node, the information bits after being encoded by the convolutional encoder are passed through the interleaver and then are mapped into quadrature phase shift keying (QPSK) symbols as shown in Figure 5.1, which are grouped into pairs $\mathbf{s}(i) = [s(1,i), s(2,i)]^T$, where $[.]^T$ indicates the transpose of the vector $\mathbf{s}(i)$ and i denotes the discrete pair index. The source node then broadcast its information to the relay nodes R_k, $k \in 1, 2, 3, 4$, and the destination node in two different time transmission periods. The corresponding signal vector $\mathbf{r}_{sd} = [r_{sd}(1,i), r_{sd}(2,i)]^T$ received at the destination node via the direct channel h_{sd} in the first phase can be expressed as follows

$$\mathbf{r}_{sd}(i) = h_{sd}\mathbf{s}(i) + \mathbf{n}_{sd}(i) \qquad (5.2.1)$$

where h_{sd} is the coefficient of the channel gain between the source node and the destination node and it is modelled as a quasi-static Rayleigh flat fading channel and $\mathbf{n}_{sd}(i) = [n_{sd}(1,i), n_{sd}(2,i)]^T$ is an additive Gaussian noise vector with elements having distribution $CN(0, \sigma_n^2)$. To detect $\hat{s}_{sd}(t,i)$, $t \in 1, 2$, i.e. the symbols that are actually transmitted, the least squares (LS) method can be used as follows

$$\hat{s}_{sd}(t,i) = arg \min_{s_t \in S} |h_{sd}^* r_{sd}(t,i) - |h_{sd}|^2 s_t|^2 \qquad \text{for} \qquad t \in 1,2 \quad (5.2.2)$$

where S is the alphabet containing M symbols for QPSK. As will be shown in the next section, even if the DT link described in (5.2.1) provides limited end-to-end performance it still contains information which can be used to initialize further processing [26].

In the second phase, the relaying nodes try to decode the information received from the source node before forwarding it to the destination node. After successfully decoding the received signals, the relay nodes re-encode it again as follows

$$
\mathbf{S} = \begin{bmatrix} x_1(1,i) & x_1(1,i) & x_2(1,i) & x_2(1,i) \\ x_1(2,i) & x_1(2,i) & x_2(2,i) & x_2(2,i) \end{bmatrix}
$$
$$
= \begin{bmatrix} s(1,i) & s(1,i) & s(2,i) & s(2,i) \\ -s^*(2,i) & -s^*(2,i) & s^*(1,i) & s^*(1,i) \end{bmatrix} \qquad (5.2.3)
$$

and then effectively forward the resulting matrix code $\mathbf{S}$ in (5.2.3) from the relay nodes to the destination node in two different time transmission periods, where each row corresponds to the particular time transmission period and the column to the relay node. In (5.2.3) the encoding data packets at the relay nodes R_k, $k \in 1,2,3,4$, corresponding to $\mathbf{s}(i)$ are denoted as $\mathbf{x}_1(i) = [x_1(1,i), x_1(2,i)]^T$ at R_1, $\mathbf{x}_2(i) = [x_1(1,i), x_1(2,i)]^T$ at R_2, $\mathbf{x}_3(i) = [x_2(1,i), x_2(2,i)]^T$ at R_3 and $\mathbf{x}_4(i) = [x_2(1,i), x_2(2,i)]^T$ at R_4.

As mentioned in previous chapters, the full data transmission rate between the relay nodes and the destination node can be achieved by using distributed open-loop EO-STBC in the case of four relay nodes but at the expense of loss in diversity gain between the relay nodes and

the destination node. To attain full data transmission rate with full diversity order equal to the number of transmitting relay nodes, the phase of different code symbols that are transmitted from the first and third relay nodes must be rotated by appropriate phase angles (phase shifted) before they are transmitted as follows,

$$U_1 = e^{j\theta_1}$$
$$U_2 = e^{j\theta_2} \tag{5.2.4}$$

while the symbols for the other two relay nodes are kept unchanged as shown in Figure 5.1. It is assumed that the channel state information (CSI) is known at the destination node requiring every relay node to broadcast training symbols that can be used to estimate the channels at the destination node. Furthermore, both the broadcast and feedback may need to be performed at every time transmission periods, because the channel coefficients can potentially vary over different time transmission periods. Therefore, the CSI assumption considered in this model may not be practical except in slowly varying environments where such regular updates ar not required. It is important to point out that the phase rotations applied to the transmitted symbols are essentially equivalent to rotating the phases of the corresponding channel coefficients to improve the effective diversity gain between the relay nodes and the destination node at the expense of increased feedback overhead [15].

As mentioned in all previous models in Chapters 3 and 4, the imperfect synchronization between R_1 and the other relay nodes resulting from different delays will induce ISI at the destination node, the transmitted signal $\mathbf{x}_k(i)$, $k \in 1, 2, 3, 4$, over two time transmission periods

from the relay nodes as in (5.2.3) will most likely arrive at the destination node in different time instants as shown in Figure 5.2, where τ_k, $k \in 2, 3, 4$, is a timing misalignment among the received versions of the signals at the destination node, which for convenience are shown identical as shown in Figure 5.2.
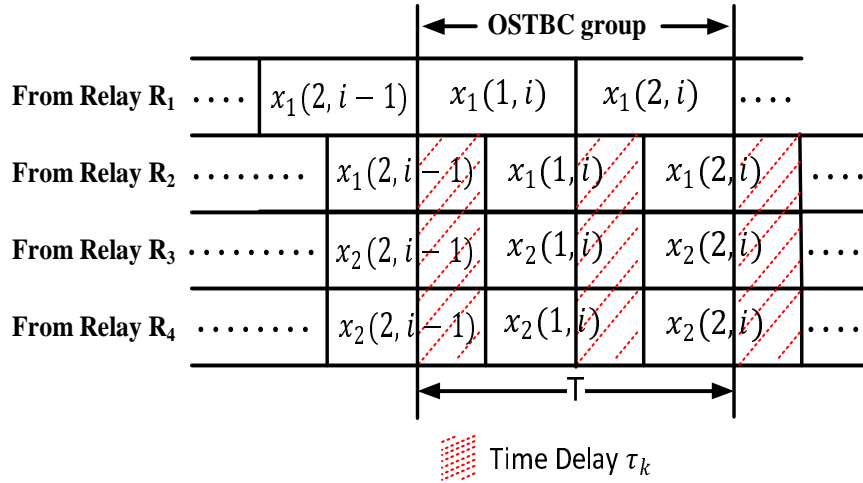
Figure 5.2. Representation of misalignment of received signals at the destination node which induces ISI in the case of four relay nodes, each relay node is equipped with a single antenna.

As mentioned previously in Chapters 3 and 4, the first relay node is assumed to be perfectly synchronized to the destination node, that is, $\tau_1 = 0$. In this work an interference is added to the received signals because of the asynchronism between the transmission from the relay nodes R_k, $k \in 2, 3, 4$, so that the received signals can be represented as follows

$$r_{rd}(1, i) = (U_1 g_1 + g_2)x_1(1, i) + (U_2 g_3 + g_4)x_2(1, i)$$
$$+ I_{int}(1, i) + n_{rd}(1, i) \tag{5.2.5}$$

$$r_{rd}(2, i) = (U_1 g_1 + g_2)x_1(2, i) + (U_2 g_3 + g_4)x_2(2, i)$$
$$+ I(2, i) + n_{rd}(2, i) \tag{5.2.6}$$

where $I_{int}(1, i)$ and $I_{int}(2, i)$ are the interference terms from R_2, R_3 and R_4 at the destination node and can be modelled as follows

$$
\begin{aligned}
I_{int}(1, i) = & \; g_2(-1)x_1(2, i-1) + (U_2g_3(-1) + g_4(-1))x_2(2, i-1) \\
& + \; g_2(-2)x_1(1, i-1) + (U_2g_3(-2) \\
& + \; g_4(-2))x_2(1, i-1) \hspace{3cm} (5.2.7)
\end{aligned}
$$

$$
\begin{aligned}
I_{int}(2, i) = & \; g_2(-1)x_1(1, i) + (U_2g_3(-1) + g_4(-1))x_2(1, i) \\
& + \; g_2(-2)x_1(2, i-1) + (U_2g_3(-2) + g_4(-2))x_2(2, i-1),
\end{aligned}
$$

$$(5.2.8)$$

where $n_{rd}(1, i)$ and $n_{rd}(2, i)$ are additive Gaussian noise terms at the destination node in the second phase with distribution $CN(0, \sigma_n^2)$ and g_k, $k \in 1, 2, 3, 4$, are the channel gains between the relay nodes and the destination node and are also assumed to be block Rayleigh fading from data block to data block. The coefficients $g_k(l)$, $k = 2, 3, 4$, and $l = -1, -2$, reflect the ISI from the previous symbols under imperfect inter node synchronization. For practical pulse shaping such as the raised cosine filter $g_k(-2)$ is generally a much less dominant coefficient and all other terms such as $g_k(-3)$ are very small even zero in value [26]. The relative strengths of $g_k(l)$, which have been used in this model will be expressed as a ratio as follows

$$
\beta_k(l) = \frac{|g_k(l)|^2}{|g_k|^2} \hspace{1cm} \text{for} \hspace{0.5cm} k = 2, 3, 4 \hspace{0.5cm} \text{and} \hspace{0.5cm} l = -1, -2 \hspace{0.5cm} (5.2.9)
$$

where $\beta_k(l)$ is defined to reflect the impact of time delay τ_k between transmission from relays R_2, R_3 and R_4 and R_1 at the destination node and the pulse shaping waveforms.

5.2.1 Conventional Distributed CL EO-STBC for Relay Node with

Single Antennas

Substituting (5.2.3) into (5.2.5) and (5.2.6), the received signals $r_{rd}(1, i)$ and $r_{rd}^*(2, i)$, conjugated for convenience at the two independent time transmission periods are expressed in vector form as follows

$$\mathbf{r}_{rd}(i) = \mathbf{H}\mathbf{s}(i) + \mathbf{I}_{int}(i) + \mathbf{n}_{rd}(i) \tag{5.2.10}$$

where

$$\mathbf{H} = \begin{bmatrix} U_1 g_1 + g_2 & U_2 g_3 + g_4 \\ U_2^* g_3^* + g_4^* & -U_1^* g_1^* - g_2^* \end{bmatrix}, \tag{5.2.11}$$

$\mathbf{n}_{rd}(i) = [n_{rd}(1, i), n_{rd}^*(2, i)]^T$ is an additive Gaussian noise vector, with elements having distribution $CN(0, \sigma_n^2)$ at the destination node and $\mathbf{I}_{int}(i) = [I_{int}(1, i), I_{int}^*(2, i)]^T$ is the interference vector containing terms from R_2, R_3 and R_4 at the destination node which can be modelled as follows

$$
\begin{aligned}
I_{int}(1, i) = {} & -g_2(-1)s^*(2, i-1) + (U_2 g_3(-1) + g_4(-1))s^*(1, i-1) \\
& + g_2(-2)s(1, i-1) + (U_2 g_3(-2) \\
& + g_4(-2))s(2, i-1) \tag{5.2.12} \\
I_{int}^*(2, i) = {} & g_2^*(-1)s^*(1, i) + (U_2^* g_3^*(-1) + g_4^*(-1))s^*(2, i) \\
& - g_2^*(-2)s(2, i-1) + (U_2^* g_3^*(-2) + g_4^*(-2))s(1, i-1)
\end{aligned}
$$

$$\tag{5.2.13}$$

On the basis of (5.2.10), it is well known from estimation theory that the matched filter is the optimum front-end receiver to obtain statistics for detection in the sense that it preserves information. Similar to [5]

the matched filtering is performed by pre-multiplying (5.2.10) by $\mathbf{H}^H$, where $(.)^H$ denotes the Hermitian (complex conjugate transpose) operations. Therefore, the conventional distributed CL EO-STBC detection can be carried out as follows

$$
\begin{aligned}
\hat{\mathbf{y}}(i) &= [y(1,i), y(2,i)]^T = \mathbf{H}^H \mathbf{r}(i) \\
&= \underbrace{((|U_1 g_1|^2 + |g_2|^2 + |U_2 g_3|^2 + |g_4|^2)}_{\lambda_c} \\
&\quad + \underbrace{2\Re(U_1 g_1 g_2^* + U_2 g_3 g_4^*)))}_{\lambda_f} \mathbf{s}(i) + \mathbf{H}^H \mathbf{I}_{int}(i) \\
&\quad + \mathbf{H}^H \mathbf{n}_{rd}(i) \qquad\qquad\qquad\qquad (5.2.14)
\end{aligned}
$$

where $\Re\{.\}$ is the real part of complex number, λ_c is the conventional diversity gain for the single antenna for four relay nodes and one receive antenna at the destination node, λ_f is the array (feedback) performance gain and $U_k = e^{j\theta_k}$, which is determined by two feedback information angles θ_k, $k \in 1, 2$, are obtained by maximizing λ_f, which corresponds to a type of array gain. It is obvious that if $\lambda_f > 0$, the designed closed-loop system can obtain additional performance gain, which leads to an improved signal-to-noise ratio (SNR) at the destination node. The design criterion of the two-bit feedback scheme can be designed as in Appendix A [15]. That is, each element of the feedback performance gain λ_f should be real and positive which can be achieved by:

$$
\begin{aligned}
\theta_1 &= -\angle(g_1 g_2^*) \\
\theta_2 &= -\angle(g_3 g_4^*) \qquad\qquad\qquad\qquad (5.2.15)
\end{aligned}
$$

where $\angle$ denotes the phase angle, in radians, for each complex element and the relation between the channel gain λ and SNR can be expressed as follows

$$SNR = \frac{\lambda_c - \lambda_f}{4} \frac{\sigma_s^2}{\sigma_n^2} \qquad (5.2.16)$$

where σ_s^2 is the total transmit power of the desired signal and σ_n^2 is the noise power at the destination node. To detect which symbols were actually transmitted from the relay nodes R_k, $k \in 1, 2, 3, 4$, the LS method can be employed as follows to estimate $\hat{s}(t, i)$, $t \in 1, 2$,

$$\hat{s}(t, i) = arg \min_{s_t \in S} |\hat{y}(t, i) - \lambda s_t|^2 \qquad (5.2.17)$$

where

$$\lambda = \underbrace{\sum_{k=1}^{4} (|g_j|^2)}_{\lambda_c} + \underbrace{2\Re(g_1 g_2^* U_1 + g_3 g_4^* U_2)}_{\lambda_f} \qquad (5.2.18)$$

As mentioned in all previous models, the conventional detection can fail due to detection error of the $\mathbf{H}^H \mathbf{I}(i)$ component in (5.2.14) which will also leads to loss of orthogonality in the CL EO-STBC.

5.2.2   Quantization

Due to practical limitations such as the bandwidth of the feedback channel, it is generally not possible to have high precision CSI at the relay nodes. One way to reduce the amount of information needed to be fed back in (5.2.15) is to rotate the signals at the first and third relay node antennas by a single phase. Feeding back the exact value of phase angle in (5.2.12) for dual phases for example, using fixed or floating point resolution requires very large feedback overhead. In practical application this may not be possible due to the very limited feedback bandwidth. Therefore, the phase angles should be quantized, and then these levels are fed back to the relay nodes. Consider, for each

phase angle, if two bits are available for feedback, then only one of four
phase level angles is fed back such that the phase angles are from the
set $\theta_1, \theta_2 \in \Omega = [0, \pi/2, \pi, 3\pi/2]$ then for the first relay node antenna
phase adjustment, the discrete feedback information corresponding to
the phases may be selected according to

$$\theta_1 = arg \min_{\theta_1 \in \Omega} \Re(g_1 g_2^*) e^{\theta_1} \qquad (5.2.19)$$

Similarly, for the third relay antenna phase adjustment, the phases may
be selected according to

$$\theta_2 = arg \min_{\theta_2 \in \Omega} \Re(g_3 g_4^*) e^{\theta_2} \qquad (5.2.20)$$

In this case the particular selection giving the largest values of (5.2.19)
and (5.2.20) might be preferable, as it would provide the largest array
gain and achieve full cooperative diversity advantage.

5.3   Sub-Optimum Detection for Distributed CL EO-STBC for Relay Nodes with Single Antennas

To overcome the impact of imperfect synchronization among the relay
nodes the interference component of $\mathbf{I}_{int}(i)$ should be removed from
(5.2.1). Since $x_k(t, i-1)$, $k, t \in 1, 2$, in (5.2.7) and (5.2.8) are al-
ready known if the detection process has been initialized properly (e.g.
through the use of pilot symbols at the start of the data block) as pre-
sented in Section 3.4 and 4.3, then the component $I_{int}(1, i)$ as in (5.2.4)
can be eliminated before applying the linear transformation in (5.2.14).
Therefore, sub-optimum detection can be used to mitigate the impact
of $\mathbf{I}_{int}(i)$ in (5.2.10) as follows

$$\hat{\mathbf{y}}(i) = [\hat{y}(1, i), \hat{y}(2, i)]^T = \mathbf{H}^H \mathbf{r}_{rd}(i)$$

$$= \Delta \mathbf{s}(i) + \mathbf{z}(i) + \mathbf{v}(i) \qquad (5.3.1)$$

where $\Delta = \mathbf{H}^H \mathbf{H}$, $\mathbf{v}(i) = \mathbf{H}^H \mathbf{n}_{rd}(i)$,

$$\mathbf{r}_{rd}(i) = \begin{bmatrix} r_{rd}(1, i) - I_{int}(1, i) \\ r_{rd}^*(2, i) - g_2^*(-2)s(2, i-1) + (U_2^* g_3^*(-2) + g_4^*(-2))s(1, i-1) \end{bmatrix}$$

and

$$\mathbf{z}(i) = \begin{bmatrix} z(1, i) \\ z(2, i) \end{bmatrix} = \mathbf{H}^H \begin{bmatrix} 0 \\ I_{int}^*(2, i) \end{bmatrix}$$

where $I_{int}^*(2, i) = g_2^*(-1)s^*(1, i) + (U_2^* g_3^*(-1) + g_4^*(-1))s^*(2, i)$.

Therefore

$$z(t, i) = z_1^t s^*(1, i) + z_2^t s^*(2, i) \qquad (5.3.2)$$

where

$$z_1^t = \Phi g_2^*(-1)$$

$$z_2^t = \Phi(U_2^* g_3^*(-1) + g_4^*(-1)) \qquad \text{for} \quad t = 1, 2$$

and

$$\Phi = \begin{cases} (U_2 g_3 + g_4) & \text{if} \qquad t = 1 \\ \\ (-U_1 g_1 - g_2) & \text{if} \qquad t = 2 \end{cases}$$

The components of (5.3.1) can thus be re-written as

$$\hat{y}(t, i) = \lambda s(t, i) + z(t, i) + v(t, i) \qquad \text{for} \quad t \in 1, 2 \qquad (5.3.3)$$

The detection result of the DT link in (5.2.2) is next used to initialize $s(2,i) = \hat{s}_{sd}(2,i)$, with the observation that as confirmed in the simulations, the reliability of these decisions is not critical to the performance of the final detector next defined. Finally, $\hat{\mathbf{s}}(i) = [\hat{s}(1,i), \hat{s}(2,i)]^T$ can be detected by using the LS detection method as follows

$$\hat{s}(1,i) = arg \min_{s_m \in S} |\hat{y}(1,i) - \lambda s_m - (z_1^1 s_m^* + z_1^2 s^*(2,i))|^2 \quad (5.3.4)$$

$$\hat{s}(2,i) = arg \min_{s_m \in S} |\hat{y}(2,i) - \lambda s_m - (z_2^1 \hat{s}^*(1,i) + z_2^2 s_m^*)|^2 \quad (5.3.5)$$

The above procedure mitigates the ISI caused by the synchronization time error as will be seen in the following section. It can be noted that, this is not a full maximum likelihood (ML) detection scheme due to the use of a separate initializer $s(2,i)$ therefore it is termed sub-optimum detection and moreover, this approach does not require multiple iterations and therefore detection complexity is only dependent upon the constellation size as compared with the approach presented in Section 3.4 and 4.3, which its detection complexity is dependent upon the number of PIC iterations.

5.4   Simulation Results

In this section, simulation results of the proposed scheme under imperfect synchronization are demonstrated. The bit error rate (BER) performance is evaluated as a function of the SNR using the QPSK mapping scheme, where the x-axis represents the SNR, while the y-axis represents the average BER. For fair comparison with a non-relay scheme, all relay nodes transmit at $1/4$ power that is $\sigma_r^2 = \sigma_s^2/4$.

Figure 5.3 shows the improvement provided by the proposed CL EO-STBC with outer convolutive coding scheme over CL EO-STBC

scheme without outer coding. To achieve a bit error probability of 10^{-3} it required approximately 5.5 dB of SNR for the approach with outer coding and approximately 11 dB for the approach without outer coding.
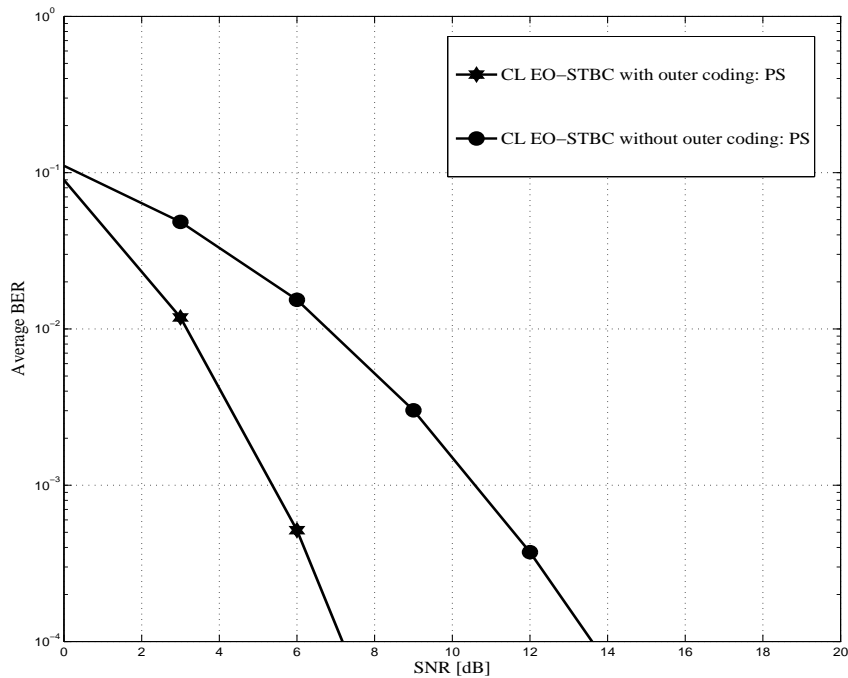
Figure 5.3. The BER performance comparison of proposed CL EO-STBC scheme with outer coding and proposed CL EO-STBC scheme without outer coding.

A comparison was made between the average BER performance of the proposed CL EO-STBC with outer convolutive coding and the proposed CL EO-STBC scheme in Section 3.3 [77], Distributed Alamouti STBC (A-STBC) in [75] and distributed orthogonal STBC (OSTBC) in [76] with outer convolutive coding in the case of perfect synchronization (PS) as depicted in Figure 5.4, it shows that the CL EO-STBC approach achieves satisfactory performance and outperforms the previous proposed schemes in [75], [76] and [77]. At a bit error probability

of 10^{-3}, the proposed scheme provides approximately 7 dB of SNR over OL EO-STBC scheme, 1.5 dB of SNR improvement over the scheme in [77] and approximately 3.5 dB of SNR over the scheme in [76]. Furthermore, the distributed convolutive coding of the Alamouti scheme for two relay nodes in [75] and DT link are included as a reference in Figure 5.4. The simulation result of a practical scenario of a two-bit quantization method is depicted in Fig. 5.4, which is very close to the performance of the un-quantized scheme (ideal phase rotation method).
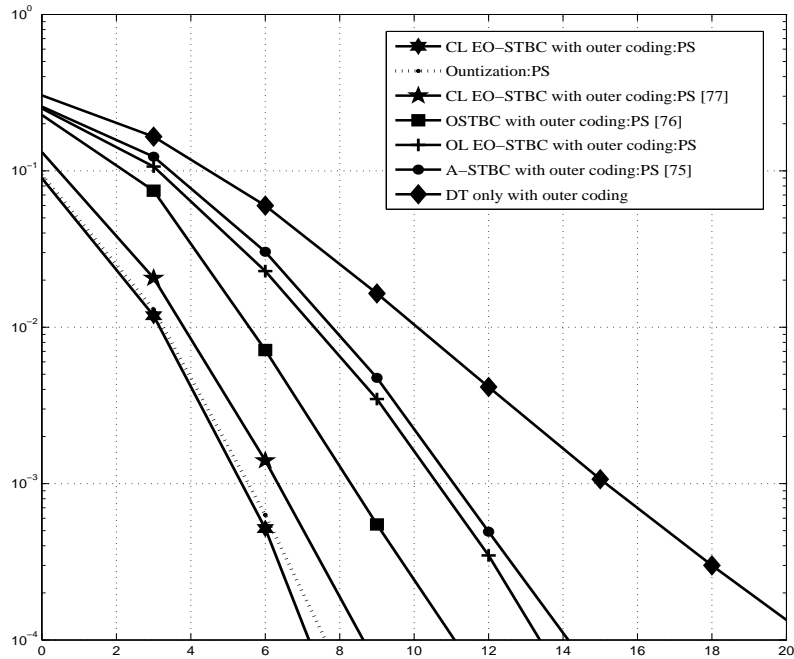
Figure 5.4. The BER performance comparisons of proposed CL EO-STBC scheme and related schemes with outer coding.

In Figures 5.5 and 5.6, the effect of synchronization error between R_1 and the other relay nodes on average BER is shown with different delay asynchronism values of $\beta_k(-1) = -6, -3, 0, 3$ dB and set $\beta_k(-2) = 0$, because $h_k(-1)$, $k \in 2, 3, 4$, are the most dominant terms. The CL EO-

STBC with outer convolutive coding under perfect synchronization and the performance with quantized feedback are included as a reference in both figures. Results in Figure 5.5 confirm that the conventional detector in CL EO-STBC is not effective to mitigate synchronization error even under small time misalignments $\beta_k(-1) = -6$ dB.
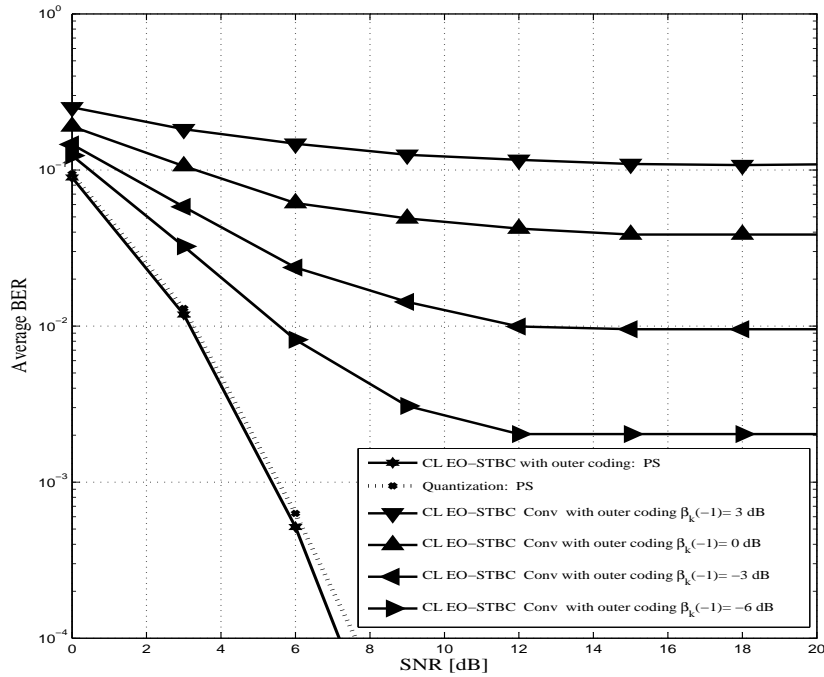
Figure 5.5. The BER performance of the conventional detector for distributed CL EO-STBC and outer convolutive coding using four relay nodes, each relay node has single antenna under different time misalignments $\beta_k(-1) = 6, 3, 0, 3$ dB.

On the other hand, the average BER performance of the proposed sub-optimum decoding scheme in Figure 5.6 is much improved. For example, at average BER 10^{-3} approximately 5.5 dB of SNR is necessary in the case of perfect synchronization with outer coding, however, in the case of sub-optimum detection approximately 11.5 dB of SNR is required when $\beta_k(-1) = 3$ dB and approximately 6.5 dB of SNR is

required when $\beta_k(-1) = -6$ dB and only 1 dB more than the perfect synchronization case.
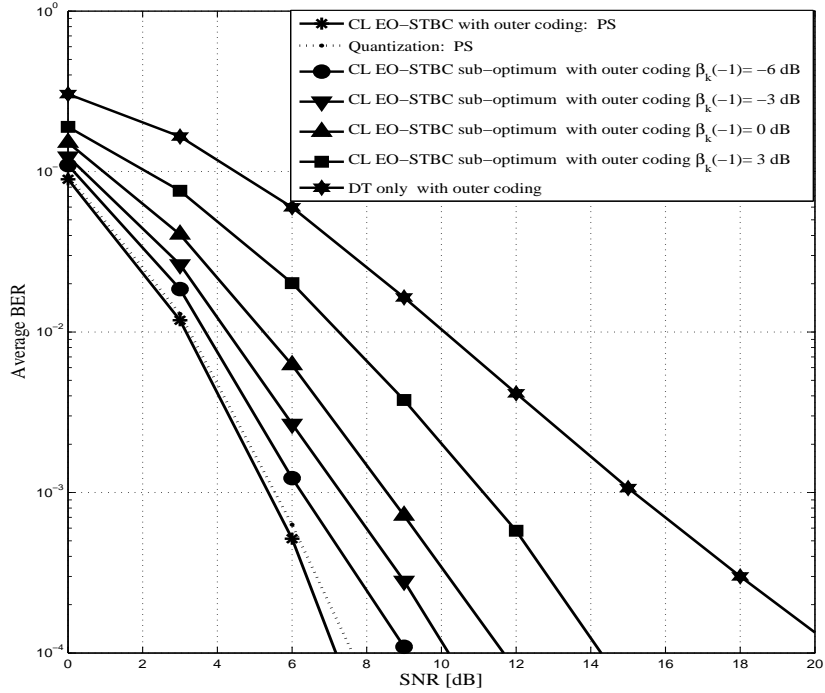
Figure 5.6. The BER performance of the sub-optimum detection for distributed CL EO-STBC and outer convolutive coding using four relay nodes, each relay node has single antennas under different time misalignments $\beta_k(-1) = 6, 3, 0, 3$ dB.

In Figure 5.7 the impact of error propagation (EP) in the decoding process on average BER performance with $\beta_k(-1) = -3$ and 3 dB where $k \in 2, 3, 4$, is considered. It can be observed that the impact of EP is very minor, only marginally degrading the BER performance at increasing SNRs, which confirms the performance behavior of the detector.
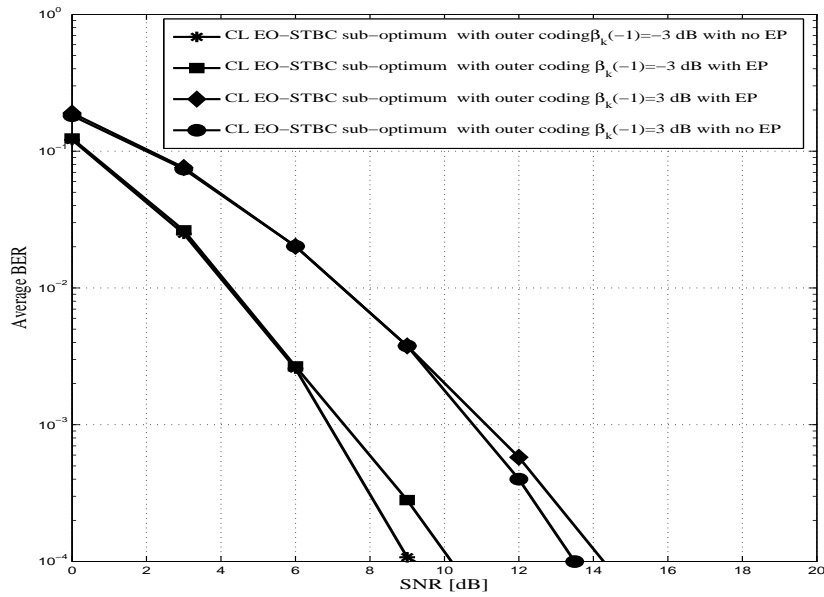
Figure 5.7. The BER performance of the sub-optimum detector showing the impact of EP under $\beta_k(-1) = -3, 3$ dB

5.5   Distributed CL EO-STBC for Two Dual Antenna Relay Nodes

In this section, a distributed CL EO-STBC scheme for the asynchronous two-hop wireless communication scenario, with a single source node, single destination node and two parallel relay nodes R_k, $k \in 1, 2$ with outer convolutive coding is considered. There is no DT connection between the source node and the destination node because it is assumed that the signal through the DT link fails to reach the destination node due to pathloss effects. Therefore, the destination node relies only on the signal from the relay nodes. It is assumed that the source node and the destination node are equipped with only one antenna, while the relay nodes are equipped with two antennas as shown in Figure 5.8. Furthermore, it is assumed that the distance between each pair of antennas on each relay node is equal to the half of transmitted wave-

length signals[1] and the CSI is assumed to be estimated without error at the destination node.
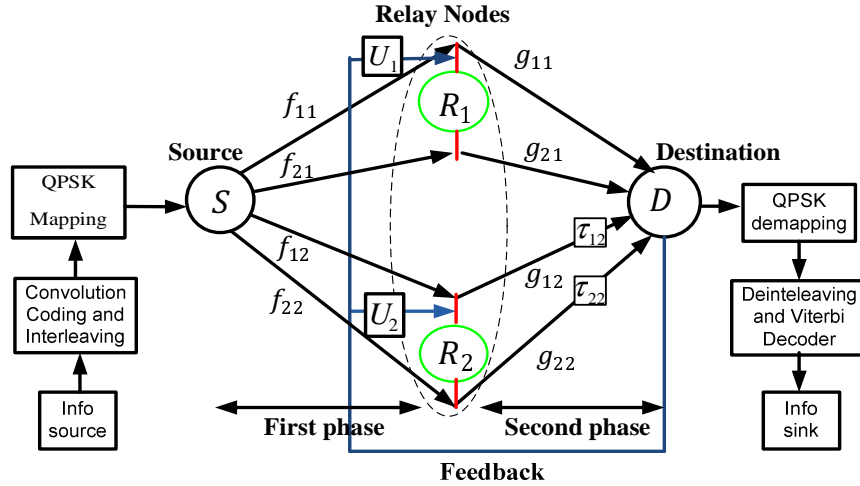
Figure 5.8. Basic structure of distributed CL EO-STBC with outer coding using two-bit feedback based on phase rotation for an asynchronous wireless relay with two antennas in each relay node and one antenna in the source and the destination node with two phases for the cooperative transmission process and time delay offset between the antennas of R_2 and the destination node.

As mentioned in Sections 3.3 and 4.2, the full cooperative diversity order between the relay nodes and the destination node cannot be achieved by applying distributed open-loop EO-STBC at the two relay nodes equipped with two antennas in each relay node due to the interference factor between the estimated symbols. Therefore, in this model the feedback scheme in [15] is adapted to overcome this issue and the coding gain is exploited in this model by combining outer convolutive code at the source node with a Viterbi decoder at the destination node as shown in Figure 5.8. All relay nodes are half-duplex and thus, all data transmission from the source node to the destination node occurs in two phases. In the first phase, the information bits

---

[1]The received signal becomes practically uncorrelated, if the antennas at the relay nodes are spaced equal to half of transmitted wavelength signals.

$\mathbf{s}(i) = [s(1,i), s(2,i)]^T$, which are encoded by the convolutional encoder are then passed through the interleaver and mapped into QPSK symbols. Then the source node broadcasts them to each antenna of each relay node R_k, $k \in 1, 2$, in two different time transmission periods.

The DF cooperation strategy is used by the relay nodes. Moreover, using the CRC scheme between the source node and the relay nodes can ensure that error free decoding is achieved at the relay nodes. Therefore, it is assumed that the relay nodes decode the source information correctly. Then the relay nodes R_k, $k \in 1, 2$, again encode the received signal as in (5.2.3) and effectively transmit the matrix code $\mathbf{S}$ as in (5.2.3) from each antenna of each relay node to the destination node in two different time transmission periods in the second phase, where the first and the second column in (5.2.3) correspond to the antennas of R_1, the third and the fourth column correspond to the antennas of R_2 and the row index corresponds to the time transmission periods. Before the entries of matrix code $\mathbf{S}$ in (5.2.3) are transmitted from each antenna of each relay node, the entries of the first antenna of R_1 and the first antenna of R_2 are multiplied by the two phase factors $U_1 = e^{j\theta_1}$ and $U_2 = e^{j\theta_2}$, respectively, whilst the other entries transmitted from the other antennas of each relay are kept unchanged as depicted in Figure 5.8 [15] to attain full cooperative diversity order between the relay nodes and the destination node as presented in Appendix A. In order to maximize the gains of the cooperative networks, each antenna of each relay node is scheduled to broadcast simultaneously. However, obtaining synchronicity at the destination node is often unrealistic owing to propagation delay as shown in Figure 5.9. This issue causes a problem in cooperative relay network systems. In the presence of a

fractional-symbol delay between the signals transmitted from different antennas of each relay node, the channel becomes dispersive even in the flat fading environment as will be shown in the simulation section.
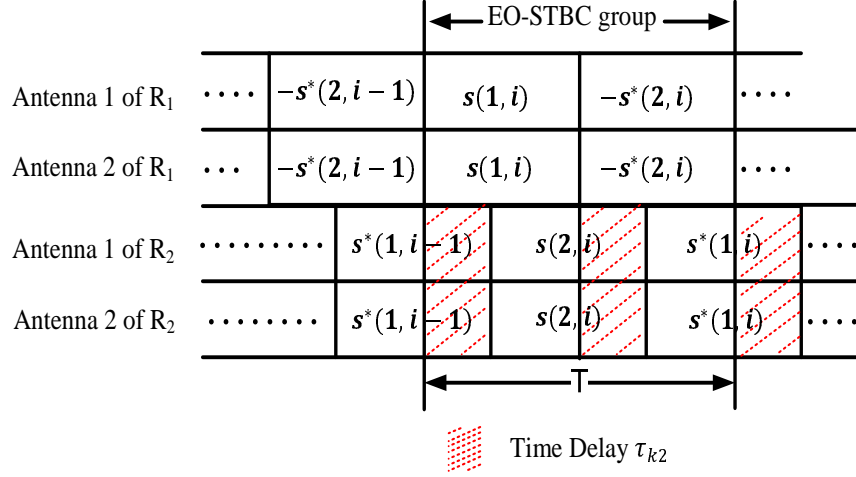
Figure 5.9. Representation of misalignment of received signals at the destination node which induces ISI in the case of two relay nodes each relay node is equipped with two antennas.

As shown in Figure 5.9 it is assumed that both antennas of R_1 are fully synchronized to the destination node, that is, $\tau_{k1} = 0$, $k \in 1, 2$. Therefore, the received signal at the destination node via relay nodes in two different time transmission periods due to time synchronization error between the antennas of each relay node can be expressed as follows

$$
\begin{aligned}
r_{rd}(1,i) = \ & (U_1 g_{11} + g_{21})s(1,i) + (U_2 g_{12} + g_{22})s(2,i) \\
& + \underbrace{(U_2 g_{12}(-1) + g_{22}(-1))s^*(1,i-1)}_{I_{int}(1,i)} \\
& + \underbrace{(U_2 g_{12}(-2) + g_{22}(-2))s(2,i-1)}_{I_{int}(1,i)} + n_{rd}(1,i) \quad (5.5.1)
\end{aligned}
$$

$$r_{rd}(2,i) = -(U_1 g_{11} + g_{21})s^*(2,i) + (U_2 g_{12} + g_{22})s^*(1,i)$$

$$+ \underbrace{(U_2 g_{12}(-1) + g_{22}(-1))s(2,i)}_{I_{int}(2,i)}$$

$$+ \underbrace{(U_2 g_{12}(-2) + g_{22}(-2))s^*(1,i-1)}_{I_{int}(2,i)} + n_{rd}(1,i) \quad (5.5.2)$$

where $I_{int}(1,i)$ and $I_{int}(2,i)$ are the interference terms from both an-
tennas of relay node R_2 in two different time transmission periods,
$n_{rd}(1,i)$ and $n_{rd}(2,i)$ represent additive Gaussian noise with zero-mean
and unity variance at the destination node and g_{k1} and g_{k2}, $k \in 1,2$,
denote complex channel coefficients from the antennas of each relay
node and the destination node. As shown in Figure 5.9, the effect of
ISI from the previous symbols is represented by $g_{k2}(l)$, $k \in 1,2$, and
$l \in -1,-2$, and as mentioned in Section 5.2, $g_{k2}(-2)$ is generally a
much smaller coefficient. Therefore, the strengths of $g_{k2}(l)$ can be ex-
pressed as a ratio as in (5.2.9), where $\beta_{12}(l) = \beta_{22}(l) = \beta(l)$ denotes
a sample of a pulse shaping waveform and the effect of the time delay
τ_{k2}, $k \in 1,2$, between transmission from the antennas of the relay node
R_1 and the antennas of the relay node R_2 at the destination node.

5.6 Near-Optimum Detection for Distributed CL EO-STBC for Relay Node with Two Antennas

As mentioned in Section (5.2.1), the received signals $r_{rd}(1,i)$ and $r_{rd}^*(2,i)$
conjugated for convenience in (5.5.1) and (5.5.2) can be represented in
vector form as in (5.2.10) with the assumption that matched filtering
is performed at the destination node. The equivalent channel matrix
$\mathbf{H}$ is as in (5.2.11).

The proposed near-optimum detection scheme can be utilized to combat the impact of $\mathbf{I}_{int}(i)$ in (5.2.10), where $s(t, i - 1)$, with $t \in 1, 2$, is in fact already known if the detection process has been initialized properly. As $I_{int}(1, i) = (U_2 g_{12}(-1) + g_{22}(-1))s^*(1, i-1) + (U_2 g_{12}(-2) + g_{22}(-2))s(2, i-1)$ then the component $(U_2^* g_{12}^*(-2) + g_{22}^*(-2))s(1, i-1)$ can be removed before applying the linear transform as in (5.2.11) and can be rewritten as follows

$$
\begin{aligned}
\hat{\mathbf{y}}(i) &= [\hat{y}(1, i), \hat{y}(2, i)]^T = \mathbf{H}^H \mathbf{r}_{rd}(i) \\
&= \Delta \mathbf{s}(i) + \mathbf{z}(i)s^*(2, i) + \mathbf{v}(i)
\end{aligned} \tag{5.6.1}
$$

where Δ and $\mathbf{v}(i)$ can be calculated as mentioned in Section (5.2.2),

$$
\mathbf{r}_{rd}(i) = \begin{bmatrix} r_{rd}(1, i) - I_{int}(1, i) \\ r_{rd}^*(2, i) - (U_2^* g_{12}^*(-2) + g_{22}^*(-2))s(1, i-1) \end{bmatrix}
$$

and

$$
\mathbf{z}(i) = \begin{bmatrix} z(1, i) \\ z(2, i) \end{bmatrix} = \mathbf{H}^H \begin{bmatrix} 0 \\ (U_2^* g_{12}^*(-1) + g_{22}^*(-1)) \end{bmatrix}
$$

Therefore, (5.6.1) can then be written as

$$
\hat{y}(1, i) = \lambda s(1, i) + z(1, i)s^*(2, i) + v(1, i) \tag{5.6.2}
$$

and

$$
\hat{y}(2, i) = \lambda s(2, i) + z(2, i)s^*(2, i) + v(2, i) \tag{5.6.3}
$$

where $\lambda = \lambda_c + \lambda_f$, where $\lambda_c = \sum_{k=1}^{2}(|g_{k1}|^2 + |g_{k2}|^2)$ and $\lambda_f = 2\Re(g_{11}g_{12}^* U_1 + g_{21}g_{22}^* U_2)$. In (5.6.3), $\hat{y}(2, i)$ is only related to $s(2, i)$ and therefore $s(2, i)$

can be detected by using the LS method as follows

$$\hat{s}(2,i) = arg \min_{s_m \in S} |\hat{y}(2,i) - \lambda s_m - z(2,i)s_m^*|^2 \qquad (5.6.4)$$

Then, the detection of $s(1,n)$ can be carried out using the LS method by substituting $\hat{s}(2,n)$ detected in $(5.6.4)$, as following:

$$\hat{s}(1,i) = arg \min_{s_m \in S} |\hat{y}(1,i) - \lambda s_m - z(1,i)\hat{s}^*(2,i)|^2 \qquad (5.6.5)$$

The above procedure totally mitigates the interference induced by different time delays from the antennas of the second relay node at the destination node. The optimality of the above procedure in terms of ML detector can be achieved if there is no decision feedback error $s(t, i-1)$, $t \in 1, 2$, therefore the above procuder is termed near-optimum detection. Moreover, the above analysis has shown that the detection complexity of this detection approach is only dependent upon the constellation size as compared with detection schemes presented in Sections 3.4 and 4.3 [77] and [80]. Also the above detection approach does not rely on the detection result of the DT link as compared with the detection approach in Section 5.3. [3].

5.7   Relay Selection Technique for Two Dual Antenna Relay Nodes

In a cooperative relay network, the cooperative relay nodes can assist the source node to broadcast the signals to the destination node, however the cooperative relay nodes have different locations so each transmitted signal from the source node to the destination node must pass through different paths causing different attenuations within the

signals received at the destination node which result in reducing the overall system performance. Therefore, to overcome this effect and benefit from cooperative communication, certain paths should be avoided by using selection techniques [92]. In this section, the conventional relay selection methods are used to ensure that the relay node with the best end-to-end path between the source node and the destination is used to improve the system performance and provide diversity gain on the order of the number of transmitting relay nodes. As mentioned in Section (5.5) and shown in Figure 5.8, each relay node is equipped with two antennas to assist the source node to transmit its signals to destination node. The resulting SNR_D at the destination node assuming maximum ratio combining, is given by

$$SNR_D = \sum_{k \in R} \sum_{ii \in 1,2} \frac{SNR_{SR_{iik}} SNR_{R_{iik}D}}{1 + SNR_{SR_{iik}} + SNR_{R_{iik}D}} \qquad (5.7.1)$$

where R denotes the set of relay indices for the relay nodes chosen in the multi-relay selection scheme. $SNR_{SR_{iik}} = |f_{iik}|^2 \frac{\sigma_s^2}{\sigma_n^2}$ is the instantaneous SNR of the paths between the source node node and the relay node antennas and $SNR_{R_{iik}D} = |g_{iik}|^2 \frac{\sigma_s^2}{\sigma_n^2}$ is the instantaneous SNR of the paths between the relay node antennas and the destination node, where $k \in 1,...,R$ and $ii \in 1,2$. These expressions give the instantaneous signal strength SNR between the source node and the relay node antennas, and the relay nodes antennas and the destination node. Then the selected relay node is chosen to maximize the minimum between

them. The two antenna relay selection policy can be expressed as

$$\Omega_{1k} = \min\{SNR_{SR_{1k}}, SNR_{R_{1k}D}\}$$

$$\Omega_{2k} = \min\{SNR_{SR_{2k}}, SNR_{R_{2k}D}\} \qquad \text{for} \quad k \in 1, ..., R \quad (5.7.2)$$

and

$$\mathcal{R} = \max_{k \in 1,...,R}\{min\{\Omega_{1k}, \Omega_{2k}\}\} \qquad (5.7.3)$$

After the best relay node has been chosen, then it can be used to forward the received signals toward the destination node. In this chapter, only two relay nodes in which each relay node is equipped with two antennas are selected to perform an appropriate encoding process to generate distributed CL EO-STBC at the destination node. Moreover, it is required to align the two signals that have different relay encoding in terms of the construction of distributed CL EO-STBC through using a feedback channel and multiplying them by the feedback value U_1 and U_2 as shown in Figure 5.8, this will enhance the system performance.

The relay selection technique used in this chapter was also utilized to minimize the time misalignment among the set of selected relay nodes in addition to selecting the best relay node with the smallest time misalignment. The procedure to perform this operation based on CSI at the destination node is as follows

- Denote the set of available relay nodes by R each of which has two antennas.

- Select the best group of relay nodes R_s from the available set of relay nodes R using the max−min selection scheme in (5.7.3).

- Without loss of generality, the destination node is assumed to be

synchronized with the best selected relay node i.e. $\tau_1 = \tau_{11} = \tau_{21} = 0$.

- Without loss of generality, the time delays from each antenna of each remaining relay nodes $R_s - 1$ are assumed to be the same, because both antennas are co-located in the same relay node $\tau_k = \tau_{1k} = \tau_{2k} \neq 0$, $k \in 2, ..., R_s - 1$.

- At this point the selection process is repeated among the remaining set of the best relay nodes $R_s - 1$ where the relay nodes with minimum relative interference strength β are selected such that

$$\beta(l) = \min \left\{ \tau_2, \tau_3, ..., \tau_{N_{R_s-1}} \right\} \quad \text{for} \quad l \in -1, -2, -3... \quad (5.7.4)$$

As mentioned in Section 3.5, normally $\beta = 1$ (i.e. 0 dB) for $\tau_k = 0.5T$ and $\beta = 0.25$ (i.e. -6 dB) for $\tau_k = 0.125T$.

- Finally, the best relay node chosen in the second point and the relay node with the smallest time delay error are used to forward the received signals toward the destination node.

5.8   Simulation Results

In this section, by assuming that each relay node is equipped with two antennas, the simulation results of the near-optimum detection developed in this chapter are carried out, without considering the DT link between the source node and the destination node. For comparison purposes the results of the near-optimum detection scheme utilizing Alamouti code in [2], sub-optimum detection as presented in Section 5.3 [3] and distributed CL EO-STBC with outer coding in perfect syn-

chronization case are also included. It is assumed that all relay nodes can detect the received signal from the source node correctly by using the DF strategy and all the channels across the network are spatially uncorrelated Rayleigh fading channels. In order to evaluate the diversity performance of the system, the average BER against SNR is plotted using QPSK mapping. The SNR is defined as SNR=σ_s^2/σ_n^2 dB, and both relay nodes transmit at 1/4 power.
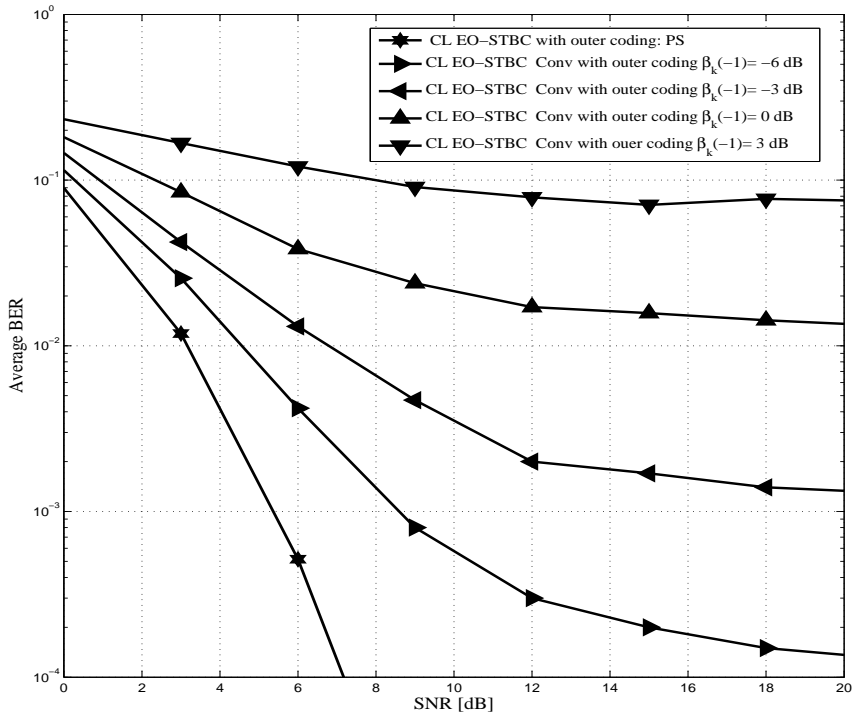
Figure 5.10. The BER performance of the conventional detector for distributed CL EO-STBC and outer convolutive coding using two relay nodes each relay node has two antennas under different time misalignments $\beta_k(-1) = -6$, -3, 0, 3 dB.

Figure 5.10 shows the BER performance of the distributed CL EO-STBC conventional detector with outer coding utilizing two antennas at each relay node under different time misalignments $\beta(-1) = -6$, -3, 0, 3 dB and set $\beta(-2) = 0$, because $g_{k2}(-1)$, $k \in 1,2$, are the most

dominate terms as mentioned earlier. It can be observed that, even under small time misalignments $\beta(-1) = -6$ dB. The conventional detector cannot deliver a good performance close to the performance of conventional detector under perfect synchronization.
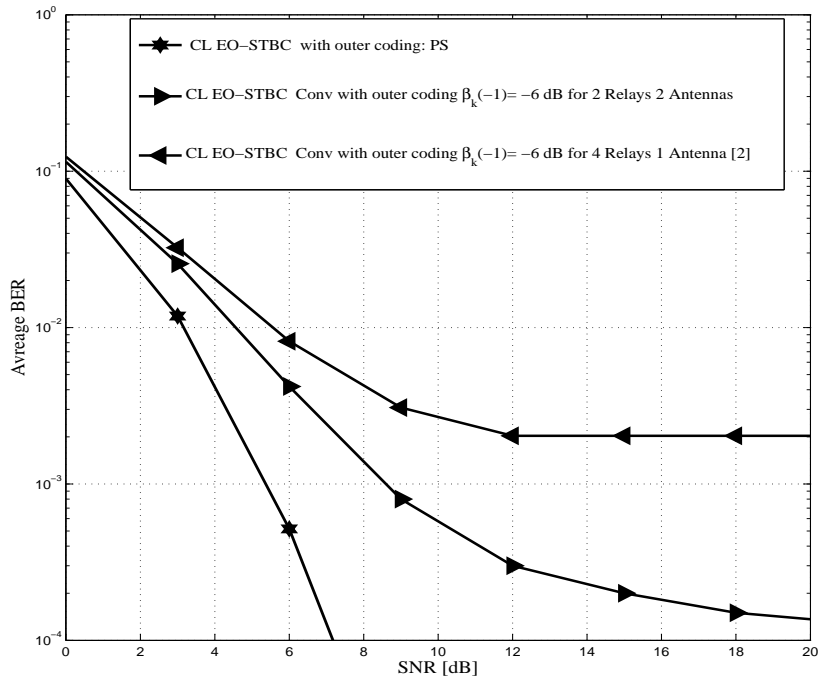
Figure 5.11. The BER performance of the conventional detector for distributed CL EO-STBC and outer convolutive coding using two relay nodes with two antennas at each relay node and four relay node with single antenna at each relay node has two antennas when $\beta_k(-1) = -6$ dB.

On the other hand Figure 5.11 illustrates the comparison between the conventional detector for distributed CL EO-STBC and outer convolutive coding using two relay nodes, each relay is equipped with two antenna and four relay nodes, each relay node is equipped with a single antenna respectively, when the time misalignments $\beta(-1) = -6$ dB. The simulation results in Figure 5.11 show that the conventional detector using two antennas at each relay node provides better perfor-

mance as compared to the conventional detector using single antenna at each relay node. For example the value of BER $= 10^{-3}$ cannot be achieved by the conventional detector using the single antenna at each relay node whereas the conventional detector utilizing two antennas at each relay node requires just approximatively 8.5 dB of SNR when $\beta(-1) = -6$ dB, in the case of two relay nodes and $\beta_k(-1) = -6$, $k \in 2, 3, 4$, in the case of four relay nodes. This is due to the number of time misalignments among the relay nodes as shown in Table 5.1.
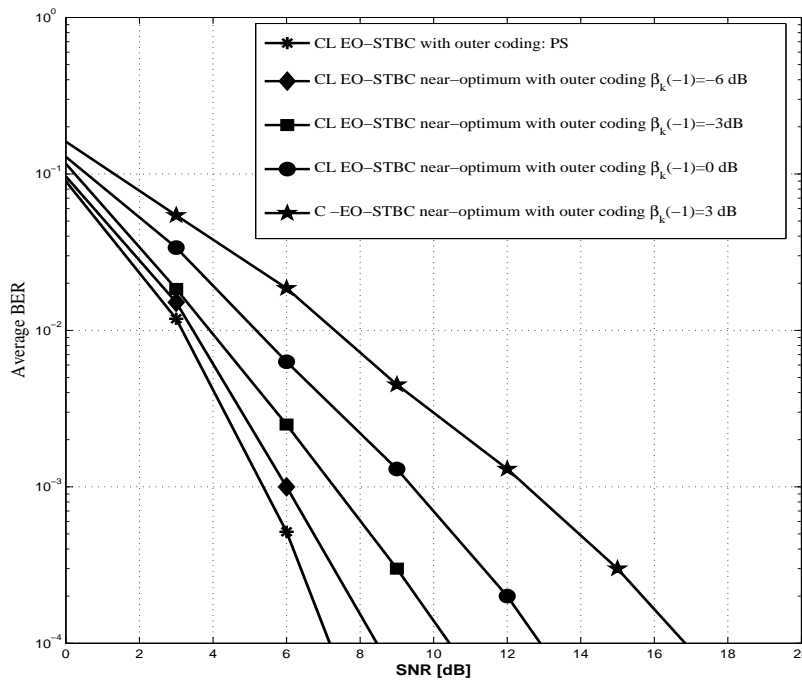
Figure 5.12. The BER performance of the near-optimum detection for distributed CL EO-STBC and outer convolutive coding using two relay nodes each relay node has two antennas under different time misalignments $\beta_j(-1) = -6$, -3, 0, 3 dB.

Figure 5.12, shows that there is a great improvement when the proposed near-optimum detection is used comparing to when the conventional detection is used under imperfect synchronization. It can be ob-

served that there is approximately a 0.5 dB degradation at BER=10^{-3} in the performance of proposed CL EO-STBC near-optimum detection when $\beta(-1) = -6$ dB as compared with the CL EO-STBC conventional detector under perfect synchronization. This degradation is increased with high time misalignments, for example when $\beta(-1) = 3$ dB there is approximately a 7 dB of SNR at BER $= 10^{-3}$ between the proposed near-optimum detection and the conventional detector under imperfect synchronization.
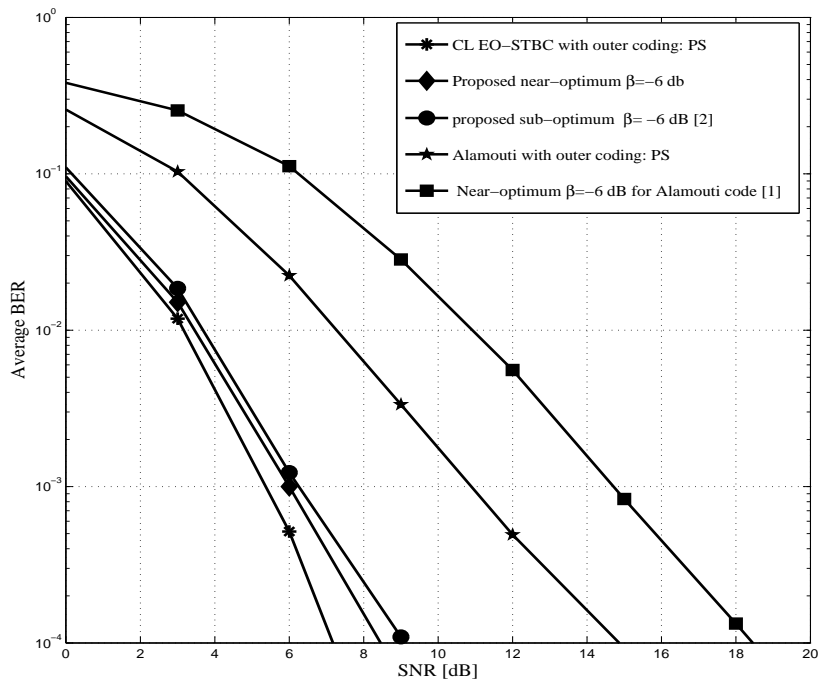
Figure 5.13. The BER performance comparison of proposed near-optimum scheme with previous detection scheme in [2] and [3].

While Figure 5.13 illustrates the BER performance comparison of the proposed near-optimum detection scheme with the previous work in [2] and [3]. For example at average BER $= 10^{-3}$ approximately 6 dB is necessary in the case of the proposed near-optimum detection,

approximately 6.2 dB is necessary in the case of sub-optimum detection scheme in [3] and approximately 14.8 dB is necessary in the case of near-optimum detection scheme in [2]. Therefore, it can be noted that the proposed near-optimum CL EO-STBC outperforms the previous work [2] and [3].

Table 5.1. Comparison of proposed near-optimum scheme with previous detection scheme in [2] and [3].

Detection Scheme	Near-optimum detection in [2]	Sub-optimum detection in [3]	proposed near-optimum detection
Number of Relay nodes	2	4	2
Number of antennas at relay nodes	1	1	2
Number of time misalignments	1	3	2
Complexity at destination	Low	High	Low
Complexity at relay node	Low	Low	High
DT Link	Not needed	Needed	Not needed
Cooperative diversity order	2	4	4

Table 5.1, illustrates the comparison between the proposed near-optimum and previous work [2] and [3], it can be seen that the cooperative diversity order of four can be obtained by using near-optimum and sub-optimum detection scheme for CL EO-STBC, however, the sub-optimum detection requires the DT link between the source node and the destination node whereas the proposed near-optimum does not require the DT link between the source node and the destination node.

While in the near-optimum detection in [2] cooperative diversity order cannot exceed more than two by utilizing the Alamouti code.
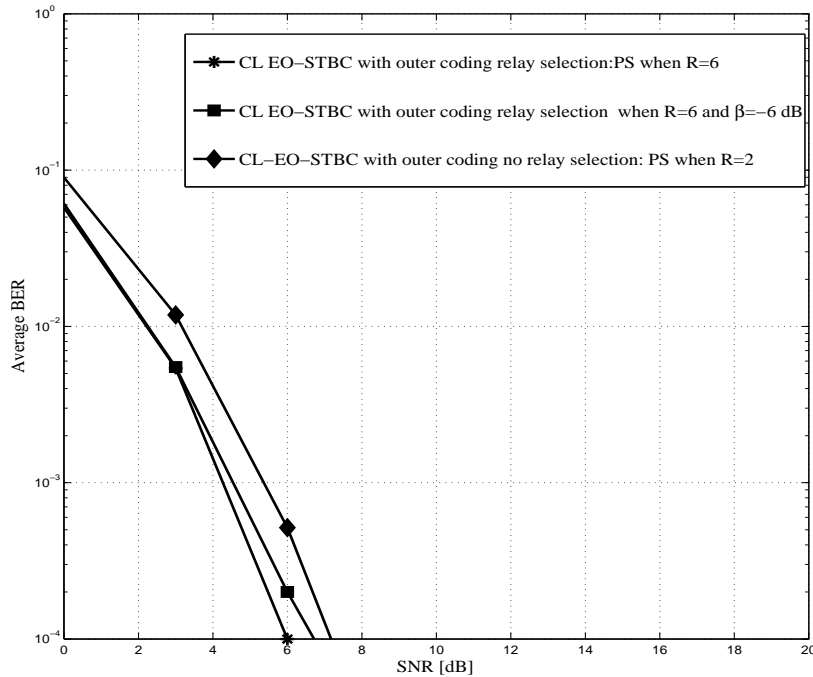
Figure 5.14. Comparison of the BER performance of the proposed selection relaying scheme with no selection relaying scheme for distributed CL EO-STBC using two relay nodes each relay node has two antennas, where $R \in 1, ..., 6$.

The performance of the proposed relay selection schemes utilizing distributed CL EO-STBC at the relay node antennas is depicted in Figure 5.14. The results confirm that the proposed relay selection schemes significantly improve the BER performance over the conventional distributed CL EO-STBC with no relay selection employed. For example, at a BER of 10^{-3}, the proposed relay selection schemes requires approximately 4.5 dB of SNR while the conventional distributed CL EO-STBC scheme requires approximately 5.9 dB of SNR. Furthermore, relay selection schemes with near-optimum detection scheme when $\beta(-1) = -6$

dB provides 0.9 dB improvement over the distributed CL EO-STBC scheme under perfect synchronization.

5.9   Chapter Summary

In this chapter the performance of two novel detection approaches were proposed and analyzed by utilizing distributed CL EO-STBC with phase rotation [15] and outer convolutive coding for wireless relay networks over frequency flat fading under imperfect synchronization. A system with two and four relay nodes, each relay has two or one antenna respectively, is demonstrated in particular.

Through the simulation results and analysis process, it was shown that both approaches are an effective at removing ISI at the destination node caused by time delay between the relay nodes with computational complexity detection at the destination node depending upon the constellation size. However, when the complexity of ML detection was considered in Section 5.6, it showed that the near-optimum detection scheme is less complex as compared with the sub-optimum detection scheme in Section 5.3 [3], this is because the near-optimum detection process relies only on the information from the relay node antennas and also due to reducing the timing error among the relay nodes when equipped with two antennas on each relay node. Furthermore, the fourth diversity order with coding gain and unity data transmission rate between the relay nodes and the destination node are exploited by both approaches.

Moreover, it has been shown through simulation results that a simple max−min relay selection method was effective in enhancing the system performance by selecting the best links and the smallest time

delay error for cooperative transmission together with exploiting the available cooperative diversity order of four as compared to distributed CL EO-STBC with outer coding under perfect synchronization among the relay nodes without relay selection.

Finally, the feedback resolution was restricted to two-bits which is practically achievable in the bi-directional control channels present in many communication systems. To reduce the high cost and high complexity due to the increased feedback information, in the next chapter a new one-bit feedback scheme for asynchronous relay network utilizing EO-STBC and orthogonal frequency division multiplexing (OFDM) type transmission over frequency flat channels will be presented.

Chapter 6

ENHANCEMENT OF

DISTRIBUTED CL EOSTBC

In this chapter a new closed-loop scheme for distributed extended orthogonal space time block coding (EO-STBC) with one-bit feedback based on selection cyclic phase rotation for two relay nodes each equipped with two antennas is proposed. Furthermore, this approach is applied to asynchronous cooperative relay networks using orthogonal frequency division multiplexing (OFDM) type transmission over frequency flat channels.

6.1 Introduction

Distributed space time block codes (STBCs) were proposed to provide both full cooperative diversity and full data transmission rate for wireless relay node networks, each relay node equipped a single antenna. However, higher order STBCs have been proposed but either cooperative diversity gain or full data transmission rate must be relaxed. A distributed quasi orthogonal STBC (QO-STBC) [43] for four relay nodes, each having only one antenna, which achieves full data transmission rate at the expenses of loss in cooperative diversity gain has been

designed [7]. In order to fully realize the benefits of distributed STBC for cooperative relay networks, channel state information (CSI) should be available at the relay nodes through feedback from the destination node. This would provide a good strategy to improve the performance of many physical layer techniques, including distributed STBC. Therefore, a closed-loop (CL EO-STBC) with two-bit feedback scheme was presented in [15] and [16] (See Appendix A) to achieve full data transmission rate and full diversity gain for point-to-point systems, however, these two closed-loop schemes required more than a single bit of feedback for each transmission block.

In this chapter a new distributed CL EO-STBC for wireless relay network with two relay nodes, each equipped with two antenna using only one-bit feedback based on selection of cyclic phase rotation is proposed to enhance cooperative diversity and improve the system performance. In particular, a new one-bit scheme is developed to eliminate the self interference from adjacent symbols in the distributed EO-STBC scheme. In this scheme, phases of symbols are rotated from relay node antennas in a prescribed way based upon CSI, which is fed back from the destination node. The rotation is effectively equivalent to rotating the phases of the corresponding channel coefficients.

As a result, the proposed one-bit feedback scheme achieves full cooperative diversity order of four for two relay nodes, each being equipped with two antennas, resulting in a significant improvement in the bit error rate (BER) performance with a significantly reduced amount of feedback compared to previous closed-loop schemes in [15] and [16] in distributed STBC for synchronous cooperative relay networks. The assumption of synchronization is not realistic due to the distributed na-

ture of each relay node, therefore, recently, asynchronous cooperative diversity has been discussed in [25], [24] and, [94].

Most of these approaches were proposed for flat fading channels and using the DF strategy at the relay nodes, where each relay has a single antenna. In [27] a simple distributed A-STBC transmission scheme based on OFDM type transmission was proposed to combat the timing error between relay nodes, however this is only valid for the case of two relay nodes as mentioned earlier. Therefore, in this chapter, the proposed one-bit feedback EO-STBC is applied along with OFDM type transmission for asynchronous relay networks over frequency flat fading channels by implementing OFDM type transmission at the source node and using amplify-and-forwared (AF) type transmission [7], time reversal (TR) and complex conjugating at two relay nodes, each being equipped with two antennas to reduce timing error among the relay nodes.

The organization of this chapter is as follows, a complete characterization of the distributed EO-STBC scheme for relay nodes with two antennas is introduced in Section 6.2. In Section 6.3 a new distributed one-bit feedback algorithm based on selection cyclic phase rotation is presented. The case of imperfect synchronization using the proposed feedback scheme along with OFDM type transmission for two relay nodes with two antenna on each relay node over frequency flat fading channels is considered in Section 6.4. In Section 6.5 the performance of the proposed feedback scheme is simulated and compared with that of existing feedback schemes. Finally, Section 6.6 concludes and summarizes this chapter.

6.2 Complete Characterization One-Bit Feedback EO-STBC

6.2.1 System Models

As shown in Figure 6.1 the proposed distributed CL EO-STBC scheme with one-bit feedback based on selection of cyclic rotation for two relay nodes with two antennas on each relay node and only a single antenna located at the source node and the destination node, without direct transmission (DT) connection between the source node and the destination node, is presented. As mentioned in Section 5.5, the distance between each pair of antennas in each relay node is assumed to be equal to half of the transmitted wavelength and all the relay nodes are subjected to half duplex constraint.
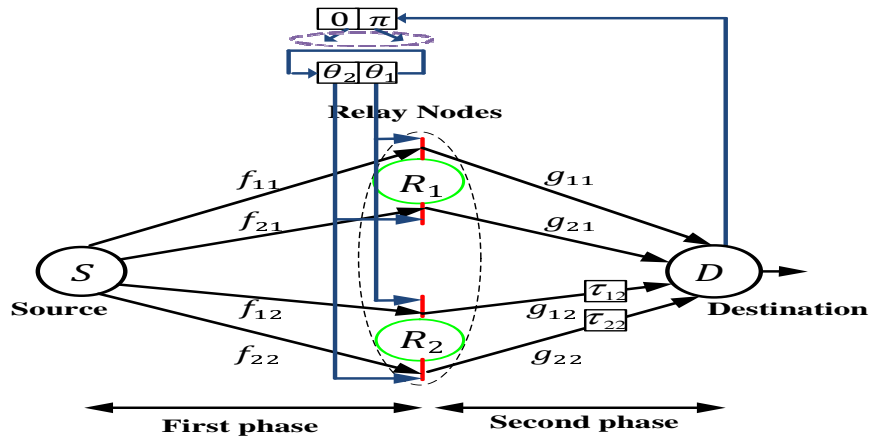
Figure 6.1. Basic structure of distributed CL EO-STBC scheme using one-bit feedback based on selection cyclic phase rotation for wireless relay networks with two antennas at each relay node and one antenna at the source and the destination node with two phases for the cooperative transmission process.

All wireless channels are assumed to be flat fading channel with zero-mean and unit-variance complex Gaussian random variables, where f_{ik} denotes the channel coefficient between the source node and each antenna of each relay node and g_{ik} denotes the channel coefficient between

each antenna of each relay node and the destination node, where $i \in 1, 2$ denotes the number of antenna on each relay node and $k \in 1, 2$ denotes the number of relay nodes in the network, also it is assumed that the destination node knows all the fading coefficients f_{ik} and g_{ik} and all relay antennas are synchronized at the symbol level. In order to achieve full cooperative diversity gain in the case of two relay nodes equipped with two antennas in each relay node, a new closed-loop scheme utilizing only one-bit feedback based on selection of cyclic phase rotation is used. Therefore the transmission signals from all relay node antennas are multiplied by two phase factor before being transmitted from each antenna of each relay node as shown in Figure 6.1 to reduce the interference factor between estimated symbols and achieve cooperative diversity gain in proportion to the number of transmitting antennas at the relaying stage.

6.2.2 Distributed One-Bit Feedback EO-STBC for Relay Nodes with Two Antennas

The communication process consists of two phases in most cooperative communication systems as mention in Section 3.2 [7] and [10]. In the first phase the source node broadcasts the signal $\sqrt{P_1}\mathbf{s}$ to antennas of each relay node, which is encoded into groups of two symbols at the source node as $\mathbf{s} = [s_1, s_2^*]^T$, where $(.)^T$ denotes the transpose and P_1 is the average transmit power at the source node for every channel use. Therefore, the received signal vector at each antenna of each relay node is represented as $\mathbf{r}_{ik}$, which is corrupted by both the fading coefficients f_{ik} and the noise term $\mathbf{n}_{ik}$ at each antenna of each relay node and can be expressed as follows

$$\mathbf{r}_{ik} = \sqrt{P_1} f_{ik} \mathbf{s} + \mathbf{n}_{ik} \qquad \text{for} \qquad i, k \in 1, 2 \qquad (6.2.1)$$

where $\mathbf{n}_{ik} = [n_{ik}^1, n_{ik}^2]^T$ is an additive Gaussian noise vector at each antenna of each relay node with distribution $CN(\mathbf{0}, \sigma_n^2 \mathbf{I}_2)$, where $\mathbf{I}_2$ is the 2×2 identity matrix. The distributed open-loop EO-STBC codeword $\mathbf{S}$ formed at the destination node has the following form

$$\mathbf{S} = [\mathbf{s}_{11} \qquad \mathbf{s}_{21} \qquad \mathbf{s}_{12} \qquad \mathbf{s}_{22}] \qquad (6.2.2)$$

where $\mathbf{s}_{i1} = [s_1, -s_2^*]^T$ and $\mathbf{s}_{i2} = [s_2, s_1^*]^T$, $i \in 1, 2$, indexes the antenna in each relay node. It is clear that $\mathbf{S}$ in (6.2.2) is the 2×4 building block form of the well known Alamouti code as presented in Section 2.2 [5]. As mentioned in previous chapters by employing distributed open-loop EO-STBC, the full cooperative diversity gain cannot be achieved in the case of two relay nodes, each relay node equipped with two antennas, due to the channel dependent interference term, which reduces the cooperative diversity gain and the signal-to-noise ratio (SNR) at the destination node. In order to overcome this issue, the new feedback scheme has been proposed with this model by using only one-bit feedback based on selection of cyclic phase rotation. Therefore, the entries of the codeword $\mathbf{S}$ in (6.2.2) are multiplied by two phase factors before transmission from each antenna of each relay node, then the code matrix of this proposed scheme can be presented as follows

$$\mathbf{S} = \begin{bmatrix} s_1 e^{j\theta_1} & s_1 e^{j\theta_2} & s_2 e^{j\theta_1} & s_2 e^{j\theta_2} \\ -s_2^* e^{-j\theta_2} & -s_2^* e^{-j\theta_1} & s_1^* e^{-j\theta_2} & s_1^* e^{-j\theta_1} \end{bmatrix} \qquad (6.2.3)$$

where the rows represent an antenna index on each relay node and the columns represent a time transmission periods for distributed CL EO-

STBC. From the code matrix $\mathbf{S}$ in (6.2.3), it is shown that all symbols are multiplied by $e^{\pm j\theta_1}$ or $e^{\pm j\theta_2}$, where θ_1 and θ_2 are available to be fed back in the angle feedback scheme. Then each antenna of each relay node, which operates in a distributed manner, transmits the received signals from the source node as a linear combination of the received signal and its conjugate denoted by $\mathbf{t}_{ik}$, $i, k \in 1, 2$. Each relay node employs with a pair of fixed 2×2 unitary matrices A_k and B_k to form the code, therefore the transmitted signal from each antenna of each relay node can be modelled as follows

$$
\begin{aligned}
\mathbf{t}_{ik} &= \sqrt{\frac{P_2}{P_1 + 1}}(A_k \mathbf{r}_{ik} + B_k \mathbf{r}_{ik}^*) \\
&= \sqrt{\frac{P_1 P_2}{P_1 + 1}}(f_{ik} A_k \mathbf{s} + f_{ik}^* B_k \mathbf{s}^*) \\
&\quad + \sqrt{\frac{P_2}{P_1 + 1}}(A_k \mathbf{n}_{ik} + B_k \mathbf{n}_{ik}^*)
\end{aligned}
\tag{6.2.4}
$$

where P_2 denotes the average transmit power at each antenna at each relay node for every channel use. In this model each antenna of each relay node is designed to use the following matrices:

$$
A_1 = \begin{bmatrix} 1 & 0 \\ 0 & 1 \end{bmatrix}, B_1 = A_2 = \begin{bmatrix} 0 & 0 \\ 0 & 0 \end{bmatrix}, B_2 = \begin{bmatrix} 0 & -1 \\ 1 & 0 \end{bmatrix}
$$

Therefore the received signal at the destination node can be modeled as follows

$$
\mathbf{y} = \sum_{k=1}^{2}(g_{1k}\mathbf{t}_{1k}U_1 + g_{2k}\mathbf{t}_{2k}U_2) + \mathbf{w}
\tag{6.2.5}
$$

where g_{ik} denotes the channel coefficients between each antenna of each relay node and the destination node and they are assumed to be zero-mean and unit-variance complex Gaussian random variables, where $i, k \in 1, 2$, $\mathbf{w} = [w_1, w_2]^T$ is the total additive Gaussian noise vector

at the destination node with distribution $CN(\mathbf{0}, \sigma_n^2 \mathbf{I}_2)$, and

$$U_1 = \begin{bmatrix} e^{j\theta_1} & 0 \\ 0 & e^{-j\theta_2} \end{bmatrix} \quad \text{and} \quad U_2 = \begin{bmatrix} e^{j\theta_2} & 0 \\ 0 & e^{-j\theta_1} \end{bmatrix}$$

In this model, it is assumed that the special case that $A_k = 0$, B_k is unitary or A_k is unitary and $B_k = 0$, then the following variables are defined as follows

$$\left. \begin{array}{cccc} \hat{A}_1 = A_1 & \hat{f}_{i1} = f_{i1} & \hat{\mathbf{n}}_{i1} = \mathbf{n}_{i1} & \mathbf{s}_{i1} = \mathbf{s}_{i1} \\ & \hat{U}_{11} = U_1 & \hat{U}_{21} = U_2 & \end{array} \right\} \quad \text{if} \ \ B_1 = 0$$

$$\left. \begin{array}{cccc} \hat{A}_2 = B_2 & \hat{f}_{i2} = f_{i2}^* & \hat{\mathbf{n}}_{i2} = \mathbf{n}_{i2}^* & \mathbf{s}_{i2} = \mathbf{s}_{i2} \\ \\ \hat{U}_{12} = \begin{bmatrix} 0 & e^{-j\theta_2} \\ -e^{j\theta_1} & 0 \end{bmatrix} & \hat{U}_{22} = \begin{bmatrix} 0 & e^{-j\theta_1} \\ -e^{j\theta_2} & 0 \end{bmatrix} \end{array} \right\} \quad \text{if} \ \ A_2 = 0$$

$$(6.2.6)$$

Therefore, the received signal (6.2.5) at the destination node can be written as follows

$$\mathbf{y} = \sqrt{\frac{P_1 P_2}{P_1 + 1}} \mathbf{S} \mathbf{H} + \mathbf{w} \tag{6.2.7}$$

where

$$\mathbf{S} = [\hat{A}_1 \hat{U}_{11} \mathbf{s}_{11} \quad \hat{A}_1 \hat{U}_{21} \mathbf{s}_{21} \quad \hat{A}_2 \hat{U}_{12} \mathbf{s}_{12} \quad \hat{A}_2 2 \hat{U}_{22} \mathbf{s}_{22}],$$

$$\mathbf{H} = [\hat{f}_{11} \hat{g}_{11} \quad \hat{f}_{21} \hat{g}_{21} \quad \hat{f}_{12} \hat{g}_{12} \quad \hat{f}_{22} \hat{g}_{22}]^T$$

and

$$\mathbf{w} = \sqrt{\frac{P_2}{P_1 + 1}} \left(\sum_{k=1}^{2} (g_{1k} \hat{A}_k \hat{U}_{1k} \hat{\mathbf{n}}_{1k} + g_{2k} \hat{A}_k \hat{U}_{2k} \hat{\mathbf{n}}_{2k}) \right) + \mathbf{n}_{rd}$$

where $\mathbf{n}_{rd} = [n_{rd}^1, n_{rd}^2]^T$ is an additive Gaussian noise vector at the destination node with zero-mean and unit-variance. Since $\mathbf{S}$ is a codeword

in distributed CL EO-STBC given in (6.2.3) and the channel coeffi-

cients f_{ik} and g_{ik} are known at the destination node, where $i, k \in 1, 2$,

the maximum likelihood (ML) decoding is given by

$$\hat{\mathbf{s}} = \arg \min_{\mathbf{S}} \|\mathbf{y} - \sqrt{\frac{P_1 P_2}{P_1 + 1}} \mathbf{SH}\|_F^2 \qquad (6.2.8)$$

where $||.||_F$ indicates the Frobenius norm and $\mathbf{S}$ is the set of all possible

vector symbols. If the total power per symbol transmission used in

the whole network is fixed as P, the optimal power allocation that

maximizes the expected receive SNR is modelled as

$$P_1 = \frac{P}{2} \qquad \text{and} \qquad P_2 = \frac{P}{M_R R} \qquad (6.2.9)$$

where R is the number of relay nodes and M_R is the number of antennas

on each relay node. Thus, the optimum power allocation is such that

the source node uses half the total power and the relay nodes share the

other half [6] and [72][1].

6.3   Enhancement by Distributed One-Bit Feedback Based on

Selection of Cyclic Rotation

By substituting (6.2.4) into (6.2.5) and taking the conjugate of y_2 in

(6.2.5), the equivalent channel matrix corresponding to the code matrix

(6.2.3) can be represented as follows

---

[1]When $log\ P \gg 1$, distributed CL EO-STBC achieves diversity $MR(1 - loglogP/logP)$. As $P \to \infty$, distributed CL EO-STBC achieves full cooperative diversity gain in proportion to the number of transmitting antennas on all relay nodes

$$\mathbf{H} = \begin{bmatrix} f_{11}g_{11}e^{j\theta_1} + f_{21}g_{21}e^{j\theta_2} & f_{12}^*g_{12}e^{j\theta_1} + f_{22}^*g_{22}e^{j\theta_2} \\ f_{12}g_{12}^*e^{j\theta_2} + f_{22}g_{22}^*e^{j\theta_1} & -f_{11}^*g_{11}^*e^{j\theta_2} - f_{21}^*g_{21}^*e^{j\theta_1} \end{bmatrix} \quad (6.3.1)$$

Therefore, the Grammian matrix can be calculated by applying the matched filter at the destination node with $\mathbf{H}^H\mathbf{H}$ matrix, where $(.)^H$ denotes Hermitian transpose and is given as

$$\mathbf{H}^H\mathbf{H} = \begin{bmatrix} \lambda_c + \lambda_f & 0 \\ 0 & \lambda_c + \lambda_f \end{bmatrix} \quad (6.3.2)$$

where λ_c indicates the conventional channel gain for two relay nodes with two antennas at each relay node, and given by

$$\lambda_c = \sum_{k=1}^{2}(\mid f_{1k}g_{1k}\mid^2 + \mid f_{2k}g_{2k}\mid^2) \quad (6.3.3)$$

and λ_f can be interpreted as the channel dependent interference parameters, and given by

$$\lambda_f = 2\Re(f_{11}^*g_{11}^*f_{21}g_{21} + f_{12}g_{12}^*f_{22}^*g_{22})e^{j(\theta_2-\theta_1)} \quad (6.3.4)$$

where $\Re\{.\}$ denotes the real part of a complex number. The feedback performance gain λ_f, which changes with the defined value of $e^{j(\theta_2-\theta_1)}$, which are determined by using one-bit feedback based on selection of the cyclic phase rotation θ_1 and θ_2. It is well known that the presence of the channel dependent interference λ_f may be negative, this leads to cooperative diversity loss. Moreover, the SNR at the destination node can be calculated as follows

$$SNR = \frac{\lambda_c + \lambda_f}{M_R R} \frac{\sigma_s^2}{\sigma_n^2} \qquad (6.3.5)$$

where σ_s^2 is the total transmit power of the desired signal and σ_n^2 is the noise power at the destination node. It is obvious that if $\lambda_f > 0$, the designed closed-loop scheme can obtain additional performance and provide fourth order diversity at the destination node by using two relay nodes with two antennas at each relay node, which leads to an improved SNR at the destination node. Therefore the design criterion of one-bit feedback scheme based on selection of cyclic phase rotation as shown in (6.2.3) is proposed. In this approach each element of the feedback performance gain of g_f in (6.3.2) should be real and positive which can be achieved by adopting one-bit feedback $b = 0$ or $b = 1$ to indicate whether

$$\Re(f_{11}^* g_{11}^* f_{21} g_{21} + f_{12} g_{12}^* f_{22}^* g_{22}) \geq 0 \qquad b = 0$$

or

$$\Re(f_{11}^* g_{11}^* f_{21} g_{21} + f_{12} g_{12}^* f_{22}^* g_{22}) < 0 \qquad b = 1$$

Then this one-bit information will be fedback to each antenna of each relay node. At relay nodes, first judge the value of b if $b = 0$, which can be achieved by seting $\theta_1 = \theta_2 = 0$ or $\theta_1 = \theta_2 = \pi$ which ensures $e^{j(\theta_2 - \theta_1)} = 1$, and if $b = 1$, which can be achieved by seting $\theta_1 = \pi$ and $\theta_2 = 0$ or $\theta_1 = 0$ and $\theta_2 = \pi$ which ensures $e^{j(\theta_2 - \theta_1)} = -1$.

The solution for the proposed closed-loop scheme using one-bit feedback based on selection cyclic phase rotation can be expressed as follows

$$b = \begin{cases} 0, & \Re(f_{11}^* g_{11}^* f_{21} g_{21} + f_{12} g_{12}^* f_{22}^* g_{22}) \geq 0 \\ & \text{set } \theta_1 = \theta_2 = 0 \ \text{ or } \ \theta_1 = \theta_2 = \pi \\ \\ \\ 1, & \Re(f_{11}^* g_{11}^* f_{21} g_{21} + f_{12} g_{12}^* f_{22}^* g_{22}) < 0 \\ & \text{set } \theta_1 = \pi \ \ \theta_2 = 0 \ \text{ or } \ \theta_1 = 0 \ \ \theta_2 = \pi \end{cases}$$

It can be seen that the proposed scheme is different from [15] and [16] in the sense that the proposed scheme chooses just one-bit feedback to maximize the value of λ_f and by selection of cyclic phase rotation.

6.4   OFDM Based Approach for Asynchronous Wireless Relay Channels

6.4.1   OFDM Based Approach for Frequency Flat Fading Channels

In this section, a distributed CL EO-STBC-OFDM scheme with one-bit feedback based on selection cyclic phase rotation for asynchronous relay networks over frequency flat fading channels is presented. As shown in Figure 6.2 the OFDM type transmission with cyclic prefix (CP) is implemented at the source node, and TR and complex conjugation are implemented at the relay nodes. The CP at the source node is used to remove the timing errors from the relay nodes as shown in Figure 6.2, which operate in simple distributed STBC type mode. It is assumed that the channels between any two nodes is quasi-static flat Rayleigh fading.
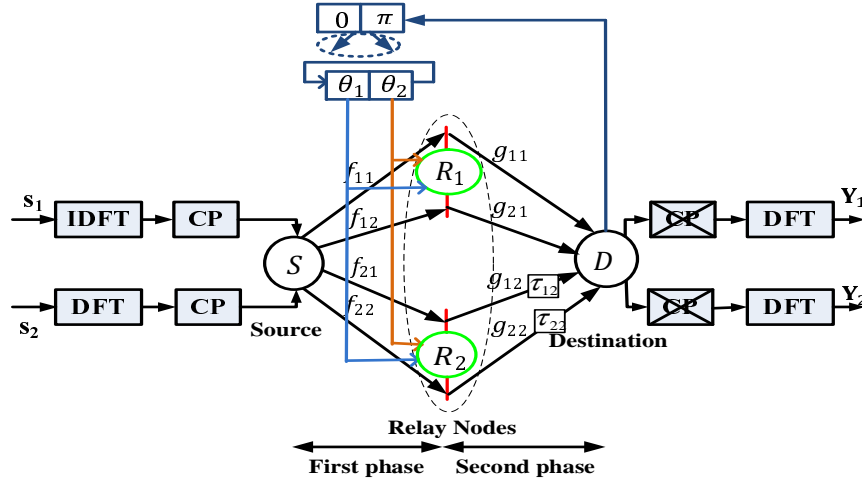
Figure 6.2. Basic structure of distributed CL EO-STBC scheme using one-bit feedback based on selection cyclic phase rotation along with OFDM and CP at the source node for wireless relay networks with two antennas in each relay node and one antenna in the source and the destination nodes with two phases for the cooperative transmission process.

As mentioned in Section (6.2.1), to transmit the signal from the source node to the destination node, they undergo two phases. In the first phase, at the source node the signal are first mapped into a block of N complex symbols $\mathbf{s}_k = [s_{0,k}, s_{1,k}, ..., s_{N-1,k}]^T$, $k \in 1, 2$. Subsequently, each length N block of modulated symbols is fed to an OFDM modulator. In the OFDM modulator, the first and second blocks are converted into samples for transmission using the N-point inverse discrete Fourier transform (IDFT) and N-point discrete Fourier transform (DFT) operations, respectively and can be represented as follows

$$\mathbf{S}_1 = \text{IDFT}(\mathbf{s}_1)$$

$$\mathbf{S}_2 = \text{DFT}(\mathbf{s}_2) \tag{6.4.1}$$

thereafter, each OFDM symbol $\mathbf{S}_k$, $k \in 1, 2$, is preceded by a CP with length l_{cp} before broadcasting them to the antennas of each relay node.

It is assumed that l_{cp} is not less than the maximum possible relative timing error τ_{max} of the signals arriving at the destination node from each antenna of each relay node $l_{cp} \geq \tau_{max}$ [27]. Denote two OFDM symbols $\mathbf{S}_1$ and $\mathbf{S}_2$ with preceded CP as $\mathbf{S}_{cp1}$ and $\mathbf{S}_{cp2}$ and thus each OFDM symbol consists of $L \triangleq N + l_{cp}$ samples.

Therefore, the received signals at each antenna of each relay node for two successive OFDM symbols duration is denoted as $\mathbf{r}_{ik}^t$, which is corrupted by both the fading coefficients f_{ik} and the noise term $\mathbf{n}_{ik}^t$ and can be represented as follows

$$\mathbf{r}_{ik}^t = \sqrt{P_1} f_{ik} \mathbf{S}_{cp_t} + \mathbf{n}_{ik}^t \quad \text{for} \quad i, k, t \in 1, 2 \qquad (6.4.2)$$

where $\mathbf{n}_{ik}^t$ is an additive Gaussian noise vector, with elements having zero-mean and unit-variance, for each antenna of each relay node in two successive OFDM symbol durations, and it is assumed that the channel coefficients are constant during two OFDM symbol intervals. Denote P_1 as the transmission power at the source node, then the mean power of the signal $\mathbf{r}_{ik}^t$ at each relay node is $P_1 + 1$ due to the unit variance assumption of the additive noise $\mathbf{n}_{ik}^t$, $i, k, t \in 1, 2$ from the source node to each antenna of each relay node in (6.4.2). Assume the total power used to transmit the information symbols vector $\mathbf{s}_k$ from the source node to the destination node is P, therefore, the optimum power allocation is used in this proposed scheme can be represented as in (6.2.9). In the second phase the one-bit feedback scheme proposed in the previous sections is used, i.e. multiplying the received noisy signal $\mathbf{r}_{ik}^t$ from each antenna of each relay node by the proper phase factor to achieve full cooperative diversity gain. Therefore, the code matrix transmited from the each antenna of each relay node can be modelled as follows

$$
\begin{bmatrix} \mathbf{t}_{11}^1 & \mathbf{t}_{11}^2 \\ \mathbf{t}_{21}^1 & \mathbf{t}_{21}^2 \\ \mathbf{t}_{12}^1 & \mathbf{t}_{12}^2 \\ \mathbf{t}_{22}^1 & \mathbf{t}_{22}^2 \end{bmatrix} = \rho \begin{bmatrix} \mathbf{r}_{11}^1 e^{j\theta_1} & -\zeta(\mathbf{r}_{11}^2)e^{-j\theta_2} \\ \mathbf{r}_{21}^1 e^{j\theta_2} & -\zeta(\mathbf{r}_{21}^2)e^{-j\theta_1} \\ (\mathbf{r}_{12}^2)^* e^{j\theta_1} & \zeta(\mathbf{r}_{12}^1)^* e^{-j\theta_2} \\ (\mathbf{r}_{22}^2)^* e^{j\theta_2} & \zeta(\mathbf{r}_{22}^1)^* e^{-j\theta_1} \end{bmatrix} \tag{6.4.3}
$$

where the row corresponds to each antenna of each relay node, the column corresponds to the particular time transmission periods, $\rho = \sqrt{\frac{P_2}{P_1+1}}$, $(.)^*$ denotes the complex conjugation, and $\zeta(.)$ represents the TR of the signals, that is, $\zeta(\mathbf{r}_{ik}^t(n)) \triangleq \mathbf{r}_{ik}^t(L-n)$, where $n = 0, 1, ..., L-1$, and $\mathbf{r}_{ik}^t(L) \triangleq \mathbf{r}_{ik}^t(0)$. The advantage at the relay nodes is that no decoding operation is required while only implementing very simple linear transform operations on the received noisy signal $\mathbf{r}_{ik}^t$ such as amplification, conjugation, TR and reordering, where $i, k, t \in 1.2$. Moreover, the proposed scheme does not need to decode the information symbols or perform Fourier transform operations at the relay nodes.

At the destination node, timing synchronization is easily implemented for the shortest path from the source node to the destination node. Without loss of generality, this will be assumed to be the paths of each antenna of the first relay node R_1 as shown in Figure 6.2. Hence the delay in sample periods of the paths from each antenna of each relay node is relative to that from each antenna of the first relay node R_1 and it is denoted as $\tau_{i1} = 0$ and there is time misalignment with each antenna of the second relay node R_2 and is denoted as $\tau_{12} = \tau_{22} \neq 0$. As shown in Figure 6.3 the time delays from the each antenna of the second relay node R_2 are shown identical because both antennas are located on the same relay node.
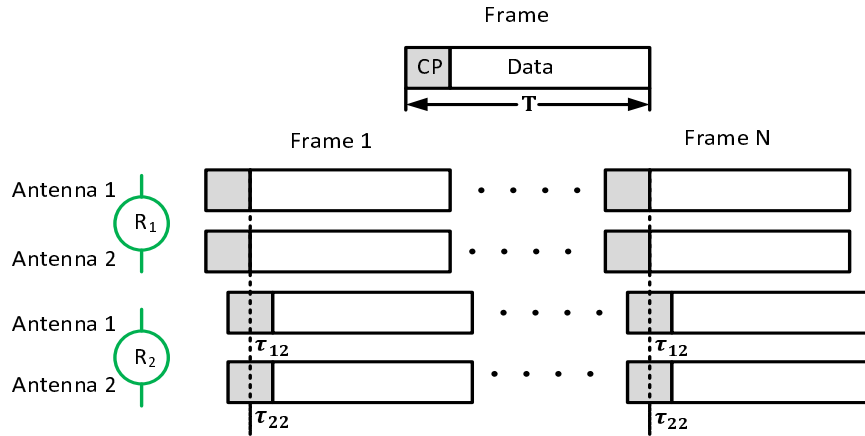
Figure 6.3. The basic structure of the transmission frames with respect to each antenna of R_1 is synchronized to the destination node, while each antenna of R_2 is not synchronized to the destination node.

To process the signals at the destination node firstly the CP removal is preformed for each OFDM symbol as in a conventional OFDM system. Then the reordering process needs to be preformed on the second OFDM received signal to correct for the misalignment caused by the TR in (6.4.3). This can be preformed by shifting the last l_{cp} samples of the N-point vector as the first l_{cp} samples. Finally, the received signals are transformed by the N-point DFT. Since the signal from each antenna of the second relay node arrives at the destination node with timing error $\tau_k = \tau_{12} = \tau_{22}$, later than the signals from each antenna of the first relay node, the orthogonality between subcarriers can still be maintained because τ_{max} is assumed to be not greater than the length of l_{cp}. The delay in the time domain corresponds to a phase term in frequency and can be expressed as follows

$$\mathbf{f}^{\tau_k} = [f_0^{\tau_k}, f_1^{\tau_k}, ..., f_{N-1}^{\tau_k}]^T \qquad (6.4.4)$$

where $f_m^{\tau_k} = e^{-j2\pi m \tau_k/N}$, where $k \in 1, 2$ and $m \in 0, 1....., N-1$, the received signals at the destination node at two time transmission peri-

ods after the CP removal, reordering the second OFDM received symbol and the DFT transformation is denoted as $\mathbf{Y}_k = [y_{0,k}, y_{1,k}, \ldots\ldots, y_{N-1,k}]$, $k \in 1, 2$ and can be written as

$$\begin{aligned}
\mathbf{Y}_1 = {} & \sqrt{\frac{P_2}{P_1 + 1}} [\mathrm{DFT}(\mathbf{t}_{11}^1)g_{11} + \mathrm{DFT}(\mathbf{t}_{21}^1)g_{21} \\
& + (\mathrm{DFT}(\mathbf{t}_{12}^1)g_{12} + \mathrm{DFT}(\mathbf{t}_{22}^1)g_{22}) \otimes \mathbf{f}^{\tau_1}] + n_{rd}^1 \qquad (6.4.5)
\end{aligned}$$

$$\begin{aligned}
\mathbf{Y}_2 = {} & \sqrt{\frac{P_2}{P_1 + 1}} [-\mathrm{DFT}(\mathbf{t}_{11}^2)g_{11} - \mathrm{DFT}(\mathbf{t}_{21}^2)g_{21} \\
& + (\mathrm{DFT}(\mathbf{t}_{12}^2)g_{12} + \mathrm{DFT}(\mathbf{t}_{22}^2)g_{22}) \otimes \mathbf{f}^{\tau_2}] + n_{rd}^2 \qquad (6.4.6)
\end{aligned}$$

where $\otimes$ is the Hadamard product and n_{rd}^t is additive Gaussian noise at the destination node with zero-mean and unit-variance where $t \in 1, 2$. Using the identities as in [27], $(\mathrm{DFT}(s))^* = \mathrm{IDFT}(s^*), (\mathrm{IDFT}(s))^* = \mathrm{DFT}(s^*)$ and $(\mathrm{DFT}(\zeta(\mathrm{DFT}(s)))) = \mathrm{IDFT}((\mathrm{DFT}(s)))$. Therefore, the received signals (6.4.5) and (6.4.6), conjugated for convenience at two transmission periods can be written as in the following EO-STBC code form at each subcarrier m; $0 \le m \le N - 1$

$$\begin{bmatrix} Y_{m,1} \\ Y_{m,2}^* \end{bmatrix} = \sqrt{\frac{P_2 P_1}{P_1 + 1}} \mathbf{H}_m \begin{bmatrix} s_{m,1} \\ s_{m,2}^* \end{bmatrix} + \mathbf{w}_m \qquad (6.4.7)$$

where $\mathbf{w}_m = [w_{m,1}, w_{m,2}]^T$ denotes the total additive Gaussian noise vector at the relay nodes and the destination node and

$$\mathbf{H}_m = \begin{bmatrix} h_{m,11}e^{j\theta_{m,1}} + h_{m,21}e^{j\theta_{m,2}} & (h_{m,12}e^{j\theta_{m,1}} + h_{m,22}e^{j\theta_{m,2}})f_m^{\tau_1} \\ (h_{m,12}^*e^{j\theta_{m,2}} + h_{m,22}^*e^{j\theta_{m,1}})f_m^{\tau_2} & -h_{m,11}^*e^{j\theta_{m,2}} - h_{m,21}^*e^{j\theta_{m,1}} \end{bmatrix}$$

$$(6.4.8)$$

where

$$
h_{m,ik} = \begin{cases} f_{m,ik} g_{m,ik} & \text{if} \quad k = 1 \\[3em] f^*_{m,ik} g_{m,ik} & \text{if} \quad k = 2, \end{cases}
$$

where $i, k \in 1, 2$, $m \in 0, 1....., N - 1$, from (6.4.7) and assuming CSI at the destination node, the conventional one-bit feedback EO-STBC-OFDM detection can be carried as follows

- Multiply the received signal $\mathbf{Y} = [Y_{m,1}, Y^*_{m,2}]^T$ in (6.4.7) by the matched filter $\mathbf{H}^H$ to form the detection vector $\hat{\mathbf{g}} = [\hat{g}_{m,1}, \hat{g}_{m,2}]^T$ as follows

$$
\begin{bmatrix} \hat{g}_{m,1} \\ \hat{g}_{m,2} \end{bmatrix} = \mathbf{H}^H_m \mathbf{H}_m \begin{bmatrix} Y_{m,1} \\ Y_{m,2} \end{bmatrix} \tag{6.4.9}
$$

- Applying the LS detection method to obtain the detection results $\hat{s}_{m,k}$

$$
\hat{s}_{m,k} = arg \min_{\mathbf{s}_{m,k} \in \mathbf{S}} \| \hat{g}_{m,k} - \sqrt{\frac{P_2 P_1}{P_1 + 1}} \mathbf{H}_m \mathbf{S}_{m,k} \|^2 \tag{6.4.10}
$$

where $\mathbf{S}$ is the set of all possible vector symbols and P is the total transmission power in the whole network, therefore the optimal power allocation that maximizes the expected receive SNR is modelled as in (6.2.9).

6.4.2   One-Bit Feedback Scheme for Asynchronous Wireless Relay Channels

As mentioned in Section 6.3, by applying the matched filter at the destination node with the channel matrix in (6.4.8) for each of m sub-

carriers, the Grammian matrix can be obtained as in (6.3.2) where $\lambda_{c_m} = \sum_{i=1}^{2} (|f_{m,i1}g_{m,i1}|^2 + |f_{m,i2}g_{m,i2}|^2)$ corresponds to the conventional gain for two relay nodes, each relay has a two antenna and $\lambda_{f_m} = 2\Re(h_{m,1} + h_{m,2})e^{j(\theta_{m,2} - \theta_{m,1})}$ corresponds to the feedback performance gain where

$$
h_{m,k} = \begin{cases} f_{m,11}^* g_{m,11}^* f_{m,21} g_{m,21} & \text{if} \quad \text{k=1} \\ \\ f_{m,12} g_{m,12}^* f_{m,22}^* g_{m,22} & \text{if} \quad \text{k=2,} \end{cases}
$$

It is clear that if λ_{f_m} is positive, it corresponds to a type of array gain, assuming the destination node knows CSI, the design criterion of one-bit feedback for each of m subcarriers can be designed by adapting the value of $b = 0$ or $b = 1$ to find the value of the phase angles which is from the set of $\{\theta_{m,1}, \theta_{m,2}\} = [0, \pi]$ as follows

$$
b = \begin{cases} 0, & e^{j(\theta_{m,2} - \theta_{m,1})} = 1 \\ & \text{set} \ \ \theta_{m,1} = \theta_{m,2} = 0 \ \ \text{or} \ \ \theta_{m,1} = \theta_{m,2} = \pi \\ \\ 1, & e^{j(\theta_{m,2} - \theta_{m,1})} = -1 \\ & \text{set} \ \ \theta_{m,1} = \pi \ \ \theta_{m,2} = 0 \ \ \text{or} \ \ \theta_{m,1} = 0 \ \ \theta_{m,2} = \pi \end{cases}
$$

It is obvious that if $\lambda_{f_m} > 0$, the closed-loop one-bit feedback design can obtain additional performance gain which leads to an improved SNR at the destination node as mentioned in Section (6.3).

6.5 Simulation Results

In this section, the end-to-end bit error performance of the proposed CL EO-STBC using only one-bit feedback based on selection of cyclic phase rotation in distributed cooperative relay network is simulated. It is

assumed that in all simulation results all the channels in the network are quasi-static flat fading channels. The average BER performance against the average transmitted power P_1 at the source node was simulated by using quadrature phase shift keying (QPSK) modulation.

In Figure 6.4, simulation results comparing the performance of the proposed closed-loop scheme with the previous closed-loop schemes by applying these schemes in a distributed manner and employing two relay nodes, each having two antennas.
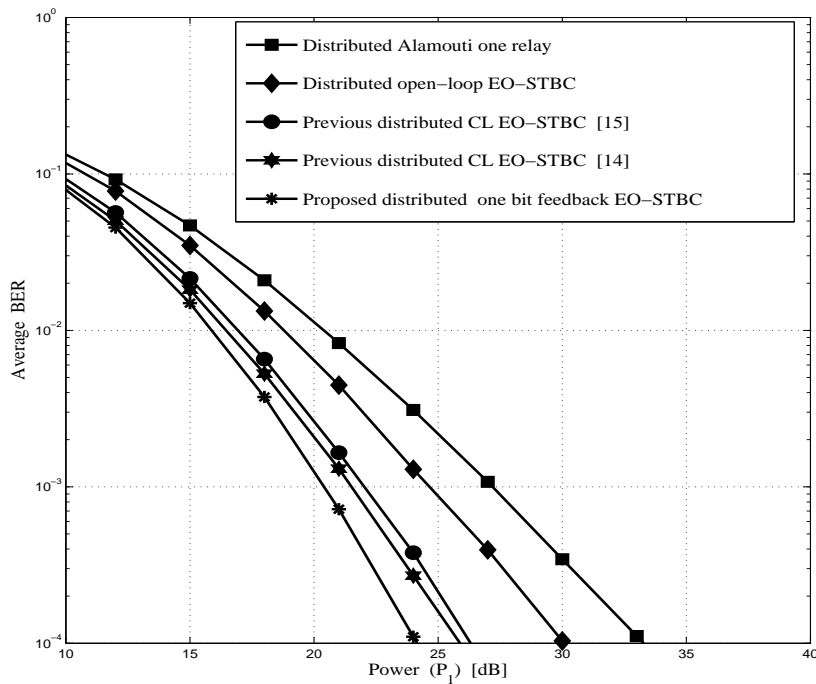
Figure 6.4. A comparison of BER performance as a function of transmit power of the proposed scheme and with the previous feedback schemes in two relay nodes with two antennas in each relay for a wireless network.

It can be observed that all the distributed CL EO-STBC schemes obtain better performance than the distributed open-loop EO-STBC. In particular, it is clear that the proposed one-bit feedback scheme

provides an improved performance for instance at 10^{-3}, it provides a power saving approximately 5 dB as compared to the distributed open-loop scheme, approximately 2.5 dB as compared to distributed CL EO-STBC in [16] and approximately 2 dB as compared to distributed CL EO-STBC in [15]. Furthermore, the distributed A-STBC using only one relay node equipped with two antennas is included as reference. The proposed scheme at bit error probability of 10^{-3} provides a power saving of approximately 8 dB improvement as compared to distributed A-STBC.
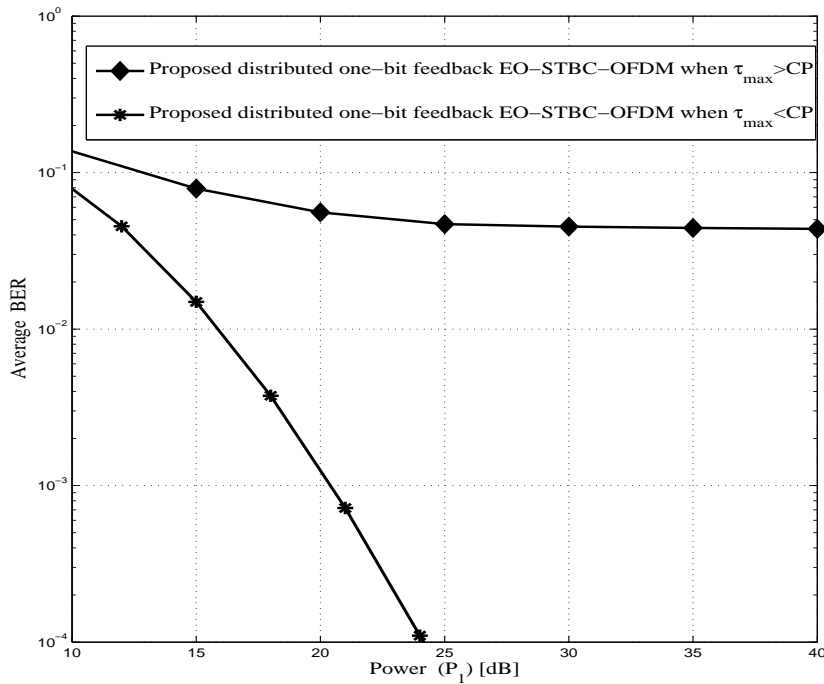
Figure 6.5. The BER performance as a function of transmit power of the proposed scheme in two relay nodes with two antennas in each relay for asynchronous wireless network.

Figure 6.5 shows the performance of the proposed scheme under timing error among the relay nodes using OFDM type transmission and CP at the source node to eliminate the timing error from the relay

nodes where the length of data block N=64 with $l_{cp} = 16$ and the time delay between the relay nodes is chosen between 0 and 11 with uniform distribution. The figure shows that when the CP is greater than the time delay the system delivers a good performance, while if the time delay is greater than the CP the system does not deliver a good performance.

6.6 Chapter Summary

In this chapter, a new one-bit feedback based on selection cyclic phase rotation is proposed along with OFDM type transmission for asynchronous relay networks over frequency flat fading channels. In this scheme, only one-bit of feedback was used to determine the transmission phase terms applied to the symbols from the antennas of each relay node. This is considerably lower feedback overhead as compared to the previous feedback schemes and this proposed scheme can effectively provide full cooperative diversity gain with array gain as well as full data transmission rate between the relay nodes and the destination node, while each symbol is decoded separately utilizing only linear processing. From the simulation results it is clear that the proposed feedback scheme can enhance the performance of the system with the feedback information limited to only one-bit, as such it outperforms previous feedback schemes in distributed cooperative relay networks and provides robustness to an asynchronous cooperative relay network link between the source node through relaying stage to the destination node. Furthermore, employing two antennas on each relay node will reduce timing error among the relay nodes as compared to using four relay nodes each having a single antenna.

Chapter 7

CONCLUSION

This concluding chapter summarizes the results that were presented in this thesis. Furthermore, some open problems are pointed out, giving possible research directions for the future.

7.1 Conclusion

In this thesis, the design of distributed space time block coding (STBC) methods over frequency flat fading channels were developed for asynchronous cooperative relay networks. The impact of synchronization error among the relay nodes in cooperative communication systems is one of the most important research areas. With asynchronism the code structure at the destination node is not orthogonal and hence the transmitted signals are prevented from being successfully decoded at the destination node with a conventional STBC decoder.

However, to mitigate such interference at the destination node and deliver a good performance with full cooperative diversity, different interference cancellation methods were proposed in this thesis.

In Chapter 3, the concept of virtual antenna array (VAA) was introduced and applied to the asynchronous cooperative relay networks, implementing distributed multiple-input multiple-output multi-stage communication networks.

In particular, a two-hop network was introduced using distributed closed-loop quasi-orthogonal STBC (CL QO-STBC) and closed-loop extended orthogonal STBC (CL EO-STBC) without outer coding in a decode-and-forward (DF) cooperative relaying system employing a parallel interference cancellation (PIC) detection scheme at the destination node for four relay nodes under imperfect synchronization assuming that there is a direct transmission (DT) connection between the source node and the destination node.

These distributed closed-loop STBCs were shown to obtain full data transmission rate between the relay nodes and the destination node and attain full cooperative diversity order of four with simple linear decoding at the destination node, unlike the distributed Alamouti STBC (A-STBC) and distributed orthogonal STBC (OSTBC).

Simulation results illustrated that the performance gain of deploying distributed CL EO-STBC design is superior to the other distributed STBC designs over the relay nodes. This suggested that in a cooperative relay network, an increase in the number of cooperating relay nodes must be accompanied with appropriate coding techniques to maximize the network performance.

Although the DT link between the source node and the destination node can reduce the effect of pathloss as well as improve the end-to-end performance, it may not be practical to always have this DT link due to potential obstacles between the two nodes. A new relaying solution that employs distributed A-STBC for two relay nodes with PIC detection at both the relay nodes and the destination node without the DT connection between the source node and the destination node was proposed. It demonstrated that the use of a multilevel cooperative

multi-hop solution yields significant gains which deliver good end-to-end bit error rate (BER) performance for a given network topology. Moreover, simulation results confirmed that a new relaying solution provided a significant improvement in network performance compared to the DT link assisted cooperation using distributed A-STBC.

The advantage of these proposed schemes is the potential delivering of full data transmission rate in each hop and cooperative diversity order equal to the number of cooperating relay nodes using a DF strategy. However, this will lead to relay node complexity.

In Chapter 4, in order to reduce the amount of processing and hardware complexity at the relay nodes, the cooperative strategy for distributed STBC based on amplify-and-forward (AF) transmission type was designed for asynchronous cooperative relay networks over frequency flat fading channels employing distributed A-STBC design and distributed CL EO-STBC design with outer coding and a PIC detection scheme at the destination node for two and four relay nodes respectively. It was demonstrated that in the first phase the source node sends signals to the relay nodes and then in the second phase the relay nodes encode their received signals into a linear dispersion STBC and transmit to the destination node without any decoding operation at the relay node, which overcomes the issue of complexity at the relay node as compared to the DF strategy mentioned in Chapter 3.

Furthermore, it was shown that both proposed schemes deliver full data transmission rate in each stage and full cooperative diversity gain with coding gain, the pairwise error probability (PEP) utilizing both proposed schemes for synchronous cooperative relay network was analyzed to confirm that the cooperative diversity gain is equal to the

number of transmitting relay nodes in the case of distributed A-STBC design and a smaller PEP was achieved due to array gain in the case of distributed CL EO-STBC design.

Simulation results confirmed the advantage of using distributed CL EO-STBC design in asynchronous cooperative relay networks as compared with the distributed A-STBC design. A practical measure was also used in demonstrating this performance advantage with distributed CL EO-STBC providing a steeper BER curve than the distributed A-STBC ensuring that a diversity order of four is achieved at the destination node for the topology considered. This means that four relay nodes using distributed CL EO-STBC promises to deliver a better performance advantage compared to two relay nodes deploying distributed A-STBC.

In all the proposed distributed STBCs which were considered in Chapter 3 and 4, the PIC detection scheme was shown to be very effective to combat the synchronization error at the destination node and deliver a good performance close to the case of distributed STBC under perfect synchronization as was showing in simulation results. Just three iterations of the PIC were required; whereas maximum likelihood (ML) detection failed to mitigate the impact of imperfect synchronization even under small time misalignments. However, the PIC detector had appreciable computational complexity dependent upon the number of iterations.

In Chapter 5, two novel detection schemes were proposed for a DF asynchronous cooperative relay network utilizing distributed CL EO-STBC with phase rotation and outer convolutive coding to mitigate the interference component at the destination node caused by time delay

error between the relay nodes, whilst reducing the detection complexity at the destination node. It was shown that both approaches do not require multiple iterations and the computational complexity is only dependent upon the constellation size Therefore, these two contributions can be considered as promising techniques for lower detection complexity at the destination node as compared to distributed STBC with the PIC detection scheme in Chapters 3 and 4.

Through the simulation results and analysis, it was shown that both approaches proved to be very effective in removing ISI at the destination node caused by time delay between the relay nodes. Unity data transmission rate was achieved between the relay node and the destination node and full cooperative diversity equal to $M_R R$ with coding gain, where M_R is the number of antennas on each relay node R, were obtained. Furthermore, the relay selection technique was considered with a near-optimum approach for two dual antenna relay nodes which offer the possibility to improve the system performance as compared to the cooperative relay system without relay selection scheme.

Finally, in Chapter 6, in order to design a closed-loop transmission method, it was desirable to have features such as a limited amount of feedback information. A novel closed-loop distributed EO-STBC design with linear dispersion code using one-bit feedback information based on selection of phase rotation was therefore proposed for two relay nodes each equipped with two antennas to enhance cooperative diversity and improve the network performance. It was shown that only one-bit of feedback is required to determine the transmission phase terms applied to the symbols from the antennas of each relay node based upon channel state information (CSI) available at the destination node.

As a result, the proposed one-bit feedback scheme achieves full cooperative diversity order of four with full data transmission rate at each hop by utilizing distributed EO-STBC design at the antennas of each relay node and provides a significant improvement in BER performance with a significant reduction in the a mount of feedback information and low decoding complexity at the relay node as compared to the previous closed-loop methods mentioned in the previous chapters.

Furthermore, this proposed scheme was applied to improve the robustness of the asynchronous wireless link between the source and the destination nodes. Orthogonal frequency division multiplexing (OFDM) type transmission with cyclic prefix (CP) was used at the source node to combat the timing errors at the relay nodes. Moreover, utilizing two antennas on each relay reduced the timing error between the relay nodes as well as the decoding complexity at the destination node. Simulation results illustrated that the proposed feedback scheme can provide substantial performance improvement as compared to the open-loop EO-STBC design and also the existing CL EO-STBC design.

The ultimate purpose of this thesis was to positively contribute to scientific knowledge through developing new strategies that could be useful in future wireless systems in particular distributed STBC in asynchronous cooperative relay networks multi-stage relaying networks, and this has been achieved, moreover, the work has opened up other challenges that may catch the imagination of future researchers.

7.2 Direction of Future Research Work

7.2.1 General Coding

- The potential concatenating of the coding schemes considered with outer channel codes such as Turbo and low-density parity-check (LDPC) codes in order to further increase the performance systems and it is still open research. Moreover, such coding could be implemented in a distributed manner.

- The investigated scenarios can be extended to any form of coding, i.e. potentially concatenated differential space-time block, Golden and Silver codes.

7.2.2 Cooperative Relaying

- Only a quasi-static Rayleigh flat fading channel is considered in this thesis, the work should be extended to investigate the effects of different fading environments.

- The performance of all proposed methods can be improved by combining the received signal of DT connection between the source node and the destination node during the first phase with the transmitted signals from the relay nodes during the second phase.

- To increase the performance of distributed CL EO-STBC in Chapters 3,4 and 5, the one-bit feedback scheme in Chapter 6, can be utilized.

- All the proposed distributed STBC schemes with interference cancellation methods in this thesis are implemented in asynchronous

one way cooperative relay networks, therefore extending the proposed schemes in this thesis for asynchronous two way cooperative relay networks is still an open research area.

- In most of the proposed schemes in this thesis so far, only the case of a single source node wishing to communicate with a single destination node via asynchronous cooperative relay nodes has been considered. The issue can be extended and generalized to asynchronous multi-user environments which is one of the major potential research directions in the future.

- In Chapter 6 extending the proposed distributed CL EO-STBC-OFDM based transmission scheme to coherent, symbol asynchronous cooperative relay networks with timing errors and frequency offsets at the relay nodes is also an interesting direction for further work. This problem has been addressed in [95] for the case of two relay nodes.

- In Chapter 6, only distributed CL EO-STBC-OFDM is considered. The same ideas could be extended to distributed CL EO-SFBC-OFDM as well and a comparison between these schemes could be performed under various Doppler and delay profiles.

7.2.3   Robustness of Distributed Space Time Block Coding

- Throughout the thesis, channel state information (CSI) at the destination node is assumed to be known perfectly. However, in a real world application, CSI can only be estimated which obviously will introduce an error in CSI. An interesting study would be examining the proposed schemes in this thesis with channel

estimate imperfections, and designing robust algorithms.

- Both sub-optimum and near-optimum detection methods in Chapter 5 can be applied to distributed CL EO-STBC in Chapter 4, However only a sub-optimum detection method can be used with distributed CL QO-STBC in Chapter 3. .

- Studying of successive interference cancelation (SIC) detection in [96] and [97] with the proposed closed-loop STBC schemes and comparisons with PIC detection schemes in frequency flat fading channels is an important open problem.

- Consideration of overloading in asynchronous multi-user cooperative multiple-input multiple-output (MIMO) [98] environments, possibly exploiting more sophisticated optimization approaches, such as genetic algorithms (GAs) in [99] and [100] is an interesting research area.

Appendix A

CLOSED-LOOP BASED METHODS FOR EXTENDED SPACE TIME BLOCK CODE FOR ENHANCEMENT OF DIVERSITY

The closed-loop based methods of STBC for the enhancement of a diversity system with four transmit and one receive antennas are proposed in [15] and [16] . In [16], for a four transmit antenna scheme, it was proposed in order to achieve full diversity gain, that the transmitted signal from the first and third transmit antenna are per-multiplied by $U_1 = (-1)^a$ and $U_2 = (-1)^b$, where $a, b = 0, 1$, respectively. Therefore, the Grammian matrix can be calculated as in (2.3.24), where

$$\lambda_c = |U_1|^2|h_1|^2 + |h_2|^2 + |U_2|^2|h_3|^2 + |h_4|^2 \qquad \text{(A.1)}$$

and

$$\lambda_f = 2\Re\{U_1 h_1 h_2^* + U_2 h_3 h_4^*\} \qquad \text{(A.2)}$$

Here, λ_c is the conventional channel gain for four transmit antennas, the feedback performance gain λ_f in (A.2) can also be represented as follows

$$\lambda_f = 2\Re(h_1 h_2^*)(-1)^a + 2\Re(h_3 h_4^*)(-1)^b \qquad \text{(A.3)}$$

This changes with the defined values $U_1 = (-1)^a$ and $U_2 = (-1)^b$, which are determined by the feedback information bits a and b. According to the above analysis, the design criterion of the two-bit feedback scheme was proposed to ensure that each element of the feedback performance gain λ_f in (??) should be nonnegative as follows

$$(a,b) = \begin{cases} (0,0), & \text{if} \quad \Re(h_1 h_2^*) \geq 0 \quad \text{and} \quad \Re(h_3 h_4^*) \geq 0 \\ (0,1), & \text{if} \quad \Re(h_1 h_2^*) \geq 0 \quad \text{and} \quad \Re(h_3 h_4^*) < 0 \\ (1,0), & \text{if} \quad \Re(h_1 h_2^*) < 0 \quad \text{and} \quad \Re(h_3 h_4^*) \geq 0 \\ (1,1), & \text{if} \quad \Re(h_1 h_2^*) < 0 \quad \text{and} \quad \Re(h_3 h_4^*) < 0 \end{cases} \qquad \text{(A.4)}$$

It can be noted that from (A.4), the feedback bits are chosen to maxmize the value of λ_f in (A.3). This can lead to a larger received signal-to-noise ratio (SNR) at the receiver and achieve full diversity order.

However, in [15] the signal transmitted from the first and the third antennas are instead rotated by phase angles (phase shifted) $U_1 = e^{j\theta_1}$ and $U_2 = e^{j\theta_2}$ respectively while the other two antennas are kept unchanged. The phase rotation on transmitted symbols is importantly effectively equivalent to rotating the phase of the corresponding channel coefficients. Therefore, the conventional channel gain for four transmit antennas can be represented as in (A.1) and the feedback performance

gain λ_f in (A.3) can be represented as follows

$$\lambda_f = 2\Re(h_1 h_2^*)e^{j\theta_1} + 2\Re(h_3 h_4^*)e^{j\theta_2} \tag{A.5}$$

where θ_1 and θ_2 can be obtained as follows

$$\theta_1 = -\angle(h_1 h_2^*)$$
$$\theta_2 = -\angle(h_3 h_3^*) \tag{A.6}$$

This design criterion of two-bit feedback was designed to ensure that the feedback performance gain should be real and positive, which leads to an improved SNR at the receiver and achieve full diversity order.

Appendix B

END-TO-END BIT ERROR

RATE (BER)

If the lth stage experiences independent probability of error BER, which is denoted here as $P_{b,l\in(1,K)(e)}$, where K is the number of relaying stages, the probability of error free transmission at stage l can be expressed as

$$1 - P_{b,l\in(1,K)(e)} \tag{B.1}$$

hence the average probability of correct end-to-end transmission $P_{c,e2e}(e)$ can be expressed as the joint probability of correct transmission at each stage, i.e.

$$P_{c,e2e}(e) = \prod_{l=1}^{K}(1 - P_{b,l(e)}) \tag{B.2}$$

A bit transmitted from a source terminal is received correctly at the destination only when at all the stages the bits have been transmitted correctly. Thus, the end-to-end BER $P_{b,e2e}(e)$ can therefore be expressed as

$$P_{b,e2e}(e) = 1 - P_{c,e2e} \tag{B.3}$$

which at low BER at each stage can be approximated as

$$
\begin{aligned}
P_{b,e2e}(e) &\approx \sum_{l=1}^{K} P_{b,l(e)} \\
&\approx \sum_{l=1}^{K} \frac{P_{s,l(e)}}{log_2(M_l)}
\end{aligned}
\tag{B.4}
$$

where M_l is the modulating index employed at the lth stage. From (B.4), it is clear that the end-to-end BER will be dominated by the worst stage [12].

REFERENCES

[1] J. Proakis, "Digital communications," *McGraw Hill, Fourth edition,* 2001.

[2] F. Zheng, A. Burr, and S. Olafsson, "Near-optimum detection for distributed space-time block coding under imperfect synchronization," *IEEE Trans. on Communications,* vol. 56, pp. 1795–1799, Nov. 2008.

[3] A. Elazreg, and J. Chambers, "Sub-optimum detection scheme for asynchronous cooperative relay networks," *IET Communications,* vol. 5, pp. 2250–2255, Nov. 2011.

[4] A. Goldsmith, "Wireless communications," *Cambridge University Press,* 2005.

[5] S. Alamouti, "A simple transmit diversity technique for wireless communications," *IEEE Journal on Selected Areas in Communications,* vol. 16, pp. 1451–1458, Oct. 1998.

[6] Y. Jing, and B. Hassibi, "Distributed space-time coding in wireless relay networks," *IEEE Trans. on Wireless Communications,* vol. 5, pp. 3524–3526, Dec. 2006.

[7] Y. Jing, and H. Jafarkhani, "Using orthogonal and quasi-orthogonal designs in wireless relay networks," *IEEE Trans. on Information Theory,* vol. 53, pp. 4106–4118, Nov. 2007.

[8] J. Laneman, and G. Wornell, "Distributed space time coded protocols for exploiting cooperative diversity in wireless networks," *IEEE Trans. on Information Theory*, vol. 49, pp. 2415–2425, Oct. 2003.

[9] E. Larsson and P. Stoica, "Space-time block coding for wireless communications," *Cambridge University Press*, 2003.

[10] L. Laneman, D. Tse, and G. Wornell, "Cooperative diversity in wireless networks: efficient protocols and outage behaviour," *IEEE Trans. on Information Theory*, vol. 50, pp. 3062–3080, Dec. 2004.

[11] J. Laneman, "Cooperative diversity in wireless networks: algorithms and architectures," *PhD Thesis Massachusetts Institute of Technology*, Sep. 2002.

[12] M. Dohler, "Virtual antenna arrays," *PhD Thesis, University of London*, Nov. 2003.

[13] A. Nosratinia, T. Hunter, and A. Hedayat, "Cooperative communication in wireless networks," *IEEE Communications Magazine*, vol. 42, pp. 74–80, Oct. 2004.

[14] M. Dohler, and Y. Li, "Cooperative communications haradware, channel and PHY," *John Wiley and Sons*, 2010.

[15] N. Eltayeb, S. Lambotharan, and J. Chambers, "A phase feedback based extended space-time block code for enhancement of diversity," *IEEE 65th Vehicular Technology Conference, (VTC)*, pp. 2269–229, May. 2007.

[16] Y. Yu, S. Keroueden, and J. Yuan, "Closed-loop extended orthogonal space-time block codes for three and four transmit antennas," *IEEE Trans. Signal Processing Letters*, vol. 13, pp. 273–276, May. 2006.

[17] C. Toker, S. Lambotharan, and J. Chambers, "Closed-loop quasi-orthogonal STBCs and their performance in multipath fading environments and when combined with turbo codes," *IEEE Trans. on Wireless Communications*, vol. 50, pp. 1890–1896, Nov. 2004.

[18] L. Li, and G. Stuber, "Orthogonal frequency division multiplexing for wireless communication," *Springer Science, USA*, 2006.

[19] A. Sendonari, E. Erkip, and B. Aazhang, "User cooperative diversity- part I: system description," *IEEE Trans. on Communications*, vol. 51, pp. 1927–1938, Nov. 2003.

[20] X. Li, "Space time coded multi-transmission among distributed transmitters without perfect synchronization," *IEEE Signal Processing Letters*, vol. 11, pp. 948–951, Dec. 2004.

[21] F. Oggier and B. Hassibi, "An algebraic family of distributed space-time codes for wireless relay networks," *IEEE International Symposium on Information Theory (ISIT), Seattle, USA*, pp. 538–541, Jul. 2006.

[22] X. Li, F. Ng, J.-T. Hwu, and M. Chen, "Channel equalization for STBC-encoded cooperative transmissions with asynchronous transmitters," *Proc. of the 39th Asilomar Conf. on Signals, Systems and Computers*, pp. 457–461, Oct. 2005.

[23] Y. Shang, and X.Xia, "Shift-full-rank matrices and applications in space-time trellis codes for relay networks with asynchronous coopera-

tive," *IEEE Trans. on Information Theory*, vol. 52, pp. 3153–3167, Jul. 2006.

[24] S. Wei, D. Goeckel, and M. Valenti, "Asynchronous cooperative diversity," *IEEE Trans. on Wireless Communications*, vol. 5, pp. 1547–1557, Jun. 2006.

[25] Y. Li, and X. Xia, "A Family of distributed space-time trellis codes with asynchronous cooperative diversity," *IEEE Trans. on Communications*, vol. 55, pp. 790–800, Apr. 2007.

[26] F. Zheng, A. Burr, and S. Olafsson, "Signal detection for distributed space-time block coding: 4 relay nodes under quasi-synchronization," *IEEE Trans. on Communications*, vol. 57, pp. 1250–1255, May. 2009.

[27] Z. Li, and X. Xia, "A simple Alamouti space-time transmission scheme for asynchronous cooperative systems," *IEEE Signal Processing Letters*, vol. 14, pp. 804–807, Nov. 2007.

[28] J. Winters, "On the capacity radio communication with diversity in a rayleigh fading environment," *IEEE Journal on Selected Areas in Communications*, vol. 5, pp. 871–878, Jun. 1987.

[29] G. Foschini, and M. Gans, "On limits of wireless communications in a fading environment when using multiple antennas," *Wireless Personal Communications*, vol. 6, pp. 311–335, Mar. 1998.

[30] I. Telatar, "Capacity of multi-antenna Gaussian channels," *European Trans. Telcommunications*, vol. 10, pp. 585–595, Dec. 1999.

[31] A. Paulraj, R. Nabar and D. Gore, "Introduction to space-time wireless communications,," *New York: Cambridge University Press*, 2003.

[32] E. Biglieri, R. Calderbank, A. Constantinides, A. Goldsmith, A. Paulraj and H.V. Poor, "MIMO wireless communications," *Cambridge University Press*, 2007.

[33] Broadcom Corporation, "802.11n: Next-generation wireless LAN technology," *White paper*, pp. 1–13, Apr. 2006.

[34] Agilent Technologies, "WiMax implementation of MIMO," *www.home.agilent.com.*, 2012.

[35] B. Evans, and K. Baughan, "Visions of 4G," *Electronics and Communication Engineering Journal*, pp. 293–303, Dec. 2002.

[36] M. Rumeny, "LTE and the evolution to 4G wireless: Design and measurement challenges," *John Wiley and Sons*, Jul. 2009.

[37] V. Tarokh, A. Naguib, N. Seshadri, and A. Calderbank, "Combined array processing and space-time coding," *IEEE Trans. on Information Theory*, vol. 45, pp. 1121–1128, May. 1999.

[38] L. Zheng, and D. Tse, "Diversity and multiplexing: A fundamentel trade-off in multiple-antenna channels," *IEEE Trans. on Information Theory*, vol. 49, pp. 1073–1093, May. 2003.

[39] D. Tse and P. Viswanath, "Fundamentals of wireless communication," *Cambridge University Press*, 2005.

[40] D. Reynolds, X. Wang, and H. V. Poor, "Blind adaptive spacetime multiuser detection with multiple transmitter and receiver antennas," *IEEE Trans. Signal Processing*, vol. 50, p. 12611276, Jun. 2002.

[41] V. Tarokh, N. Seshadri, and A. Calderbank, "Space time block codes for high data rate wireless communication: Performance criterion and code construction," *IEEE Trans. Information Theory*, vol. 44, pp. 744–765, Mar. 1998.

[42] V. Tarokh, H. Jafarkhani, and A. Calderbank, "Space time block codes from orthogonal design," *IEEE Trans. on Information Theory*, vol. 45, pp. 1456–1467, July. 1999.

[43] H. Jafarkhani, " A quasi-orthogonal space time block code," *IEEE Trans. on Communications*, vol. 49, pp. 1–4, Jan. 2001.

[44] M. Jankiraman, "Space-time codes and MIMO systems," *Norwood: Artech House*, 2004.

[45] LetWorld, "3GPP / 3G LTE tutorial - Long Term Evolution," *http://lteworld.org/tutorial/3gpp-3g-lte-tutorial-long-term-evolution*, Jul. 2009.

[46] H. Jafarkhani, "Space time block coding: theory and practice," *New York: Cambridge University Press*, 2005.

[47] C. Papadias and G. Foschini, "A space-time coding approach for systems employing four transmit antennas," *IEEE International Conference on Acoustics, Speech, and Signal Processing (ICASSP)*, vol. 4, pp. 2481–2488, May. 2001.

[48] W, Su, and X. Xia, "Quasi-orthogonal space time block codes with full diversity," *in Proc. CLOBECOM*, vol. 2, pp. 1098–1102, Nov. 2002.

[49] W. Su, and X. Xia, "Signal constellation for quasi-orthogonal space-time block codes with full diversity," *IEEE Trans. on Information Thoery*, vol. 50, pp. 2331–2347, Oct. 2004.

[50] O. Tirkkonen, "Optimising space-time block code by constellation rotation," *Finnish Wireless Communications. Workshop (FWWC)*, Oct. 2001.

[51] N. Sharma and C. Papadias, "Improved quasi-orthogonal codes through constellation rotation," *IEEE 56th Vehicular Technology Conference. (VTC)*, vol. 51, pp. 332–332, Mar. 2003.

[52] R. Yates, "A coding theory tutorial," *White Paper, Digital Signal Labs*, p. 111, Aug. 2009.

[53] N. Benvenuto, L Bettella, and R. Marchesani, "Performance of the Viterbi algorithm for interleaved convolutional codes," *IEEE Trans. vehicular Technology*, vol. 47, pp. 919–923, Aug. 1998.

[54] I. Glover, and P. Grant, "Digital communications," *Prentice Hall*, 2010.

[55] M. Varanasi, and B. Aazhang, "Multistage detection in asynchronous code division multiple-access communication," *IEEE Trans. on Communications*, vol. 38, pp. 509–519, Apr. 1990.

[56] J. Bingham, "Multicarrier modulation for data transmission: An idea whose time has come," *IEEE Commun. magazine*, vol. 28, pp. 5–14, May. 1990.

[57] A. Bahai, B. Saltzberg, and M. Ergen, "Multi-carrier digital communications: Theory and applications Of OFDM ," *Springer Sciences*, 2004.

[58] H. Yang, "A road to future broadband wireless access: MIMO-OFDM based air interface," *IEEE Communications Magazine*, vol. 43, pp. 53–60, Jan. 2005.

[59] M. Simon, and M. Alouini, "Digital communication over fading channels: A unified approach to performance analysis ," *New York, John Wiley and Sons*, 2000.

[60] E. Meulen, "Three-terminal communication channels," *Advanced Appl. probaboility*, vol. 3, pp. 120–154, 1971.

[61] T. Cover, and A. El Gamal, "Capacity theorems for the relay channel," *IEEE Trans. on Information Thoery*, vol. 25, pp. 572–584, Sep. 1979.

[62] T. Cover, and J. Thomas, "Elements of information theory," *Johns Wiley and Sons*, 1991.

[63] A. Sendonari, E. Erkip, and B. Aazhang, "User cooperative diversity- part II: system description," *IEEE Trans. on Communications*, vol. 51, pp. 1939–1948, Nov. 2003.

[64] T. Hunter, S.Sanayei, and A. Nosratinia, "Outage analysis of coded cooperation," *IEEE Trans. on Information Theory*, vol. 52, pp. 375–391, Feb. 2006.

[65] T. Hunter, "Coded cooperation: A new framework for user cooperation in wireless networks," *PhD Thesis. University of Texas at Dallas, Richardson*, 2004.

[66] P. Anghel, and M. Kaveh, "On the diversity of cooperative systems," *IEEE International Conference on Acoustics, Speech, and Signal Processing (ICASSP)*, vol. 4, pp. 577–580, May. 2004.

[67] Y. Hua, Y. Mei, and Y. Chang, "Wireless antennas-making wireless communications perform like wireline communications," *IEEE Topical Conf. on Wireless Communications Technology*, pp. 47–73, Oct. 2003.

[68] B. Hassibi, and B. Hochwald, "High-rate codes that are linear in space and time," *IEEE Trans. on Information Theory*, vol. 48, pp. 1804–1824, Aug. 2002.

[69] T. Kiran and B. Rajan, "Distributed space-time codes with reduced decoding complexity," *IEEE International Symposium on Information Theory (ISIT), Seattle, USA*, pp. 542–546, Jul. 2006.

[70] Y. Jing, and B. Hassibi, "Cooperative diversity in wireless relay networks with multiple-antenna nodes," *IEEE International Symposium on Information Theory (ISIT)*, pp. 815–819, Sep. 2005.

[71] X. Liang, "Orthogonal designs with maximal rates," *IEEE Trans. on Information Theory*, vol. 49, pp. 2468–2503, Oct. 2003.

[72] J. Harshan, and B. Rajan, "Co-ordinate interleaved distributed space-time coding for two-antenna-relays networks," *IEEE Trans. on Wireless Communications*, vol. 8, pp. 1783–1791, Apr. 2009.

[73] Y. Li, and X. Xia, "Full diversity distributed space-time trellis codes for asynchronous cooperative communications," *IEEE International Symposium on Information Theory (ISIT)*, pp. 911–915, Sep. 2005.

[74] F. Zheng, A. Burr, and S. Olafsson, "Signal detection for orthogonal space time block coding over time selective fading channel: a PIC approach for the $\mathcal{G}_i$ system," *IEEE Trans. on Communications*, vol. 53, pp. 969–972, Jun. 1998.

[75] F. Zheng, A. Burr, and S, Olafsson, "PIC detector for distributed space-time block coding under imperfect synchronization," *IET Electronics Letters*, vol. 43, pp. 580–581, Jun. 2007.

[76] F. Zheng, A. Burr, and S, Olafsson, "Distributed space-time block coding for 3 and 4 relay nodes: imperfect synchronization and a solution," *IEEE International Symposium on Personal, Indoor and Mobile Radio Communications (PIMRC)*, pp. 1–5, Sep. 2007.

[77] M. Elazreg, and J. A. Chambers, "Closed-loop extended orthogonal space-time block coding for four relays node: Under imperfect synchronization," *IEEE Workshop on Statistical Signal Processing (SSP)*, pp. 545–545, Oct. 2009.

[78] A. Elazreg, F. Abdurahman, and J. Chambers, "Distributed closed-loop quasi-orthogonal space time block coding with four relay nodes: overcoming imperfect synchronization," *IEEE International Conference on Wireless and Mobile Computing (WIMOB)*, pp. 320–325, Nov. 2009.

[79] A. Elazreg, U. Mannai, and J. Chambers, "Distributed cooperative space-time coding with parallel interference cancellation for asynchronous wireless relay networks," *IEEE International Conference on Software, Telecommunications and Computer Networks (SoftCOM)*, pp. 360–364, Sep. 2010.

[80] A. Elazreg, W. Qaja, and J. Chambers, "PIC detector with coded distributed closed-loop EO-STBC under imperfect synchronization," *IEEE International Conference on Software, Telecommunications and Computer Networks (SoftCOM)*, pp. 1–5, Sep. 2012.

[81] Z. Li and X. Xia, "An Alamouti coded OFDM transmission for cooperative systems robust to both timing errors and frequency offsets," *IEEE Trans. on Wireless Communications*, vol. 7, pp. 1839–1844, May. 2008.

[82] G. Rajan and B. Rajan, "OFDM based distributed space time coding for asynchronous relay networks," *IEEE International Conference on Communication (ICC)*, pp. 1118–1122, May. 2008.

[83] A. Elazreg, and J. Chambers, "Distributed one-Bit feedback extended orthogonal space time coding based on selection of cyclic rotation for cooperative relay networks," *IEEE International Conference Acoustics, Speech and Signal Processing (ICASSP)*, pp. 3340–3343, May. 2011.

[84] A. Elazreg, S. Kassim, and J. Chambers, "Cooperative multi-hop wireless networks with robustness," *IEEE Europe Wireless Conference (EW)*, pp. 449–453, Apr. 2010.

[85] X. Li, F. Ng, J. Hwu, and M. Chen,, "Channel equalization for STBC encoded cooperative transmissions with asynchronous transmitter," *Proc, of the 39th Asilomar conf. on Signals Systems and Computer*, pp. 457–361, Oct. 2005.

[86] L. Le, and E. Hossain, "Multihop cellular networks: potential hains. research chanllenges, and a resource allocation framework," *IEEE Communication Magazine*, vol. 45, pp. 66–73, Sep. 2007.

[87] H. Li, M. Lott, M. Weckerle, W. Zirwas, and E. Schulz, "Multihop communications in future mobile radio networks," *IEEE Personal Indoor and Mobile Radio Communications (PIMRC)*, vol. 1, pp. 54–58, Sep. 2003.

[88] Y. Jing, and B. Hassibi, "Diversity analysis of distributed space-time codes in relay networks with multiple transmitter/receiver antennas," *EURASIP Jounral, Advance in Signal Processing*, vol. 2008, Article ID 254573, 17 pages, 2008.

[89] J. Harshan and B. Sundar Rajan, "High-rate, single-symbol ML decodable precoded DSTBCs for cooperative networks," *IEEE Trans. on Information Theory*, vol. 55, pp. 2004–2015, May. 2009.

[90] S. Wei, "Diversity-multiplexing tradeoff asynchronous cooperative diversity in wireless networks," *IEEE Trans. on Information Theory*, vol. 53, pp. 4150–4172, Nov. 2007.

[91] L. Le, and E. Hossain, "Multihop cellular networks: Potential gains, research challenges, and a resource allocation framework ," *IEEE Communication Magazine*, vol. 45, pp. 66–73, Sep. 2007.

[92] A. Bletsas, A. Khisti, D. Reed, and A. Lippman, "Simple cooperative diversity method based on network path selection," *IEEE Journal on Selected Areas in Communications*, vol. 24, pp. 659–672, Mar. 2006.

[93] A. Adinoyi, Y. Fan, H. Yanikomeroglu, H. Vincent Poor and F. Al-Shaalan, "Performance of selection relaying and cooperative diversity," *IEEE Trans. on Wireless Communications*, vol. 8, pp. 5790–5795, Dec. 2009.

[94] Y. Mei, Y. Hua, A. Swami, and B. Daneshrad, "Combating synchronization errors in cooperative relay," *IEEE International Conference on Acoustics, Speech, and Signal Processing,(ICASSP)*, pp. 1–6, Mar. 2005.

[95] L. Zheng, and X. Xia, "An Alamouti coded OFDM transmission for cooperative systems robust to both timing errors and frequency offsets," *IEEE Trans. on Wireless Communications*, vol. 7, pp. 1839–1844, May. 2008.

[96] M. El Astal, and A. Abu-Hudrouss, "SIC detector for 4 relay distributed space-time block coding under quasi-synchronization," *IEEE Communications Letters*, vol. 15, pp. 1056–1058, Oct. 2011.

[97] Z. Wu, X. Wang, and L. Zhou, "Signal detection in distributed cooperative cellular systems without perfect synchronization," *IEEE International Conference on Communications (ICC)*, pp. 1–5, Jun. 2009.

[98] C. Tan, and A. Calderbank, "Multiuser detection of Alamouti signals," *IEEE Trans. on Communications*, vol. 57, pp. 1–10, Jul. 2009.

[99] Q. Guo, S. Kim, and D. Park, "Antenna selection using genetic algorithm for MIMO systems," *IEICE Trans. on Fundamentals of Electron-*

ics, Communications and Computer Sciences, vol. E89, pp. 1773–1775, Jun. 2006.

[100] M. Jiang, and L. Hanzo, "Multi-user MIMO-OFDM for next generation wireless system," *Proceeding of the IEEE*, vol. 95, pp. 1431–1469, Jul. 2007.